Performance Adaptation of Gas Turbines for Power Generation Applications

Elias Tsoutsanis

Submitted for the degree of PhD

Department of Power and Propulsion

Cranfield University

Cranfield, UK

2010

Cranfield University

School of Engineering

PhD

2010

Elias Tsoutsanis

Performance Adaptation of Gas Turbines for Power Generation Applications

Academic Supervisor: Dr Yi-Guang Li

Academic Advisor: Professor Pericles Pilidis

Industrial Advisor: Mr. Michael Newby

June 29, 2010

Abstract

One of the greatest challenges that the world is facing is that of providing everyone access to safe and clean energy supplies. Since the liberalization of the electricity market in the UK during the 1990s many combined cycle gas turbine (CCGT) power plants have been developed as these plants are more energy efficient and friendlier to the environment. The core component in a combined cycle plant is the gas turbine. In this project the MEA's Pulrose Power Station CCGT plant is under investigation. This plant consists of two aeroderivative LM2500+ gas turbines of General Electric for producing a total of 84MW power in a combined cycle configuration.

Accurate gas turbine performance simulation and adaptation leads to robust diagnostic analysis which saves time and money in a sector where even a percent change in thermal efficiency is translated to thousands of pounds. For satisfying the needs of such a competitive environment various software capabilities have been developed for performance and financial analysis of a power plant. The software that Cranfield's University has built for performance simulation and diagnostics is PYTHIA. This has a graphical user interface (GUI) and performs thermodynamic calculations through the Turbomatch code, which has an international reputation and experience of 30 years.

The limitations that, exclusive manufacturer's property, compressor maps have imposed at off-design performance prediction of a gas turbine have been overcome by the development of a novel off-design performance adaptation method. The new approach is capable of adapting the performance of an engine model to that of a service engine at part load conditions. This method has been developed in visual basic and integrated into PYTHIA's environment. The proposed adaptation method initially generates a series of compressor maps, which in turn provide the performance of the engine model at off-design conditions. Thence from a family of possible solutions the best set of compressor map coefficients is determined through a genetic algorithm optimiser. The genetic algorithm optimisation is based on a maximum fitness criterion between the

engine model simulated measurements and the target measurements of the adaptation, which are available from the service engine.

Through a series of case studies the developed adaptation's quality and accuracy have been validated and tested. The proposed method in conjuction with a novel compressor map generation approach, which is integrated in the adaptation process, is able to match very accurately the performance of a gas turbine at part load conditions. Apart from adaptation of the engine model to a single operating point set of service engine target data the method is able to match multiple off-design operating points simultaneously. The developed method's limitations, which are due to the interaction between PYTHIA'S code and Turbomatch code, affect the range of operating conditions that the adaptation can capture in a single simulation.

The new adaptation approach is a fast and accurate method for matching a gas turbine's performance at off-design conditions and has the prospects, after a series of proposed modifications, to extend its application span to that of an engine's operating envelope. The establishment of a robust off-design performance adaptation method is a fundamental contribution to knowledge in the gas turbine energy sector.

Acknowledgements

I would like to take this opportunity to thank and express my sincere gratitude to Professor Pericles Pilidis for giving me the opportunity to do a research degree in a project where I feel very fortunate to be a part of, and for his expert guidance and support.

I am deeply indebted to my supervisor Dr. Yi-Guang Li for his constant support, invaluable advice and constructive suggestions that greatly has enriched my knowledge with his exceptional insights in gas turbine performance and diagnostics. His guidance has helped me construct a robust theoretical background and he has given much time and devotion for this project.

I also would like to thank my industrial supervisor Mr. Mike Newby for his support and for regularly devoting much of his invaluable time in the project.

In the initial period of the project I had the pleasure to collaborate with Mr. Marco Mucino and his challenging suggestions and motivating discussions are greatly appreciated.

I would like to thank my colleagues Nikolaos Asproulis, Antony Milonas, Christos Vamvakoulas and Dimitris Mantzalis that have been and still are an excellent companion and very good friends. I am deeply thankful to my office mate doctoral researcher Emad Hamid for all the constructive discussions and his kindness. I would also like to acknowledge my departmental colleagues Pavlos Zachos, Dimitrios Fouflias and Konstantinos Kyprianidis with who we harmoniously shared the same corridor of the 183 building.

Thanks also to Angelos Varelis of hellenic air force for all the suggestions and discussions we had through the duration of my PhD. I also have to acknowledge Panagiotis Stathopoulos of hellenic air force and his family for their excellent companion and friendship.

A big “thank you” goes to my parents Dimitrios and Aggeliki for their continuing

support and to my brother Panagiotis, who has also completed his PhD in Cranfield University, for his conststructive comments and suggestions. Last but not least I would like to express my appreciation to my girlfriend Kelly for her patience and understanding during my study.

The financial support provided by Manx Electricity Authority (MEA), the Engineering and Physical Sciences Engineering Council (EPSRC), and Cranfield University is greatly acknowledged.

To my parents Dimitrios and Aggeliki who instill in me the drive and determination to follow my dreams and pursue my goals.

Contents

List of Figures

List of Tables

Chapter 1

Introduction

One of the greatest challenges facing humanity during the twenty-first century is that of giving everyone on the planet access to safe, clean and sustainable energy supplies. Energy demand is increasing and major improvements for higher energy efficiency are explored. A industrial revolution in the UK took place during the 1990s after the liberalization of electricity generation market. During this period more energy efficient plants as the CCGTs have been built. A combined cycle is characteristic of a power producing plant that employs more than one thermodynamic cycle. Combining two or more "cycles" such as the Brayton and Rankine cycle results in improved overall efficiency.

The CCGT plants have a higher thermal efficiency than old-fashioned coal plants and in business terms are more profitable. At the same time their emissions are far lower than conventional coal/lignite plants therefore they are environmentally friendlier. These plants evolved when natural gas was present, as this is the more efficient way to produce energy from this type of fossil fuel. The combined cycle plant works around a gas turbine which is its core component. The MEA's power station in the Isle of Man is such a combined cycle plant which produces 84MW of power and is using the LM2500+ aero-derivative gas turbines of General Electric.

The major advantages of the gas turbine is its size and power to weight ratio. Even with the latest heavy duty industrial machines capable of producing 600MW of power in a combined cycle, the gas turbine's size remains a strong feature compared to the old diesel engines and coal/lignite plants. There is margin for further improving the performance and thermal efficiency of such machines till they reach the theoretical maximum as defined in Carnot cycle. As boards of directors and business corporations

will always pursue more efficient "money machines" the large gas turbine manufacturers will be addressed with the task of developing new gas turbines that in the future might reach the aforementioned limit in an advanced CCGT configuration.

Better performance is always required from the gas turbines. This affects operational and maintenance costs which play a significant role in the competitive energy market. Minimizing these costs and ensuring that the plant is always running efficiently is a key ingredient for a profitable energy plant. Under this scope various software capabilities have been developed for performance and financial analysis of a CCGT plant. The software that Cranfield's University has built for performance simulation and diagnostics is PYTHIA. This has a graphical user interface (GUI) and performs thermodynamic calculations through the Turbomatch code, which has an international reputation and experience.

The industrial gas turbines are packed with instrumentation systems for measuring almost everything. However, there are various thermodynamic parameters that can not be physically measured and these are mass flow rates and turbine entry temperature (TET) which is very high even for the latest of instrumentation sets. These parameters are the ones that can verify the actual performance of a gas turbines. There are various ways of estimating these, but the simulation software that combines both performance simulation and actual assessment of engine health is the PYTHIA software which has been integrated with performance adaptation and gas path analysis diagnostics. Performance adaptation simulates the engine's capabilities and control logic which self-adjusts its operation and therefore its performance by any change in operating and ambient conditions.

The cooperating body and one of the major financial sponsors of this project is the Manx Electricity Authority's (MEA) Pulrose power station in the Isle of Man. This CCGT plant produces 84MW of power and is using the LM2500+ aero-derivative gas turbines of General Electric.

1.1 Aims and Objectives

The aim of this research project is the development of a new version of PYTHIA software based on the development of gas turbine performance adaptation and GPA diagnostics that is going to be integrated to the MEA environment for easier decision making.

The project objectives are summarized here:

1. Using PYTHIA's software as a starting point build a LM2500+ engine model that will have the capacity to capture accurately the performance of the MEA gas turbines .

2. Development an off-design adaptation method that will enable the engine model to match the MEA's service engine performance at part load conditions.

3. Development of a gas turbine performance platform for MEA for their two existing LM2500+ gas turbine engines implemented with fully adapted engine performance model. The platform should provide a graphical user interface, be flexible enough to implement varying operating conditions in performance and diagnostics analysis and user friendly so that important performance parameters can be displayed conveniently.

1.2 Thesis Contribution

The work conducted in this thesis has made significant contributions to the field of gas turbine performance and diagnostics for power generation applications. In particular

- A more accurate engine model of GE LM2500+, that is the prime mover of MEA's combined cycle power plant, has been developed in Cranfield's University performance simulation and diagnostics software programme called PYTHIA.

- The engine model is enabled by the design point and off-design performance adaptation to readapt its performance to the performance of the service engines of MEA during the whole span of its operation.

- A novel method for generating a compressor performance map, which is a useful performance and diagnostic tool for the whole engine, has been developed and is capable of producing compressor maps tailored to the engine specifications that an engine under investigation implies.

- An off-design performance adaptation has been developed which employs the compressor generating method and genetic algorithms optimisation technique for matching the engine's model performance to the service engine of MEA at off-design conditions, which has enhanced the applicability of PYTHIA's simulation and diagnostics software tool.

- Apart from single point adaptation the developed off-design adaptation is able to handle multiple operating points adaptation from a series of service engine data.
- The gas turbine diagnostics option of PYTHIA has therefore much more accurate prediction of the engine's health at design and off-design conditions.
- Results from this thesis have been presented in a number of international conferences including the 5th International Condition Monitoritng and Machine Failure Prevention Technology Conference, July 2008, Edinburgh, and the Gas Turbine Conference of the Institution of Diesel and Gas Turbine Engineers, November 09, Milton Keynes, along other key meetings and events.

A list of the papers published and the ones that are currently under preparation are enlisted here.

1. "Gas Turbine Off-Design Performance Adaptation by Compressor Map Generation and Genetic Algorithms Part I & II", E.Tsoutsanis Y.G.Li P.Pilidis and M.Newby, under preparation for journal article publication.
2. 'Applied GPA diagnostics for gas turbines used in combined cycle power plants', E.Tsoutsanis Y.G.Li M.Newby and P.Pilidis, 5th GAS TURBINE CONFERENCE IDGTE, 10-11 November, 2009
3. 'Industry – University Collaboration: A case study between Manx Electricity Authority and Cranfield University', E.Tsoutsanis M.Newby Y.G.Li and P.Pilidis, Annual Board Meeting of the Institution of Diesel and Gas Turbine Engineers, 19th March, 2009
4. 'Gas path analysis applied to an aeroderivative gas turbine used for power generation', E.Tsoutsanis Y.G.Li P.Pilidis and M.Newby, 5th International Condition Monitoring and Machine Failure Prevention Technology, Proceedings, 15th July, 2008
5. 'GPA diagnostics: an application to an industrial gas turbine', E.Tsoutsanis Y.G.Li P.Pilidis and M.Newby, Cranfield Multi-Strand Conference, Proceedings, 6th May, 2008,

1.3 Thesis Overview

This thesis is organised as follows.

Chapter 2 presents a detailed description of the combined cycle gas turbine power plant. From the factors that drove the CCGT evolution in the early 90's up to a description of Manx Electricity Authority Power plant at the Isle of Man are presented. The aeroderivative gas turbine of GE the LM2500+, which is the prime mover of the combined cycle configuration, is analysed in terms of the function, operation and the thermodynamics that each gas turbine component has. Finally key topics such as gas turbine performance simulation, operation and maintenance, of the MEA's power plant along with a brief description of the MEA-Cranfield University's collaboration objectives and goals during this period are presented.

Chapter 3 presents the design point performance adaptation that has been employed in order to continuously adapt the engine model to service engine and therefore be able to model very accurate the design point of the gas turbine. A description of the methodology which is based on the Gas Path Analysis, similar to the GPA for diagnostics, takes place before a simple test case application. The purpose of the test case was to compare the performance deterioration of both gas turbines during a six month operation period. The practical considerations of measurement corrections and natural gas flow recalculation enabled the design point adaptation to provide a fast and accurate tool for assessing the performance of a gas turbine.

Chapter 4 takes over from the limitations of design point adaptation, which motivated the development of a novel compressor generation method with the ability to improve performance adaptation at off-design conditions. The methodology used for this analytical process of expressing a compressor map mathematically is also presented. The coefficients that provide the gas turbine user with a useful guide for the shape that a compressor map has, based on the engine's design specifications, are outlined. A sensitivity analysis for the map's coefficients also takes place. A demonstration of the compressor generation software tool along with the algorithm and the associated steps of calculations are presented.

Chapter 5 presents the off-design point performance adaptation by initially outlining the associated steps for a successful adaptation process. As long as these have been satisfied the methodology for this adaptation procedure at off-design conditions becomes an optimisation problem that genetic algorithms can handle. The relationship between compressor map generation and the genetic algorithms has the capacity to predict

the performance of a gas turbine at off-design conditions quite accurately. Several multiple operating point test cases have been used for validating and testing the off-design performance adaptation against simulated and service engine data respectively.

Chapter 6 presents the gas turbine performance based diagnostics. From a general description of the types of degradation, that an engine suffers during its lifespan, up to practical consideration that are a-priori required for accurate assessment of an engine's health condition, Gas Path Analysis is the method used for this process and described in detail. The application of this powerful diagnostic tool aims to predict the degradation that the engine's components have experienced, in terms of performance, over a period of three months. The findings of this analysis indicated that there was significant compressor fouling and negligible turbine erosion.

Chapter 7 presents the conclusions drawn from this research project and possible future research directions in the context of gas turbine performance off-design adaptation and diagnostics.

Chapter 2

Combined Cycle Gas Turbines

2.1 Introduction

Since the early days of electricity production, power plant efficiency has been improving steadily. The efficiency of a power plant is the percentage of the energy content of the fuel input that is converted into electricity output over a given time period [1].

The most advanced form of fossil-fuel led power plant now available is the CCGT. combined cycle power plants are more than 50% efficient compared with the older steam turbine power plant that is still in widespread use, where the efficiency is only about 30%, and thus two thirds of the energy content of the input fuel is wasted in the form of heat, usually dumped in the atmosphere via cooling towers.

CCGTs are more climate friendly than older, coal fired steam turbine plant, not only because they are more efficient but also because they burn natural gas, which on combustion emits 40% less CO2, than coal per unit of energy generated [2, 3, 4]. Overall taking into account both the higher efficiency and natural's gas lower CO2 emissions, when compared with traditional coal fired plant CCGT-based power plants release about half as much CO2 per unit of electricity produced. Most of the reductions that occurred in Britain's CO2 emissions during the 1990s were due to the so-called 'dash for gas' as a substitute for coal power generation.

After fuels have been converted to electricity, whether in combined cycle or steam turbine only plant, further losses occur in the wires of transmission and distribution systems that convey the electricity to customers. In UK these amounts to 8%. Overall this means that even when a modern engine, high efficiency CCGT is the electricity generator, less than half the energy in its input fuel emerges as electricity at the customers'

sockets. In the case of older power stations the figure is around one-quarter.

Clearly, there is room for further improvements in the supply-side of electricity systems, by further increasing the efficiency of generating plant and by ensuring the whatever waste heat remains is piped to where it can be used.

2.2 MEA Power Station

The concept of CCGT is based on the law of conservation of energy which states that energy can not be created or destroyed, it can only be changed from one form to another, such as when heat energy is converted to electrical energy. The power station utilizes advanced "Combined Cycle Gas Turbine technology, based on aeroderivative gas turbines. Air is drawn into the turbine compressor and compressed to 22barg. The air is then passed to the combustion chamber where it mixes with natural gas or oil fuel and the mixture is ignited. The resulting hot combustion gas rotates firstly the high pressure turbine that drives the compressor and then the low pressure turbine that drives an electrical generator.

The now cooler exhaust gases then pass to the Once Through Steam Generator (OTSG). The energy in the exhaust gas from the gas turbine is not wasted, but heats up water inside the steam generator tubes and converts it into superheated steam. The steam is then piped to the Steam Turbo Generator Set (ST8), which produces further electrical power.

The spent team falls through a Condenser where cooling water cools the steam back into water. This condensate is extracted from the condenser and pumped to the feed-pumps, which raise the pressure sufficiently to the feedwater to be returned to the steam generator and once more be turned into steam.

The cooling water is circulated through air cooled heat exchangers which dissipate the energy from the condensed steam to the atmosphere. The closed circuit cooling system does away with the vapor plume of the earlier wet cooling towers, requires less water from the river and discharges nothing to the river.

Each gas turbine can produce 32 MW and the steam turbine 23MW giving a gross output of 87MW. The station consumes 3MW of power for its own needs and hence the station net output is 84MW.

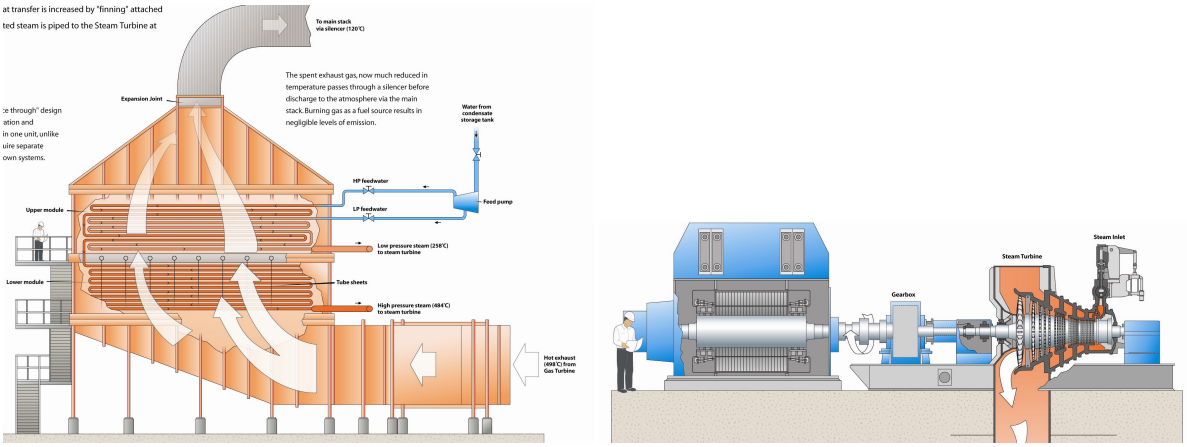

(a) OTSG (b) Steam Generator

Figure 2.1: CCGT

The total power output is 84MW capable of satisfying the island's demand and even exporting electricity back to the mainland UK through the cable under Irish sea.

The MEA is a statutory body charged with providing the people of the Isle of Man with a safe, reliable and economic electricity supply. The authority has responsibility for the generation, transmission and distribution of electricity and for the billing and collection of revenue from these activities.

The MEA is directed by a statutory board of Tynwald. The chief executive is responsible for the day to day functions of the authority who is supported by 4 Directors, who are responsible for generation, network Services, corporate services and finance.

The authority constructed an 88MW combined cycle gas turbine power station at Pulrose in 2003 together with a natural gas pipeline from Glen Mooar to Pulrose power station. This provides a diversity of fuel and a supply of natural gas to the island. Power stations are situated at Pulrose, Peel, Ramsey and Sulby as seen here. Pulrose including the CCGT has a capacity of nearly 135MW. Peel a capacity of nearly 40MW, a diesel generating station at Ramsey with a capacity of 3.6MW, and a small hydro station at Sulby with a capacity of 1.0MW.

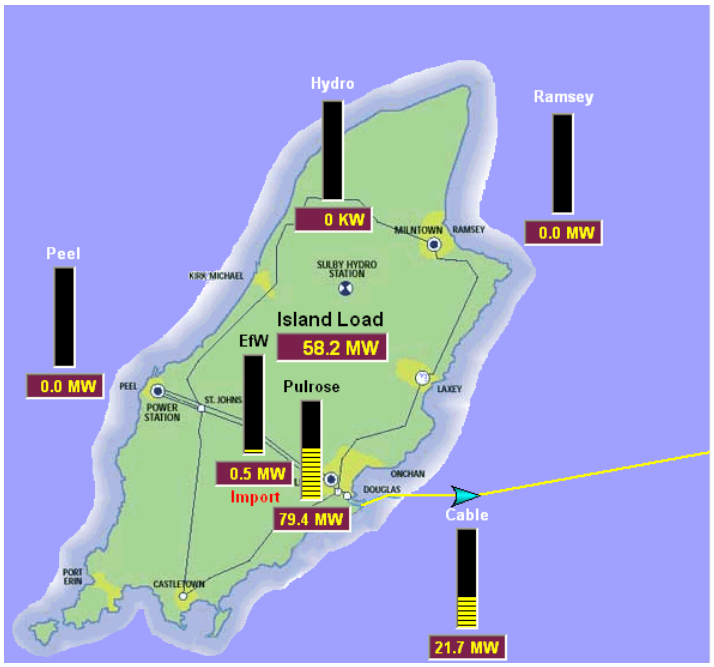

Figure 2.2: Isle of Man Generation

The MEA operates the 40MW sub sea cable link in a customer services orientated manner whilst obtaining power on a least cost basis. This is in line with the electricity supply industry best practice.

2.3 GE LM2500+ Gas Turbine

The LM2500+ is an aeroderivative gas turbine of General Electric. It is a descendant of the CF6 family of GE aero engines modified for Land and Marine applications as LM notation stands for. While aircraft engines have multiple operating points such as take-off, cruise, etc, where performance is crucial, the LM2500+ is required to operate at close to its peak efficiency near its high-speed design point [5, 6]. The high cycle pressure ratio achieved in the CF6-6 core results in gas generator with a high thermal efficiency of 39% [7].

In this case two engines are used for power generation in a CCGT power plant in the Isle of Man. Each engine is coupled to a power turbine which delivers the power output and therefore being the main contributor in the total power generated in the CCGT plant.

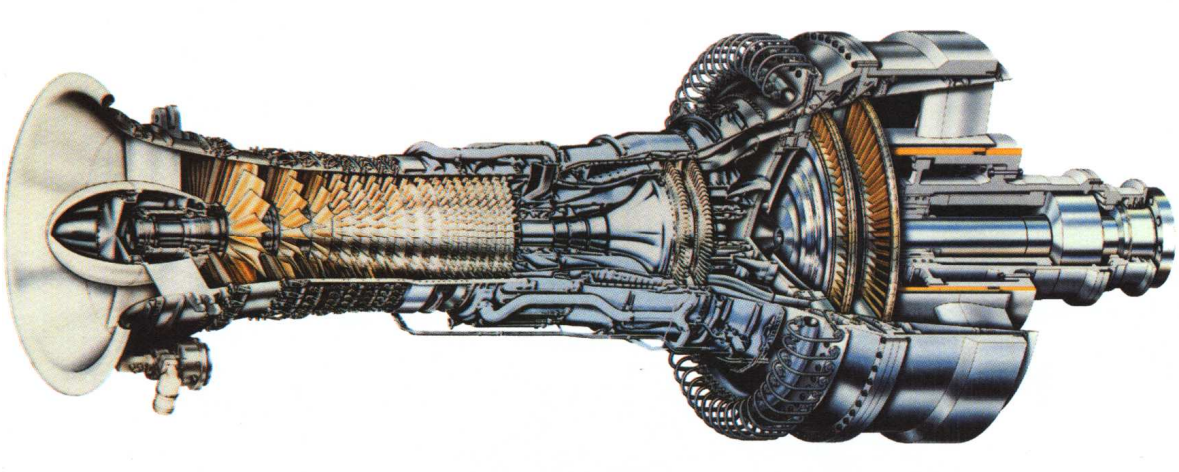

Figure 2.3: GE LM2500+ HSPT

There are many possible configurations of this engine concerning the type of combustor and power turbine. There are both advantages and disadvantages for each possible configuration and the final decision is up to the customer's needs and requirements. The specific engines are configured with a single annular combustor (SAC) and with a two stage high speed power turbine (HSPT). The main gas generator operates in the range of 9,000rpm whereas the power turbine is coupled to this with a gearbox down to 6,100rpm at a frequency of 50Hz. It is essential at this stage to analyze each component of the engines individually as follows.

Intake

Function

The primary purpose of the inlet is to bring the air required at the engine of the compressor with minimum total pressure loss. The inlet interchanges the organized kinetic and thermal energies of the gas in an essentially adiabatic process. The inlet design is a very challenging aerodynamic task for designers as its property is to attract the air by providing a minimum loss in pressure.

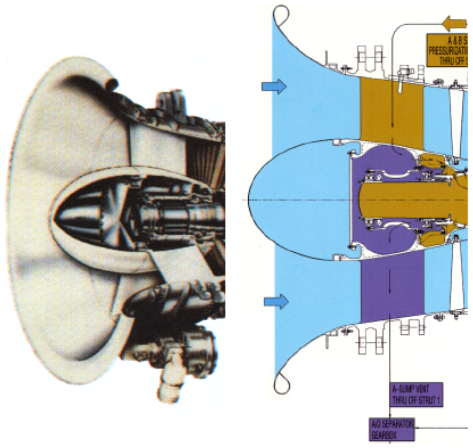

(a) Inlet (b) Inlet cutaway

Figure 2.4: Inlet

This temporarily satisfies the airflow which always follows the easiest in terms of pressure drop path (i.e. from high pressure to lower pressure) to be later compressed and satisfy the thermodynamic cycle with a series of instant processes. Ambient air is cleared by the air filtration system and then guided to each engine at the enclosure. It is then fed to the intake of the engine where the thermodynamic process begins.

Operation

The inlet guide vane (IGV) design was important because it has to deliver the required swirl distribution to the zero stage blade at the design condition and it has to be able to operate adequately at part speed when the airfoil is closed by as much as 60deg [7].

Thermodynamic Analysis

The numbering system used for this simple analysis can be seen here.

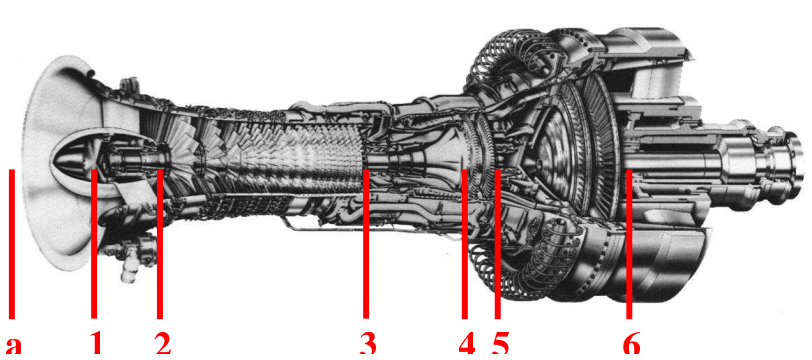

Figure 2.5: Engine's Numbering system

Following the path of the air from far upstream the air is brought to the intake. In the thermodynamic cycle calculations the stagnation conditions are the ones required (T_{0x}, P_{0x}). The total stagnation temperature at intake T_{01} can be calculated by:

- Obtaining the ambient static temperature T_a from the following equation:

$$M_a = \frac{V_a}{\sqrt{\gamma_a R_a T_a}} \tag{2.1}$$

- Assuming that T_a is equal to the static temperature at intake T_1 and
- Applying the relation between static and stagnation temperatures T_1, T_{01}:

$$\frac{T_{01}}{T_1} = 1 + \frac{\gamma - 1}{2} M_a^2 \tag{2.2}$$

The air velocity is decreased as the air is carried to the compressor inlet through the inlet diffuser and ducting system. The steady flow energy equation (SFEE) is modified by the following assumptions:

$SFEE$:

$$q - w_s = c_{pa}(T_{02} - T_{01}) \tag{2.3}$$

- The process is adiabatic: $q = 0$
- No work done by the diffuser on the fluid: $w_s = 0$
- So equation SFEE is reduced to $T_{02} = T_{01}$

That shows that the stagnation temperature at the diffuser inlet T_{01} and that of the compressor inlet T_{02} are equal. Therefore, the stagnation pressure at compressor inlet P_{02} can be calculated by the temperature pressure isentropic relation.

$$\frac{T_{02}^{'}}{T_1} = \left(\frac{P_{02}}{P_1}\right)^{\frac{\gamma_a - 1}{\gamma_a}} \tag{2.4}$$

where $T_{02}^{'}$ is the isentropic temperature at compressor inlet. State is $02^{'}$is defined as the state that would be reached by isentropic compression to the actual outlet stagnation pressure. Since the system has losses $T_{02}^{'}$ is reduced to the stagnation temperature at the compressor inlet T_{02}. For the inlet diffuser, an isentropic efficiency η_d may be defined as the ratio of the ideal to the actual enthalpy change during process or

$$\eta_d = \frac{h_{02}^{'} - h_1}{h_{02} - h_1} \approx \frac{T_{02}^{'} - T_1}{T_{02} - T_1} \tag{2.5}$$

From this equation $T_{02}^{'}$ is obtained in order to use it in previous equation to find P_{02}.

Compressor

Function

The function of the compressor is to convert mechanical work into enthalpy as near isentropically as possible or in other words to increase the pressure of the incoming air so that the combustion process and power extraction process after the combustion can be carried out more efficiently [8]. By increasing the pressure of the air, the volume of the air is reduced, which means that the combustion of the fuel/air mixture will occur in a smaller volume. The compressor of this engine is a 17 stage highly sophisticated design as seen from the figure below.

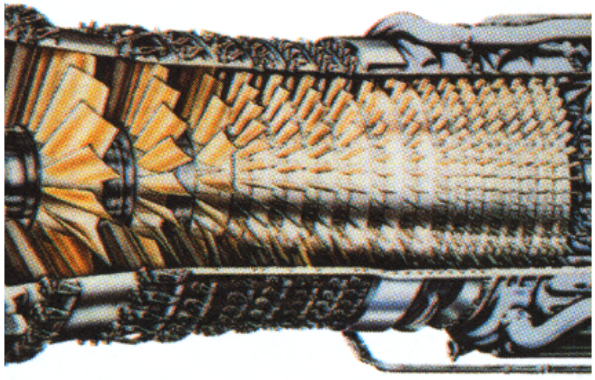

(a) Compressor drawing

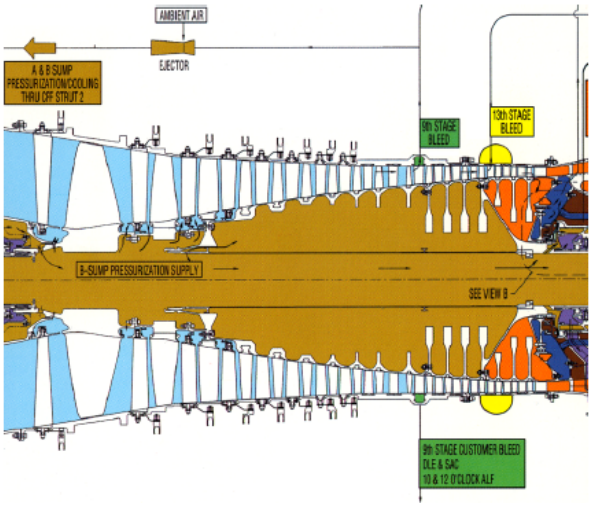

(b) Compressor cutaway

Figure 2.6: LM2500+ compressor

Operational

The aero performance has been obtained by measuring the inlet total pressure and temperature by rakes mounted between strats in the forward frame. The discharge total pressures and temperatures are measured by rakes mounted behind the OGV in the discharge diffuser [7].

The compressor has two interstage bleeds flows for cooling purposes and these are:

1. Stage 9 bleed air for cooling the low pressure turbine and uses up to 1.5% of the air mass flow rate

2. Stage 13 bleed air for anti-icing, cooling the high pressure turbine and uses up to 3.3% of the air mass flow rate

To ensure stall-free operation at part speed, the inlet guide vanes and the first six stators are variable in the LM2500+. The LM2500+ uses two torque shaft assemblies located 180deg apart to actuate the compressor variable stator vanes. This configuration has the capability to schedule each stage with stator angle schedule that are nonlinear to each other.

The compressor operating line was set with minimum of 12% stall margin [7]. Stall margin is defined at constant corrected flow and is:

$$\left|\frac{P_{stall} - P_{o.l}}{P_{o.l}}\right|_{constant flow} \tag{2.6}$$

A 4-deg open stator stall margin requirement was conservatively set for the LM2500+ to account for variable stator vanes (VSV) control/rigging variation and deterioration in the field [7]. The schedule was checked for satisfactory aeromechanical behavior of all blade and vane rows at all combinations of flows and corrected speeds over a wide range of stator angles far exceeding the control tolerance band, and over the full range of customer bleed capabilities.

Thermodynamic Analysis

The air is compressed in the dynamic compressor so the pressure and temperature both increase. Since the pressure increases at the compressor the SFEE is again modified by the following assumptions:

$$SFEE: \; q - w_s = c_{pa}(T_{03} - T_{02}) \tag{2.7}$$

- The process is adiabatic: $q = 0$
- So equation SFEE is reduced to $-w_s = c_{pa}(T_{03} - T_{02})$ or $w_c = c_{pa}(T_{03} - T_{02})$

where w_s is the specific work done on the gas by the compressor and w_c is the specific work done by the compressor on the gas. The total power output from the compressor is:

$$W_c = m_a c_{pa}(T_{03} - T_{02}) \tag{2.8}$$

.

The isentropic temperature at the compressor outlet T'_{03} can be calculated by the isentropic temperature-pressure relation:

$$\frac{T'_{03}}{T_{02}} = \left(\frac{P_{03}}{P_{02}}\right)^{\frac{\gamma_a - 1}{\gamma_a}} \tag{2.9}$$

Again losses must be taken into consideration. a useful definition of an isentropic efficiency of the compressor η_c is the ratio of the work required in an isentropic process to that required in the actual process, for the same stagnation pressure ratio and inlet state:

$$\eta_c = \frac{h'_{03} - h_{02}}{h_{03} - h_{02}} \approx \frac{T'_{03} - T_{02}}{T_{03} - T_{02}} \tag{2.10}$$

Also the compressor pressure ratio is defined as the ratio of stagnation pressure of compressor outlet to the stagnation pressure of the compressor inlet:

$$R_c = \frac{P_{03}}{P_{02}} \tag{2.11}$$

combining the above two equations it is found

$$T'_{03} = T_{02}\,(R_c)^{\frac{\gamma_a - 1}{\gamma_a}} \tag{2.12}$$

and for the isentropic efficiency of the compressor and the compressor pressure ratio this is

$$\eta_c = \frac{T_{02}\left(R_c^{\frac{\gamma_a - 1}{\gamma_a}} - 1\right)}{T_{03} - T_{02}} \tag{2.13}$$

Combustor

Function

The combustor is designed to burn a mixture of fuel and air and to deliver the resulting gases to the turbine at a uniform temperature. The thermal energy of the fuel/air mixture flowing through an air breathing engine is increased by the combustion process [9, 10]. Both gas turbine engines GT6 and GT7 have a single annular combustor (SAC) which can be seen from the figure below. The annular combustor results in a smoother operating line compared with the dry low emissions (DLE) combustor where the additional air required for the combustion's processes is subtracted from the compressor and several steps characterize its operating line.

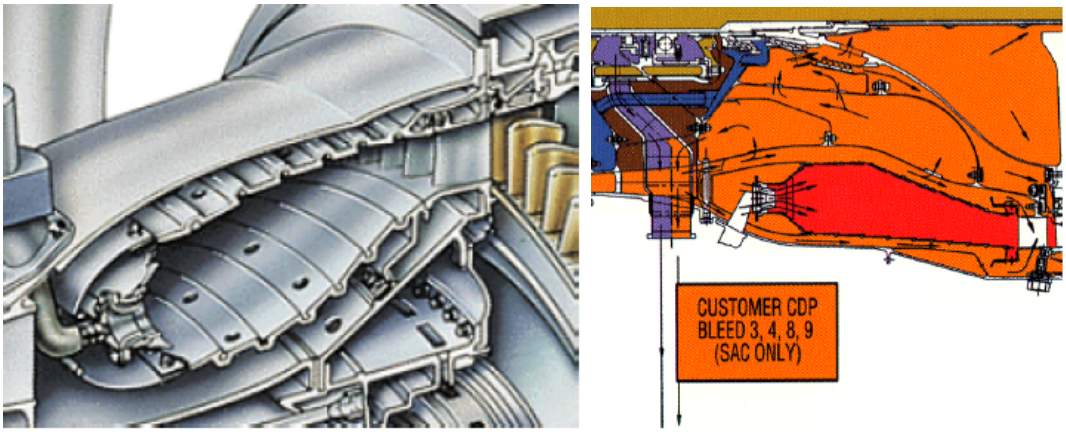

(a) SAC drawing (b) SAC cutaway

Figure 2.7: LM2500+ Combustor

The GT6 engine and the GT7 are equipped with the G84 SAC combustor which has dense vertical microcrack (DVM) for better Life cycle fatigue and reduction of thermal gradient between liner and dome among a variety of advantages.

Thermodynamic Analysis

The fuel is mixed with air which supplies the oxygen for the combustion process. The efficiency of the burner is usually almost 100%. The equation governing the energy balance across the burner is:

$$\dot{F} \cdot LHV = m_a \cdot c_{pp} \cdot (T_{04} - T_{03}) \tag{2.14}$$

where $\dot{F}$ is the fuel mass flow rate.
the pressure drop across the burner ΔP_b which is taken into account is defined as :

$$\Delta P_b = \frac{P_{04} - P_{03}}{P_{04}} \tag{2.15}$$

The total power released by the combustor is:

$$W_b = (m_a) \cdot c_{pp}(T_{04} - T_{03}) \tag{2.16}$$

Turbine

Function

The function of a turbine is exactly the opposite of that of a compressor. The objective in a turbine is to convert enthalpy into mechanical work as isentropically as possible. The turbine extracts kinetic energy from the expanding gases which flow from the combustion chamber [8]. The kinetic energy is converted to shaft horsepower to drive the compressor and the accessories.

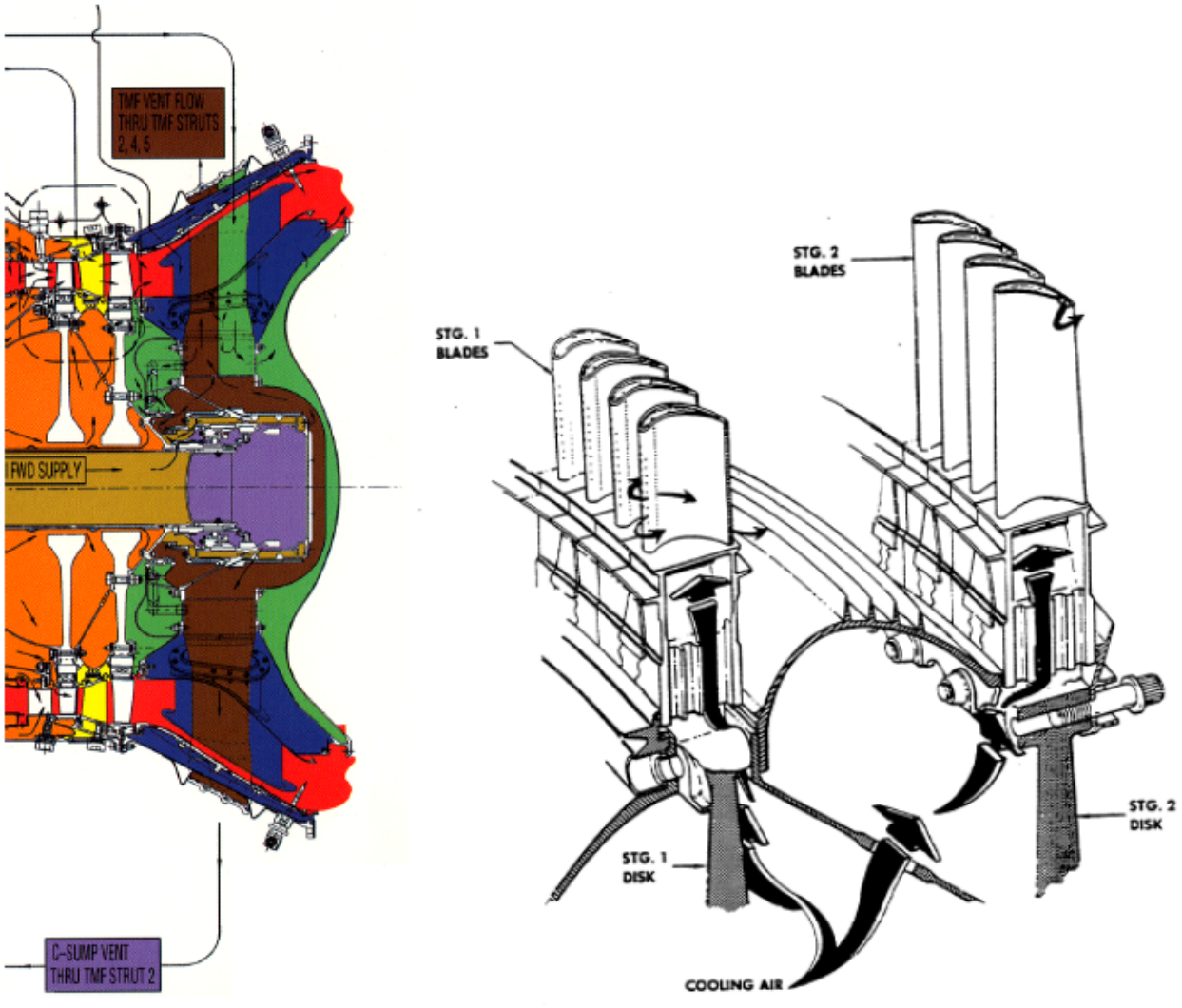

(a) Cutaway

(b) HPTurbine

Figure 2.8: High Pressure Turbine

The specific engine has a two stage high pressure turbine (HPT) with nozzle guide

vanes (NGV). Whereas compressor efficiency represents the advances in aerodynamic design the turbine's efficiency illustrates the advances in used material.

Thermodynamic Analysis

Since the pressure decreases at the turbine the SFEE is again modified by the following assumption:

$$SFEE: \; q - w_s = c_{pp}(T_{05} - T_{04}) \tag{2.17}$$

- The process is adiabatic: $q = 0$
- So equation SFEE is reduced to $-w_s = c_{pp}(T_{05} - T_{04})$ or $w_t = c_{pp}(T_{05} - T_{04})$

where w_s is the specific work done on the gas by the turbine and w_t is the specific work done by the turbine on the gas. The total power output from the turbine is:

$$W_t = (m_a + m_f)c_{pp}(T_{05} - T_{04}) \tag{2.18}$$

The isentropic temperature at the compressor outlet $T_{05}^{'}$ can be calculated by the isentropic temperature-pressure relation:

$$\frac{T_{05}^{'}}{T_{04}} = \left(\frac{P_{05}}{P_{04}}\right)^{\frac{\gamma_p - 1}{\gamma_p}} \tag{2.19}$$

Losses must be taken into consideration. The isentropic efficiency of the turbine, which is the ratio of actual turbine work to that which would be obtained during an isentropic expansion to the same exhaust stagnation pressure is defined as:

$$\eta_t = \frac{h_{04} - h_{05}}{h_{04} - h_{05}^{'}} \approx \frac{T_{04} - T_{05}}{T_{04} - T_{05}^{'}} \tag{2.20}$$

Also the turbine pressure ratio is defined as the ratio of stagnation pressure of turbine inlet to the stagnation pressure of the turbine outlet:

$$R_t = \frac{P_{04}}{P_{05}} \tag{2.21}$$

combining the above two equations it is found

$$T_{05}^{'} = T_{04}\,(R_t)^{\frac{\gamma_p - 1}{\gamma_p}} \tag{2.22}$$

and for the isentropic efficiency of the turbine and the turbine pressure ratio this is

$$\eta_t = \frac{T_{04} - T_{05}}{T_{04}\left(1 - \left(\frac{1}{R_t}\right)^{\frac{\gamma_p - 1}{\gamma_p}}\right)} \tag{2.23}$$

Power Turbine

Function

The combined cycle power plant of MEA uses a freepower turbine of Nuovo Pignone coupled to each of the gas turbines. In this arrangement the high pressure turbine drives the compressor and the combination acts as a gas generator for the low pressure power turbine. Several successful jet engines have been converted to shaft power use by substituting a free power turbine for the propelling nozzle. The gas generator is matched to the power turbine by the fact that the mass flow leaving the gas generator must equal that at entry to the power turbine, coupled with the fact that the pressure ratio available to the power turbine is fixed by the compressor and the gas generator turbine pressure ratio.

(a) Gas generator and Power turbine (b) Power turbine

Figure 2.9: High Speed Power Turbine

Each gas generator is coupled to a two stage HSPT which rotates at 6100rpm and produces 30MW of power.

Thermodynamic Analysis

Since the pressure decreases at the turbine the SFEE is again modified by the following assumption:

$$SFEE: \; q - w_s = c_{pp}(T_{06} - T_{05}) \tag{2.24}$$

- The process is adiabatic: $q = 0$
- So equation SFEE is reduced to $-w_s = c_{pp}(T_{06} - T_{05})$ or $w_{PT} = c_{pp}(T_{06} - T_{05})$

where w_s is the specific work done on the gas by the power turbine and w_t is the specific work done by the turbine on the gas. The total power output from the compressor is:

$$W_{PT} = (m_a + m_f)c_{pp}(T_{06} - T_{05}) \tag{2.25}$$

The isentropic temperature at the compressor outlet $T_{06}^{'}$ can be calculated by the isentropic temperature-pressure relation:

$$\frac{T_{06}^{'}}{T_{05}} = \left(\frac{P_{06}}{P_{05}}\right)^{\frac{\gamma_p - 1}{\gamma_p}} \tag{2.26}$$

Losses must be taken into consideration. The isentropic efficiency of the power turbine, which is the ratio of actual turbine work to that which would be obtained during an isentropic expansion to the same exhaust stagnation pressure is defined as:

$$\eta_{PT} = \frac{h_{05} - h_{06}}{h_{05} - h_{06}^{'}} \approx \frac{T_{05} - T_{06}}{T_{05} - T_{06}^{'}} \tag{2.27}$$

Also the power turbine pressure ratio is defined as the ratio of stagnation pressure of power turbine inlet to the stagnation pressure of the power turbine outlet:

$$R_{PT} = \frac{P_{05}}{P_{06}} \tag{2.28}$$

combining the above two equations it is found

$$T_{06}^{'} = T_{05}\left(R_{PT}\right)^{\frac{\gamma_p - 1}{\gamma_p}} \tag{2.29}$$

and for the isentropic efficiency of the turbine and the turbine pressure ratio this is

$$\eta_{PT} = \frac{T_{05} - T_{06}}{T_{05}\left(1 - \left(\frac{1}{R_{PT}}\right)^{\frac{\gamma_p - 1}{\gamma_p}}\right)} \tag{2.30}$$

The useful work of this cycle is:

$$UW = (m_a + m_f) c_{pp} (T_{05} - T_{06}) \tag{2.31}$$

The thermal efficiency of this thermodynamic cycle is:

$$\eta_{th} = \frac{UW}{HI} \times 100\% \tag{2.32}$$

2.4 Plant's Simulation

The gas turbine performance affects operational and maintenance costs which play a significant role in the competitive energy market. Minimizing these costs and ensuring the plant always running efficiently is a key ingredient for a profitable energy plant. Under this scope various software capabilities have been developed for performance and financial analysis of a CCGT plant. Some of the most acclaimed existing programs are enlisted here:

1. EcoSim Pro is an object-oriented simulation tool designed through FEA and CFD performance component analysis.
2. Gas Turb commercial software which is built on Borland Delphi
3. GSP which is built by NLR on Borland Deplhi and makes full use of object oriented features
4. ONYX is Java based and distributed through CORBA at Toledo University
5. NPSS developed by NASA which has open and extensible architecture, interface at C++ like language, geometry computing at fortran and deploying simulation at a computing layer
6. TURBOMATCH Object Oriented program developed in Fortran
7. PYTHIA diagnostic program based on TURBOMATCH source code for diagnostics.

8. Other in house customised programs developed by gas turbine manufacturers.

Object orientation provides an efficient means to implement functionality common to the different modelling elements in a simulation environment [11]. The inheritance principle of object orientation enables the introduction of additional gas turbine component model capabilities in a single "ancestor" component model class. The basic element is the object: a reusable, self contained entity that consists of both data and methods to manipulate data. An object can be assessed (by other objects) only through its external interface. Consequently, its internal (private) data and methods are hidden (encapsulated) from the other objects. Simulation of gas turbine's thermodynamic performance is governed by the fundamental laws enlisted here.

1. Mass Conservation
2. Conservation of Momentum
3. Conservation of Energy

PYTHIA software, which has an interface built in Microsoft's Visual Basic 6.0 and uses the fortran developed turbomatch performance code for calculations, has been extensively used for performance simulations and diagnostics. PYTHIA's software programme, which has a graphical user interface is seen in figure 2.10, is a user friendly tool that has been used from postgraduate students, researchers and industrial partners.

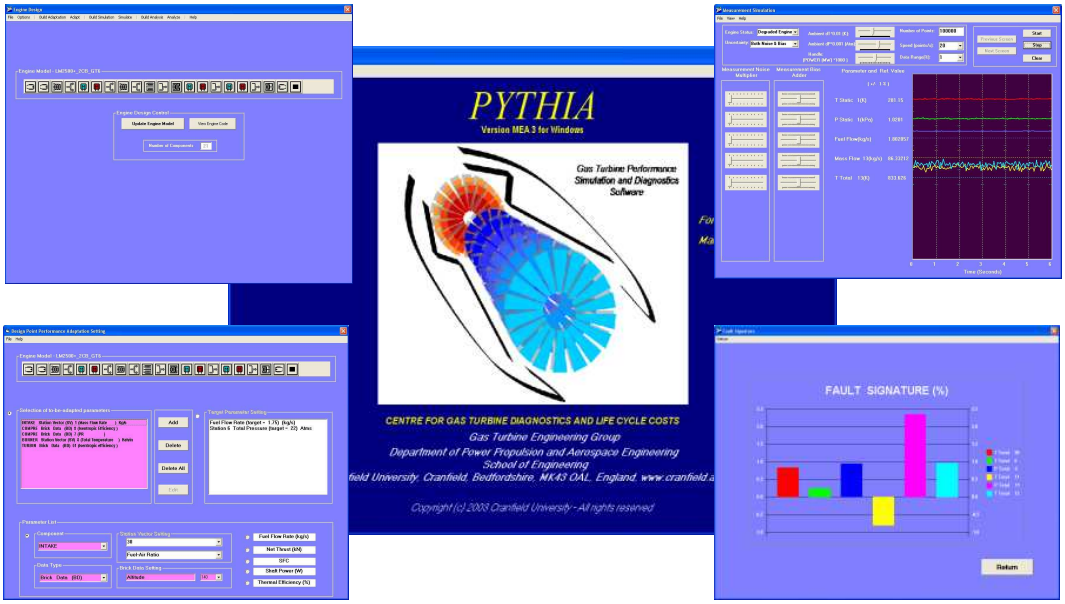

Figure 2.10: PYTHIA's software platform graphical user interface

At the start of the project the project team developed an initial model of the LM2500+ engine, based upon the published literature about the engine. The initial model was quite simple, utilising a single compressor element, no air bleeds and no variable geometry capability. The model operated only with liquid fuel and had no facility for water injection. This model could thus only produce generally representative simulated data, near to the design point of the engine when run on liquid fuel.

During this period service engine data were collated that allowed the performance models to be progressively refined. This so called refinement has been facilitated by the application of performance adaptation [6]; a method which enables the engine model to adapt its performance to the service engine data measurements. In addition to the performance adaptation itself the developed engine model includes variable geometry compressors, bleed cooling flows, multi-fuel capability and water injection through the combustion chamber. The engine performance models are regularly updated with the data of MEA for accurate performance prediction and diagnostic analysis.

The software developed by gas turbine manufacturers provide useful tools to the gas turbine users, however the expenses of such services are considerable high. Cranfield's diagnostics software PYTHIA with the use of turbomatch simulation code has the capacity to facilitate the diagnostic analysis and aid the gas turbine user towards the successful maintenance strategy of the power plant. There is still ongoing research and development that will establish PYTHIA as a robust commercial attractive software for performance simulation and real time diagnostics tool.

2.5 Plant's Maintenance

As a result of rising energy costs, users of individual gas turbines are seeking ways of reducing operating costs [12]. It is essential to develop maintenance schedules based on the characteristics of the engine and is operating environment and/or cycle in order to balance the maintenance costs with lost revenue and extra fuel costs [4, 13]. The gas turbine's hot gas path parts have a relative short lifespan of 4 to 8 years depending on overall condition. In addition these parts are used under hard conditions-high flow rates, hot gases and frequent changes that occur during startup and shutdown. Oftenly suffer degradation damage such as cracking, creeping and corrosion. Such damage is tolerated in these hot gas path parts unlike steam turbine.

Currently software systems are responsible for real time online diagnostic analy-

sis. The MEA power station condition monitoring systems enables them to have a continuous assessment of the power plant's performance and prompts the gas turbine user to take action when it is required. The MEA's maintenance division schedule includes compressor washing and replacement of inlet filters among other corrective based maintenance actions.

Compressor Washing

One method to reduce the maintenance costs by decreasing the degradation rate and improving the efficiency of the powerplant is to wash the compressor both online and off-line. In online wash, distilled water is injected into the compressor while the gas turbine is running such that water droplets impact the blades at high speeds to loosen and partially remove deposits. However complete performance recovery can be achieved by off-line wash where distilled water (sometimes mixed with a special detergent) is sprayed into the gas turbine while being isolated by the started at the crank speed [14].

As indicated by gas turbine manufacturer's point of view which also operates a power station [14], in order assess the effectiveness of online washes with distilled water only in a Frame 7 GE engine, trends on the capacity factor for both engines shown here indicate several facts.

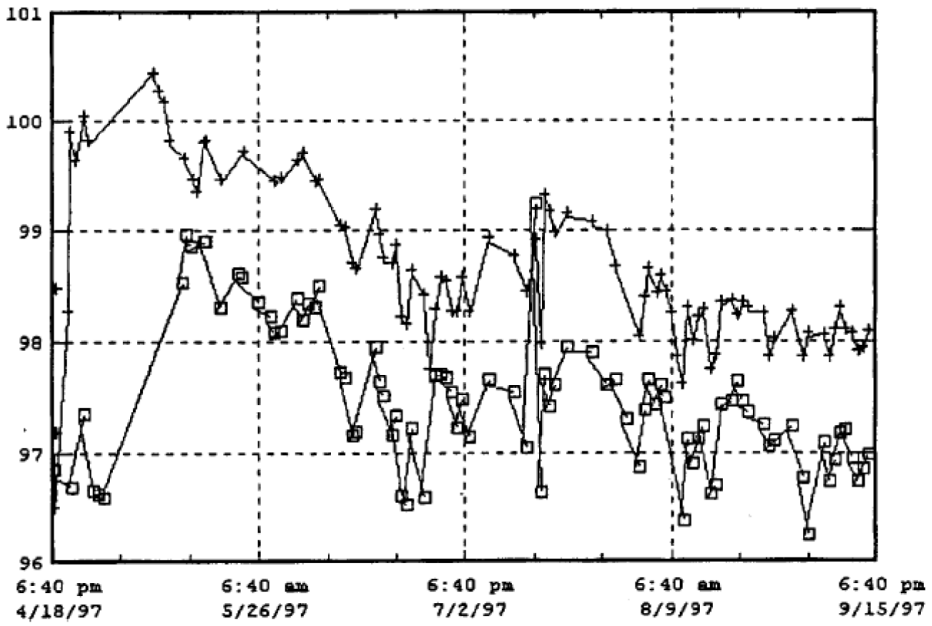

Figure 2.11: Compressor capacity factor for both engines [14]

- for both units engine degradation progresses at a rate of roughly one percent a month.
- after about 2months engine degradation stabilized at the level of two percent
- there was two discernible benefits associated with using detergent in on-line washes as opposed to using distilled water online
- there was a constant one percent difference between units A and B although both engines were identical

For a quick evaluation of the compressor degradation pressure and flow parameters have be plotted on the compressor performance map as shown in

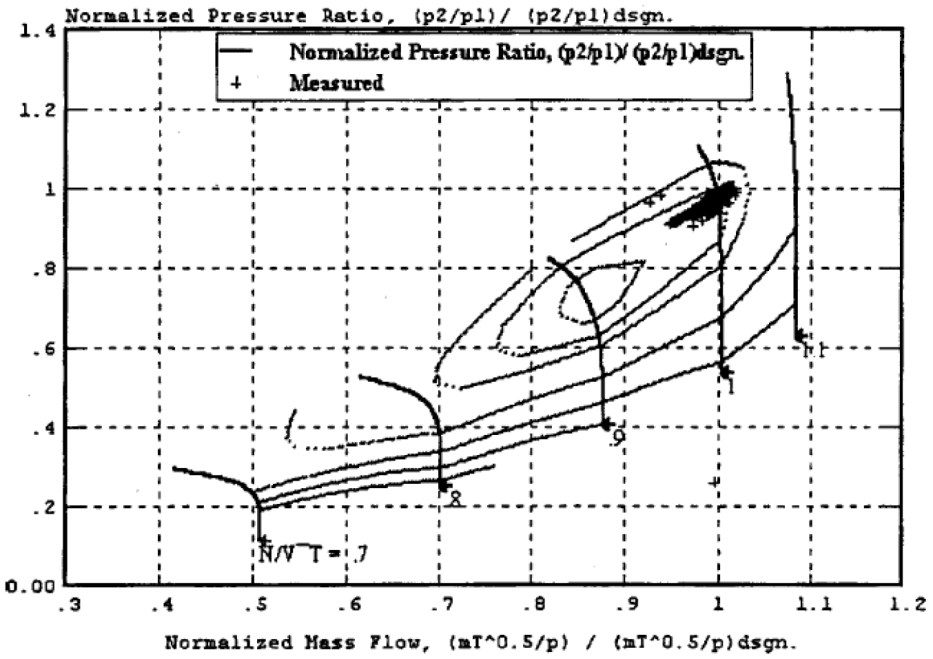

Figure 2.12: Normalized and corrected compressor performance parameters [14]

Note that the horizontal and vertical axis are normalized and corrected, compressor air mass flow rate parameter and pressure rise parameter respectively.

Inlet Filters

Each gas turbine has a single stage self-cleaning intake air filtration system with an evaporative cooler downstream. The inlet filter utilizes cylindrical filter elements that

are sequentially cleaned by reverse flow pulses of compressed air. A performance degradation of roughly 25KW per month due to inlet filter clogging has been presented by Gulen [14]. Balancing the effects of both performance changes with the cost of filter replacement, a filter replacement date of 3 years from the last replacement date has been predicted. However samples of filter units revealed that they were deteriorated to the point of performing below minimum filter specifications. This demonstrates that the pressure drop by itself is not a sufficient criterion to determine inlet filter performance degradation which prompts the gas turbine power plants to follow an economic based maintenance.

Hot End Components

An important diagnostic parameter that is calculated by the monitoring software is the ratio of the maximum exhaust thermocouple reading to the average of all exhaust temperature thermocouple known as the temperature spread. The plot of the difference between the two thermocouples i.e. the spread, shows a clear upward trend in the next figures [14].

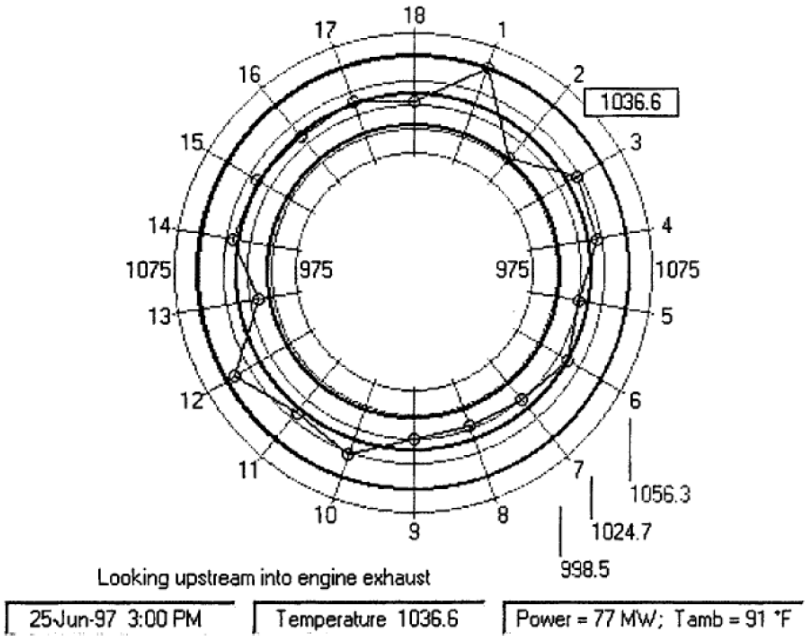

(a) Exhaust temperature profile for engine's turbine

Figure 2.13: Temperature spread of gas turbine [14]

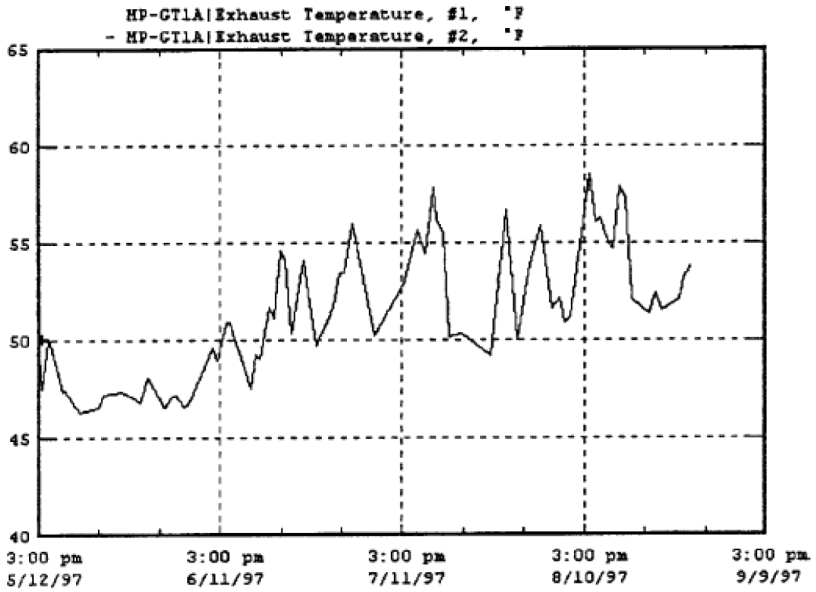

(a) Exhaust temperature spread

Figure 2.14: Exhaust temperature profile of gas turbine [14]

An important performance degradation source can be the combustor problems. Most gas turbine controllers are able to detect and discard bad thermocouple readings to generate a relative control signal. However, if the individual deviations (due to possible combustor problems) are not excessive, the resulting bias of a few degrees can still result in significant loss of output. This identifying and continuously trending exhaust thermocouple spread can pinpoint problems resulting from presently mild deviations that can lead to potentially serious engine problems or result in lost revenue.

A combustor inspection is required when this spread reaches a value of 70deg as suggested by GE [14]. An important performance degradation source can be the combustor problems. Most gas turbine controllers such as GE's Speedtronic Mark IV are able to detect and discard bad thermocouple readings to generate a relative control signal. However, if the individual deviations (due to possible combustor problems) are not excessive, the resulting bias of a few degrees can still result in significant loss of output. This identifying and continuously trending exhaust thermocouple spread can pinpoint problems resulting from presently mild deviations that can lead to potentially serious engine problems or result in lost revenue.

Condition Monitoring

The performance based Gas Path Analysis has been applied to the PYTHIA's developed engine model, for assessing the health of each gas turbine at regular time intervals and improving the plant's availability. An application of this approach for an operation period of three months along with the findings of the degraded components, measured by the GPA Index, has been produced [15, 16] . This diagnostic analysis offers a great potential to improve plant economics. The condition monitoring process has been enhanced by reviewing the instrumentation systems, use redundant set of measurements located in the gas path of the gas turbine and apply the appropriate corrections for reducing repeated uncertainties like measurement noise and varying ambient conditions. Therefore the current condition monitoring system provides a clear view of the gas turbine performance. Real time trends of the fundamental performance parameters monitored are available to the gas turbine user as seen in figure 2.15.

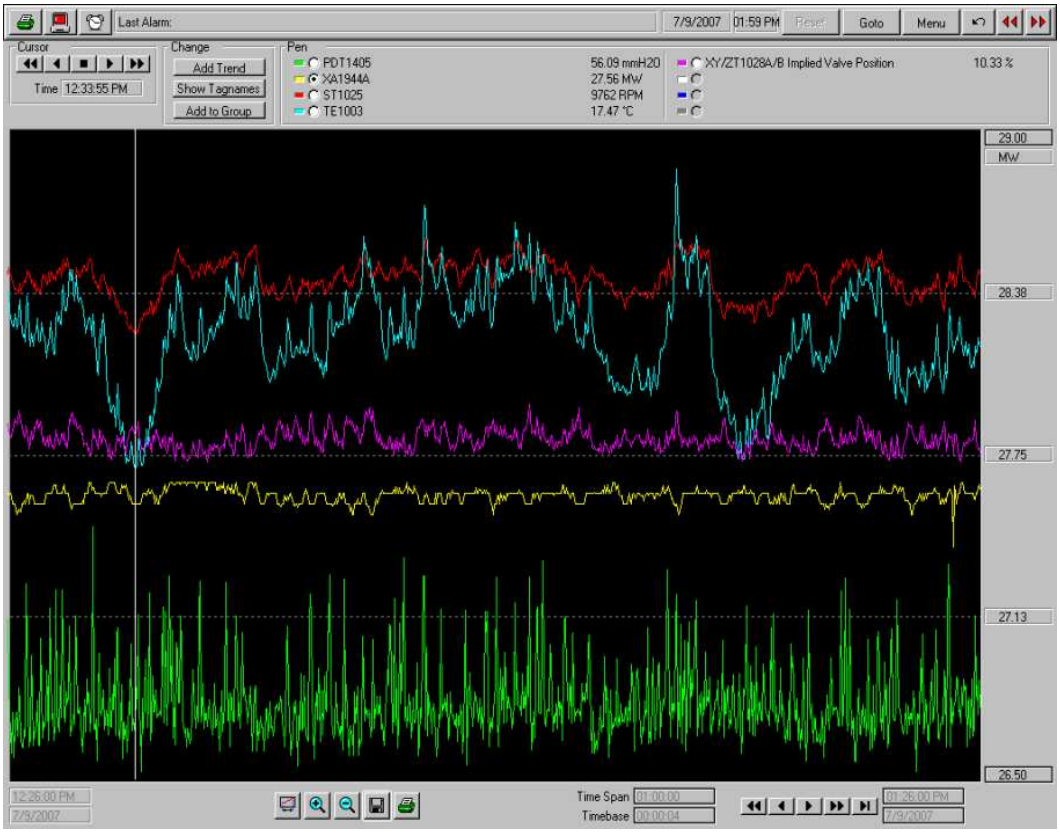

Figure 2.15: MEA's Condition Monitoring Tool

CCGT Performance Modeling

The combined cycle performance analysis, which is monitored by MEA, includes the performance simulation of the two gas turbines, two OTSG and the Steam turbine. The CCGT performance simulation program was created from the integration of existing and new individual performance simulation codes of the main components of a CCGT power station using the Visual Basic for Applications (VBA) in Excel [2]. In the case of the steam cycle, an initial model for a double pressure OTSG was produced by Mucino [2]. A novel approach using theoretical thermohydraulic models for heat exchangers and empiric correlations delivered positive results. Steamomatch, another code developed at the university, was used for the combined cycle performance simulation [2]. Extensive research is still being carried out for further improving the CCGT performance simulation program by developing a series of novel simulation techniques. This enables the project team to acknowledge the complexity involved with optimising the operation of the CCGT by taking into consideration the limitations that each component implies through this configuration.

2.6 Plant's Trading Model

Since the electricity market liberalization in UK, powerplant companies want to be energy efficient and profitable. In such a complex and competitive energy market it is fundamental to ensure that production of electricity is profitable most of the plant's operation time. An important measure which utilizes companies determine their bottom line (profit) is the spark spread. The spark spread is the theoretical net income of a gas-fired power plant from selling a unit of electricity, having bought the fuel required to produce this unit of electricity. All other costs (operation and maintenance, capital and other financial costs) must be covered from the spark spread. If the spark spread is small on a particular day, electricity production might be delayed until a more profitable spread arises.

Specifically the amount of fuel required to generate a unit of electricity is linked to the plant's thermal efficiency. The heat rate, the inverse quantity of the thermal efficiency, hence is defined as the ratio between the heat input and the power output. The financial industry defines the spark spread [17] using the operating heat rate (HR) of the plant in MMBtu/MWh, the electricity price in £/MWh (Pe) and gas price in

£/MMBtu (Pg) in basic expression as follows:

$$\pi = max(P_e - HR \cdot P_g, 0) \tag{2.33}$$

Practitioners in the power industry replace the heat rate with the thermal efficiency η_{th} which is a more accessible parameter calculated during the operation of the plant. In addition, two more coefficients representing different operating marginal costs are introduced [18]. C_e represents the costs incurred by the company in maintenance, T&D and electricity trading to and from the network. On the other hand, C_g, correspond to the cost related to the transport and trade of gas

$$\pi = max\left([P_e - C_e] - \left[\frac{P_g + C_g}{\eta_{th}}\right], 0\right) \tag{2.34}$$

For the MEA, a negative spark spread would send an economic signal to import power along the interconnector (and back-off or resell gas) while a positive spread would indicate that it would be profitable to generate from the CCGT and export the surplus to the UK through the interconnector. The following is a list of these costs, followed by the actual expression used:

1. Actual electricity (export) price in £/MWh (E)
2. Cable losses and charges in £/MWh (C)
3. Actual gas price in p/th (G)
4. Transco's incremental variable costs between NBP and Moffat in p/th (S)
5. Gas Interconnector (IC2) commodity charge in p/th (I)
6. CCGT variable maintenance costs in £/MWh (M)
7. Thermal efficiency (T)
8. Gas price "swing" premium in p/th (P)

$$\pi = max\left([E - C - M] - \left[\frac{(G + S + I + P) \cdot 0.3412}{\eta_{th}}\right], 0\right) \tag{2.35}$$

Computational method

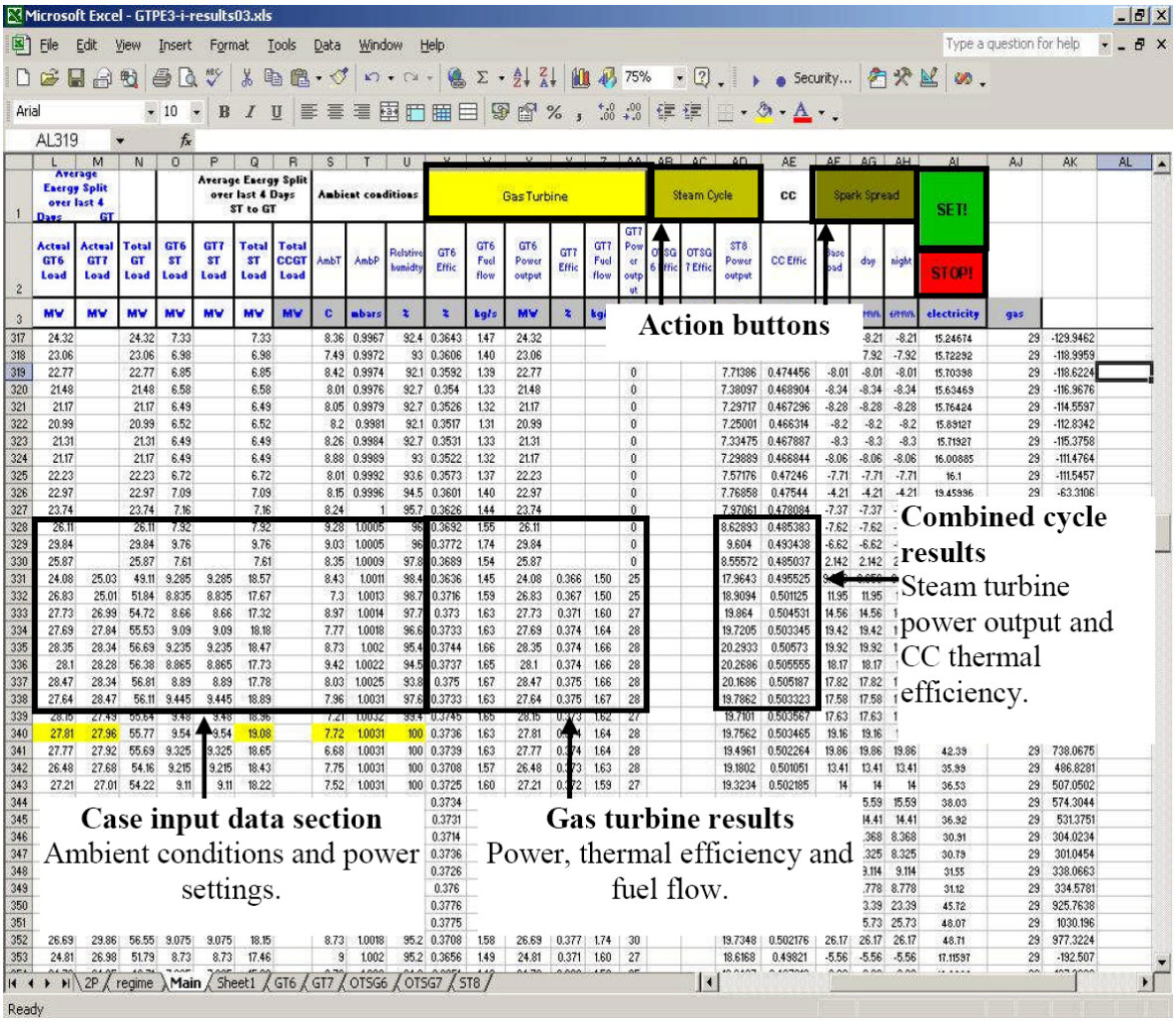

Figure 2.16: eCCGT Trading Model program

The performance of the CCGT in terms of finance has been assessed and a software program called eCCGT, shown in figure 2.16, that monitors the trading capability and performance has been developed by Marco Mucino [19] and integrated to the MEA environment for the economic analysis of the CCGT. This module delivers good interconnectivity with other modules, flexibility and graphical interface. The module has been developed in Excel VBa environment.

A study that has been carried out quantified the loss making operation strategy of the plant during the off peak market period of a day. But it also demonstrated the profit made during the peak hours lead to an overall positive cash flow for the day. The sensitivity analysis showed the positive effect of increase the GT7 load factor (overall plant thermal efficiency) is partially or completely offset by an increase in S,I,C and M.

Whereas, the GT7 load factor has a secondary order of magnitude when the electricity or gas prices are modified [19].

A number of operations optimisation strategies, which are based on the technical performance simulation of the plant under these specific conditions, have been proposed in order to increase the profitability of the plant. The developed techno-economic software eCCGT is positively affecting the way an operator manages a power generation asset through the implementation of virtually proven optimisation and risk management strategies.

2.7 Industry-University Collaboration

Detailed understanding and monitoring of power plant performance, prime mover health condition and associated costs have a deep impact in the decision making process concerning the plant's operational and maintenance strategy. In this context, research collaboration between Manx Electricity Authority (MEA) and Cranfield University has been carried out since 2001 and a series of technologies and software have been and are still being developed at Cranfield University and some of them have been integrated into MEA Combined Cycle Gas Turbine Power Plant in Pulrose, Isle of Man. During this constructive and successful collaboration period, the University has been fortunate to acknowledge the industrial needs and make significant academic contributions through ongoing research projects jointly supported by both MEA and EPSRC. On the other hand, MEA has valued the complexity of asset management concerning the gas turbine and the combined cycle, therefore enhancing its trading and operational capabilities through the application of developed performance, diagnostic, trading and economic analysis software.

The Manx Electricity Authority (MEA) is an Island based electricity generation utility. The company undertook a massive expansion in its operations during the period between 1999 and 2004 in response to the Isle of Man Department of Trade and Industry's strategic objectives for the island economy at that time. As part of this technology upgrade programme the MEA took the decision to invest in a high technology state of the art Combined Cycle Gas Turbine (CCGT) power station in Pulrose, Isle of Man and trade the excess output from this power station in the UK wholesale electricity and gas markets. The design of the plant started in 2001 just after the Interconnector cable began its operations. Since then and as part of this process the MEA

has closely collaborated with the department of Power and Propulsion of Cranfield University, which has established an international reputation for its advanced postgraduate education, extensive research activity and applied continuing professional development. A series of software programmes, which have been developed in the university, for performance simulation of gas turbines, heat exchangers and steam turbines have been integrated to MEA power station. Diagnostics tools based on the Gas Path Analysis (GPA) method have also been used for the gas turbines. These along with the economic and trading analysis software tools have enriched MEA's understanding and knowledge for successful asset management of their power plant with significant benefits for both parties.

The objectives of this collaboration have been classified in two categories: technical contribution and personnel training. The technical contribution has been achieved through the development of new technology and new analytical tools through ongoing academic research activities at Cranfield University [20]. The personnel training have been established through part-time MSc programme attended by the personnel of MEA and PhD programme attended by PhD researchers at Cranfield . Invited lectures at Cranfield provided by MEA senior managers also enhance educational programme at Cranfield University. The aim of this process was to enhance MEA's technical understanding and facilitate its decision making capability concerning the CCGT's performance, maintenance and operations through the appropriate software tools. Some of the technical development has already been implemented in MEA and more capabilities are being developed at Cranfield University and will be transferred to MEA to meet further industrial needs.

The project team considered fundamental for this collaboration to deliver the appropriate academic training to the MEA personnel through a number of seminars held in the authority's headquarters and career development short courses attended by a number of MEA's technical personnel. This has been essential for enhancing MEA's knowledge and understanding for the complexity involved in operational and maintenance as part of asset management skills. On the other hand the academic team, during this period, has organised the platform for successful research activities by assigning research projects directly related to MEA to doctoral researchers and postgraduate students as part of their research degrees and taught postgraduate courses offered by the University.

The joint research activities between Cranfield University and MEA have resulted in academic contributions and publications in research communities. Four conference

papers on gas turbine performance adaptation [21], gas turbine performance diagnostics [22, 15, 16, 23] and gas turbine combined cycle performance [24] have been published where one of them [21] was recommended by the conference for publication in Journal of Engineering for Gas Turbines and Power. The academic contributions from the joint research have been well recognized both nationally and internationally

The accomplishment of the objectives of this collaboration from the current research include the development of a gas turbine software platform with fully adapted engine models and with capability of the off design performance adaptation. The off design performance adaptation enables the engine model to adapt its performance to the service engines actual performance at part load conditions. The condition monitoring system will be updated with real time on line performance and diagnostic analysis tools provided by PYTHIA's latest version. New computer software to simulate the performance of steam cycle at different operating conditions and is adapted to real cycle performance is under development. These software tools along with the CCGT performance simulation system can be used in conjunction with the control systems monitoring process at MEA for successfully managing the operations and maintenance of MEA's CCGT power plant.

The collaboration between Manx Electricity Authority and Cranfield University has being constructive and successful in all the associated levels. Intense research activities in different technical and economic areas relevant to the operation and maintenance of MEA CCGT power plant and technical training have been accomplished and are still being carried out. Improvement in the analysis capability and understanding in gas turbine performance, condition monitoring diagnostics, steam cycle performance and economic trading are fundamental aspects of the collaboration's objectives. The deep impact that quality measurement data provided by MEA have towards the validation of the research techniques developed through the academic research has been recognized and the effort made by MEA to improve the measurement quality is greatly appreciated. MEA's personnel are able to use the developed analytical software to make an informed judgement based on the information from both power plant measurement systems and the analytical results from the software. The result is that assets are better managed; the plant availability increases and maintenance and life cycle costs are significantly reduced.

Chapter 3

Design Point Performance Adaptation

3.1 Introduction

Accurate simulation and understanding of gas turbine performance is fundamental for gas turbine users. A performance simulation should always start from the design point of the engine that is modeled. When some of the engine component parameters for an existing engine are not available, they must be estimated in order that the performance analysis can be carried out. However, the initially simulated design point performance of the engine using estimated engine component parameters may give a result that is different from the actual measured performance. This difference may be reduced with better estimation of these unknown component parameters. However, this can become a difficult task for performance engineers, let alone those without enough engine performance knowledge and experience, when the number of design point component parameters and the number of measurable/target performance parameters become large [25, 23, 26]. The gas turbine design point performance adaptation approach that has been developed by Li [27] is used for adapting the engine model of the GE LM2500+ gas turbine. In the approach, the initially unknown component parameters may be compressor pressure ratios and efficiencies, turbine entry temperature, turbine efficiencies, air mass flow rate, cooling flows, by-pass ratio, etc. The engine target (measurable) performance parameters are shaft power and thermal efficiency for industrial engines, gas path pressures and temperatures, etc.

The adaptation procedure suggests values of performance parameters (efficiencies, mass flows, TET) that would satisfy the target measurements (temperatures and pressures at various locations). The success of this analysis depends on the thermodynamic

relationships between the performance parameters and the measurements.

3.2 Methodology

Design point performance adaptation is an inverse mathematical problem. The information of the dependent parameters in a system is used to estimate the quantity of the independent variables of the model as described by Li [27]. The matrix inverse mathematical model used in the GPA approach used by Escher and Singh [28]in their diagnostics method is an effective solver to model-based inverse problems and can be applied to engine design point performance adaptation. The thermodynamic relationship between gas turbine to-be-adapted component parameters and target performance parameters of a gas turbine can be expressed with the following equation

$$\vec{z} = h(\vec{x}) \tag{3.1}$$

where $\vec{z} \in \Re^M$ is the target performance parameter vector and M is the number of target performance parameters, and $\vec{x} \in \Re^N$ is the to-be- adapted component parameter vector and N is the number of to-be-adapted component parameters and $h(\,)$ is a vector valued function.

At an initially given design point which is denoted with subscript "0" equation x can be expanded in a Taylor series as:

$$\vec{z} = z_0 + \frac{\partial h(\vec{x}, \vec{y})}{\partial x} \cdot (\vec{x} - \vec{x_0}) + HOT \tag{3.2}$$

HOT represent higher order terms which can be neglected. This assumption linearises the relationship between the deviation of the design point to-be-adapted component parameters and the deviation of their corresponding design point target performance parameters of a gas turbine and can be expressed as:

$$\Delta\vec{z} = H \cdot \Delta\vec{x} \tag{3.3}$$

For any expected deviation of $\Delta\vec{z}$ from its initial point, the deviation of to-be-adapted component parameters from its initial point can be predicted by inverting the influence coefficient matrix (ICM) H to a adaptation coefficient matrix (ACM) H^{-1} leading to equation xx when $N = M$

$$\Delta\vec{x} = H^{-1} \cdot \Delta\vec{z} \tag{3.4}$$

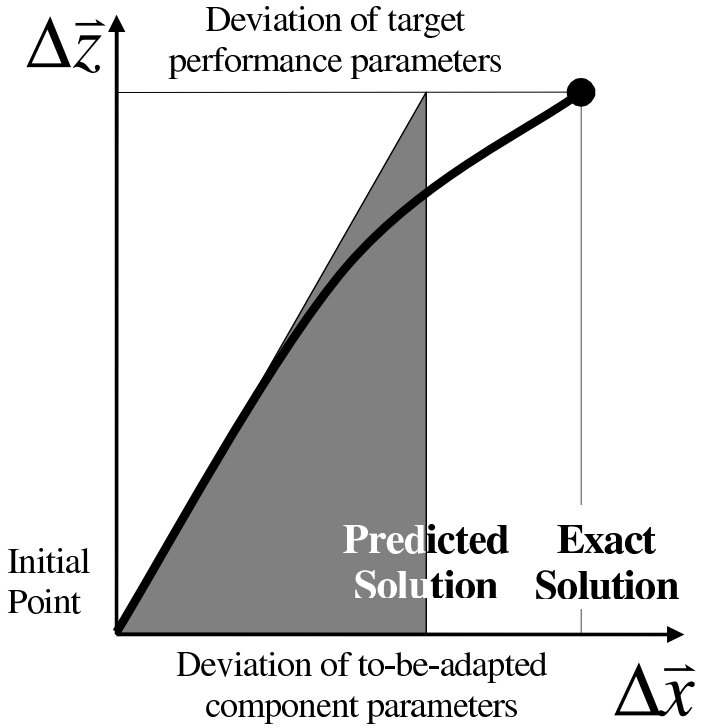

Figure 3.1: Linear |performance adaptation

The idea of linear adaptation is shown here where the linear prediction of $\Delta\vec{x}$ will be a good estimate of the engine to-be-adapted component parameters from their initial values when the shift is small and the thermodynamic behavior of the engine around the initial design point is linear.

It is very likely that when the nonlinearity of the relationship between the to-be-adapted component parameters and the target performance parameters is significant, the predicted deviation of to-be-adapted components will not the same accuracy. The nonlinearity of of the thermodynamic behavior is taken into account by using the Newton-Raphson iterative method, Escher and Singh [28],where linear prediction process is applied iteratively until a converged solution is obtained as seen here.

In many cases, the number of to-be-adapted component parameters N and the number of target performance parameters N may not be equal. If $N > M$ equation x is under-determined and this leads to an infinite number of least-squares solutions. A pseudoinverse matrix is defined as:

$$H^{\#} = H^T \cdot (HH^T)^{-1} \tag{3.5}$$

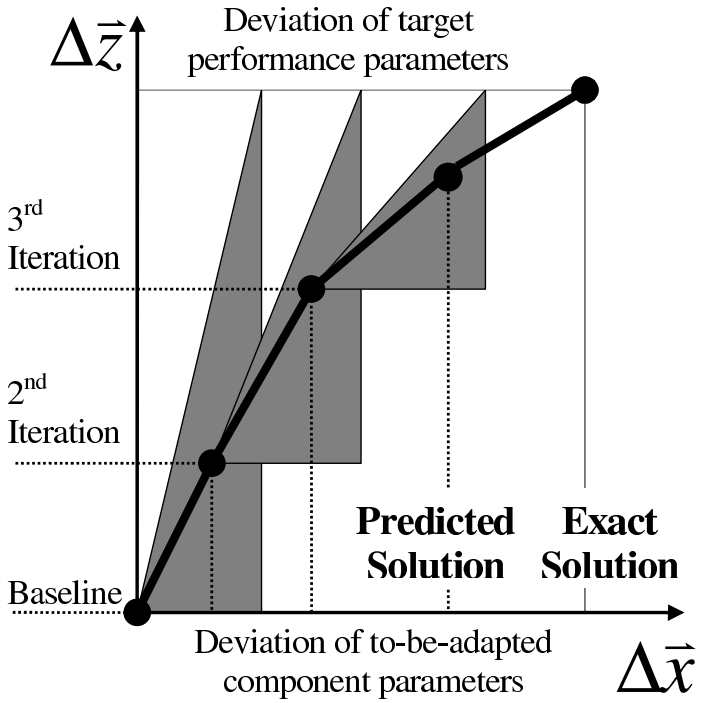

Figure 3.2: Non-Linear performance adaptation

The solution resulting from this, which is the best in a least square sense, is:

$$\vec{x} = H^{\#} \cdot \vec{z} \tag{3.6}$$

If $N < M$ equation x is over-determined and there are redundant equations. A pseudoinverse matrix is defined as:

$$H^{\#} = (H^T H)^{-1} \cdot H^{-T} \tag{3.7}$$

The resulting resulting, which is also the best in a least square sense, is:

$$\vec{x} = H^{\#} \cdot \vec{z} \tag{3.8}$$

The convergence of this iterative adaptation calculation process is declared when the performance is very close to the real target performance. The root mean square (RMS) of the difference between predicted and target performance is smaller than

$\sigma$when convergence criterion is satisfied.

$$RMS = \sqrt{\frac{\sum(z_{i,predicted} - z_{i,measured})^2}{M}} < \sigma \tag{3.9}$$

where σ is a very small number (σ=0.001 is usually chosen). The adaptation error ε_i for the i_{th} performance parameter is:

$$\varepsilon_i = \frac{z_{i,predicted} - z_{i,measured}}{z_{i,measured}} \cdot 100\% \tag{3.10}$$

For the design point adaptation procedure to be successful the compressor map has to be scaled with the following scaling factors. The definition of the design point scaling factors is shown here

$$SF_{N,DP} = \frac{N_{DP}}{N_{DP0}} = 1 \tag{3.11}$$

$$SF_{PR,DP} = \frac{PR_{DP} - 1}{PR_{DP0} - 1} \tag{3.12}$$

$$SF_{WAC,DP} = \frac{WAC_{DP}}{WAC_{DP0}} \tag{3.13}$$

$$SF_{ETA,DP} = \frac{ETA_{DP}}{ETA_{DP0}} \tag{3.14}$$

where WAC is the corrected mass flow rate, PR is the pressure ratio, ETA is the isentropic efficiency and N is the non-dimensional shaft rotational speed. The scaling factors need to be applied to the whole default compressor characteristic map with the next four equations in order to make it representative of the behavior of the compressor of interest.

$$N = N_{DP0} \tag{3.15}$$

$$PR_{DP} = SF_{PR,DP} * (PR_{DP0} - 1) + 1 \tag{3.16}$$

$$WAC_{DP} = SF_{WAC,DP} * WAC_{DP0} \tag{3.17}$$

$$ETA_{DP} = SF_{ETA,DP} * ETA_{DP0} \tag{3.18}$$

The scaled map compared with the old default compressor map can be seen here

Every single point is scaled by the scaling factors in order to match the new set design point. This adaptation procedure provides excellent results for target measurements close to the design point of the engine but cannot deliver solutions of the same accuracy

at off-design conditions.

3.3 Application

Many test cases have been performed with the design point adaptation capabilities of PYTHIA. One of this test cases presented here involves the design point Adaptation procedure for assessing the health of the MEA LM2500+ engines during a six month period. A model of the engine that has been initially developed in PYTHIA accurately match the design point performance of the engine. The model schematic diagram can be seen from the following figure.

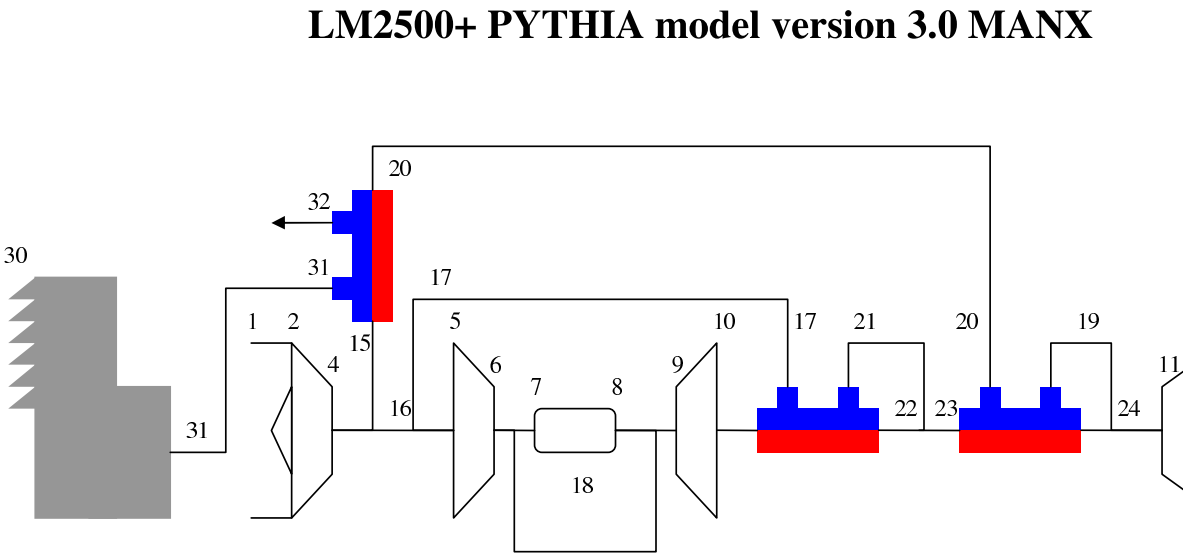

Figure 3.3: LM2500+ PYTHIA Model

The inlet air is used for cooling the 9th stage bleed from the compressor that is used for cooling the power turbine. The 13th stage is also used for power turbine cooling. The compressor discharge bleed cools the high pressure turbine. The cooling is modeled by the use of Heat exchangers. The bleed flow are considered constant and are not modeled dynamically. This PYTHIA model, which is the latest version of the MEA's configured LM2500+ engines, has simulated very accurately the design point performance of the engine which is the starting point for further analysis. This model illustrates the complexity involved for simulating the engine and will probably become even more complex as more accurate performance simulation and diagnosis are pursued.

Engine Operating History

The GT6 engine has operated for a total amount of 19678 hours, which is 25% more than the GT7. This simply indicates that the GT6 engine will theoretically have greater degradation. However this is not always true since the operating hours that a gas turbine has maintenance wise is a function of actual operating hours, number of start-ups, trips, load dumps and peak operating hours. Considering only the fact that GT7 has experienced more start-ups than the GT6 contributes significantly to the EOH which might be equal to the GT6.

Maintenance Action

The fuel nozzles at the GT6 have been replaced back in April. This action is going to affect the performance analysis as this will lead at higher combustion efficiency.

Data analysis

Two similar power setting points have been selected for this analysis. The one from 18th of January at 06:50am and the other at the 18th of June at 11:26am for GT6. A similar set of points has been selected for the GT7 as well. The data are tabulated below.

Parameter	GT6@Jan(Jun)	GT7@Jan(Jun)	Units
Power	28.1(28.1)	28.1(28.1)	*MW*
Operating hours	16645(19678)	12776(15188)	*Hrs*
Ambient Temperature	286.65(288.55)	280.65(288.45)	*K*
Ambient Pressure	0.9716(1.0048)	0.9967(1.0048)	*Bar*
Ambient Humidity	99.8(95.1)	88.9(95.1)	*%*
NGG	9751(9778)	9649.5(9775)	*rpm*
VSV Position	–(9.4233)	–(9.52)	*%*
Comp. Bleed Pres.	0.9(9.2)	9.4(0.8)	*Bar*
Comp. Bleed Temp.	420.45(423.95)	425.35(429.45)	*K*
Comp. Discharge Pres.	21.3(21.5)	22(21.8)	*Bar*
Comp. Discharge Temp.	757.05(758.85)	743.45(758.85)	*K*
Turbine Exit Pressure	4.3(4.4)	4.4(4.4)	*Bar*
Turbine Exit Temperature	1118.15(1109.15)	1085.15(1097.15)	*K*
Exh. Temp. out of HSPT	792.75(800.35)	770.25(787.65)	*K*
Spread	86(37)	53(51)	*K*
Mass Flow Calculated	75(–)	78.5(–)	*kg/s*
Fuel Flow	7571.2(7525)	7552.8(7451.8)	Sm^3/Hr
Thermal Efficiency	36.67(36.94)	36.71(37.21)	*%*

Table 3.2: MEA Data

The correct thermal efficiencies should be higher than the data that were initially received as there is an additional calculation involved for determining the actual fuel flow. This is summarized below by taking into account the density of natural gas, since the measurement of gas fuel flow is specific to its properties as indicated by the units. Natural gas density varies from 0.7kg/m^3 to 0.9kg/m^3 and an average value is assumed. The natural gas supplier provides the value of this property, which has a significant impact in the efficiency of the GT.

$$\dot{F} = \frac{GasFlow * Density}{3600Secs} = \frac{7571.2Sm^3/s * 0.8kg/m^3}{3600} = 1.6722kg/s \tag{3.19}$$

The temperature spread is dramatically reduced as the fuel nozzles have been replaced. A published paper on real time maintenance by GE engineers described that the company suggests relevant maintenance action when the spread exceeds the 70deg limit. The time to reach this limit from 50deg takes about 5 to 6 months. The exhaust temperatures of both engines have increased. This is a very important parameter that

tells a lot about the engine itself. As the engine degrades the exhaust temperature will increase and will act beneficially to the efficiency of the OTSG. Although measurements provide useful indications, there are not sufficient for engine diagnosis. Every diagnostic analysis is based on parameters that cannot be directly measured like mass flow rates, component efficiencies, TET etc. At this study the PYTHIA design point adaptation is performed to determine these fundamental for diagnosis parameters and notice their deviations. After this simulation it would prove more reasonable to compare the one engine with the other, for both dates, than comparing the engine with itself. The reason for this approach is amplified at the limitation's subsection. The figure below indicates the setup procedure for the adaptation procedure. The pink table indicates the to-be adapted parameters and the white table the measured parameters.

After setting up the model for adaptation the results that are presented here were suggesting values for achieving these measurements. As expected the Non Linear GPA Adaptation provides more accurate results than the Linear one after 34 iterations as seen from the figure.

Results

The following table summarizes the results obtained from the Design Point Adaptation. Although the absolute values might differ from the real ones a shift in these values can be a good indication of degradation. This is true only when a carefully selected design point of the engine matches accurately all the measurements. This design point is the benchmark for further performance adaptation analysis.

Parameters	GT6@Jan(Jun)	GT7@Jan(Jun)	Deviation (GT6)/(GT7)	Units
1st Comp. Efficiency	86(84.9)	85(82)	(-1.1)/(-3.0)	%
1st Pressure Ratio	10.2(10.02)	10.2(10.1)	(-0.18)/(-0.10)	
2nd Comp. Efficiency	85(84.6)	87(85.6)	(-0.4)/(-1.4)	%
2nd Pressure Ratio	2.2(2.16)	2.2(2.17)	(-0.04)/(-0.03)	
Turbine Efficiency	85(87.7)	86(89)	(+2.7)/(+3.0)	%
Intake Flow Rate	76(75.7)	78.75(78.5)	(-0.3)/(-0.25)	kg/s
Comb. Efficiency	95(95.6)	98(99)	(+0.6)/(+1.0)	%
TET	1560(1558)	1552(1561)	(-2.0)/(+9.0)	K
Efficiency of HX	73(72.7)	80(79.2)	(-0.3)/(-0.8)	%

Table 3.4: Design Point Adaptation Results

What is clearly seen from this table is that the reduction in compressor efficiency

is higher in GT7 than in GT6. This might result from the difference in the amount of compressor washes that each engine has experienced. The second useful conclusion is that the combustion efficiency has increased in GT6 because of the fuel nozzle change. The counteracting effect of combustion degradation is hidden in this incremental increase. The turbine efficiency has increased as well as a consequence of the increase in combustion efficiency. The Power turbine efficiencies were not involved in this analysis as they didn't deviate because a well defined thermodynamically relationship with a measurement could not be established. The performance adaptation results presented here may be used only for a general evaluation of the engine and by no means are eligible to provide accurate engine diagnosis which in turn might suggest the appropriate maintenance strategy. The setting window and results window of the off-design adaptation can be seen from the following figures.

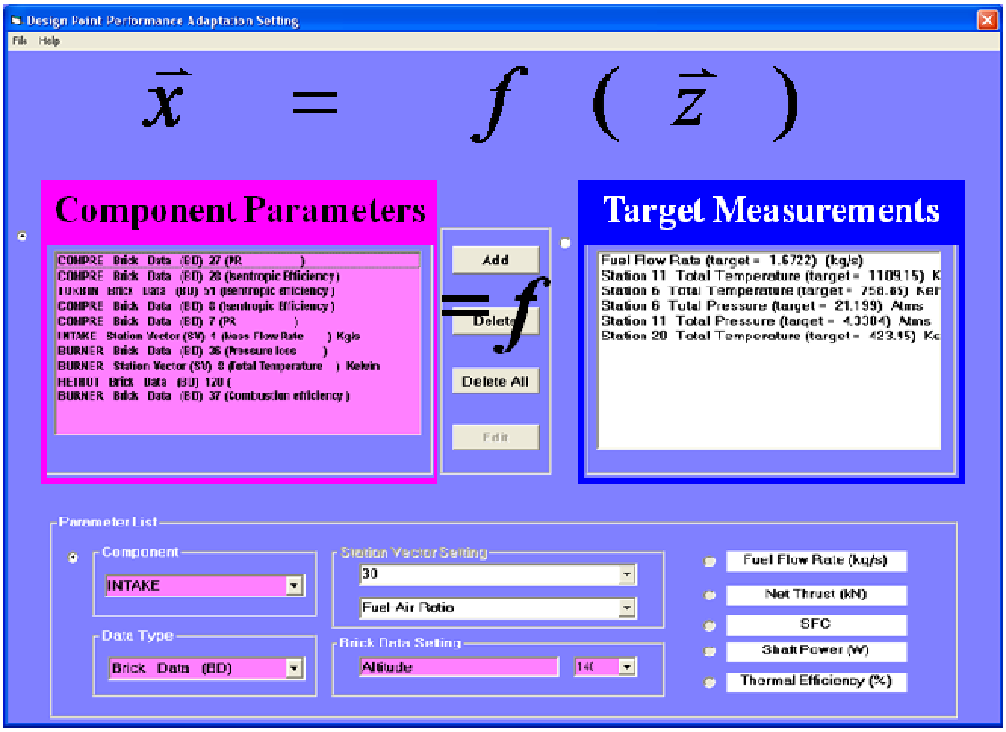

Figure 3.4: Design Point Adaptation Setting Window

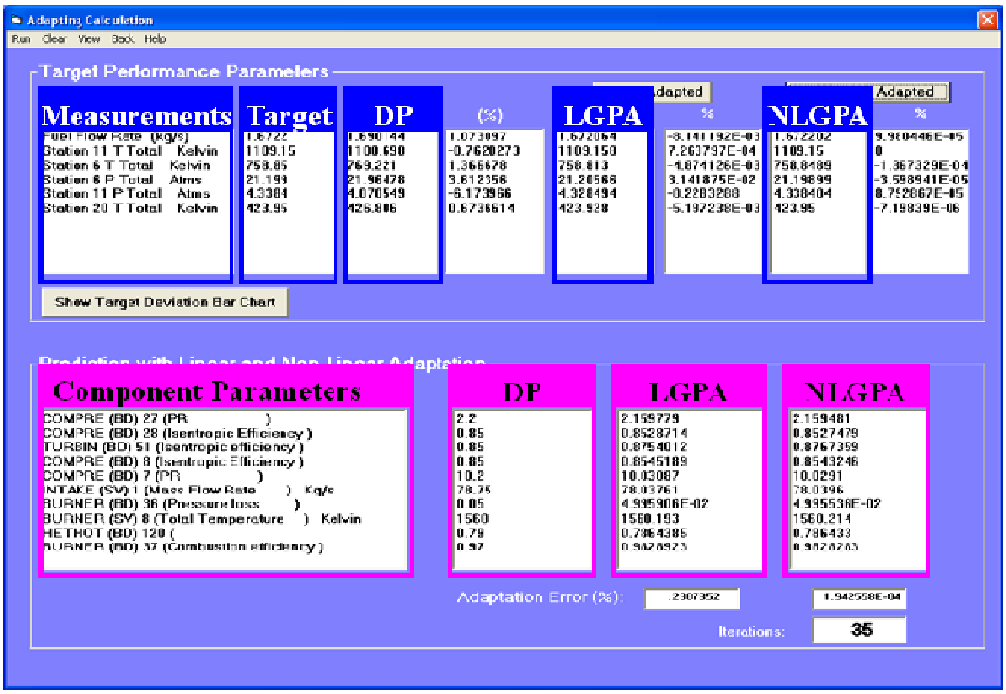

Figure 3.5: Design Point Adaptation Result Window

In this adaptation procedure the user has no control over the other simulated measurements that are not engaged for this analysis. The procedure assumes that the engine is operating at constant speed and defines a new point that will match the predetermined engine measurements. Although this method is working accurately, and provides very useful and meaningful conclusions, it can not be used for diagnostic analysis since speed and operating conditions change. The diagnostic analysis should be based on accurate off-design performance prediction which has been enhanced by the off-design adaptation and the compressor map generation method that are described in the following chapters.

Chapter 4

Compressor Performance Map Generating Method

4.1 Introduction

Prediction of gas turbine performance is strongly dependent on detailed understanding of engine component behavior. For a given rotational shaft speed, there is a characteristic line that describes the flow versus pressure ratio relationship for any axial or centrifugal compressor. This line has an upper limit that is referred to as surge point and a lower limit that is commonly called as the choke or stonewall point. The performance map usually also includes line of constant adiabatic efficiency which are referred to as efficiency contours as seen from the figure 4.1.

When flow, rotational speed and compressor discharge pressure are expressed in non dimensional terms effects of any changes in the compressor air inlet condition and physical properties are eliminated. Further more, such normalized performance maps of a variety of compressors are found to be nearly identical.

Compressor maps are based on various engine tests [29]. Shape of map helps to determine the values of measurable parameters at off-design operating condition. When a specific target of off-design performance is pursued then the maps must be shifted to match the target. In order to describe the off-design performance of gas turbine power-plant accurately, good prediction of characteristic curves of gas turbine power-plant components is essential. A generalized compressor map developed by Saravanamutto and Mac Isaac [17] has been used by Zhu and Saravanamuto [18]. Kurzke [19] introduced auxiliary coordinates (beta lines), having no physical meaning, which are superimposed

on the characteristic curves.

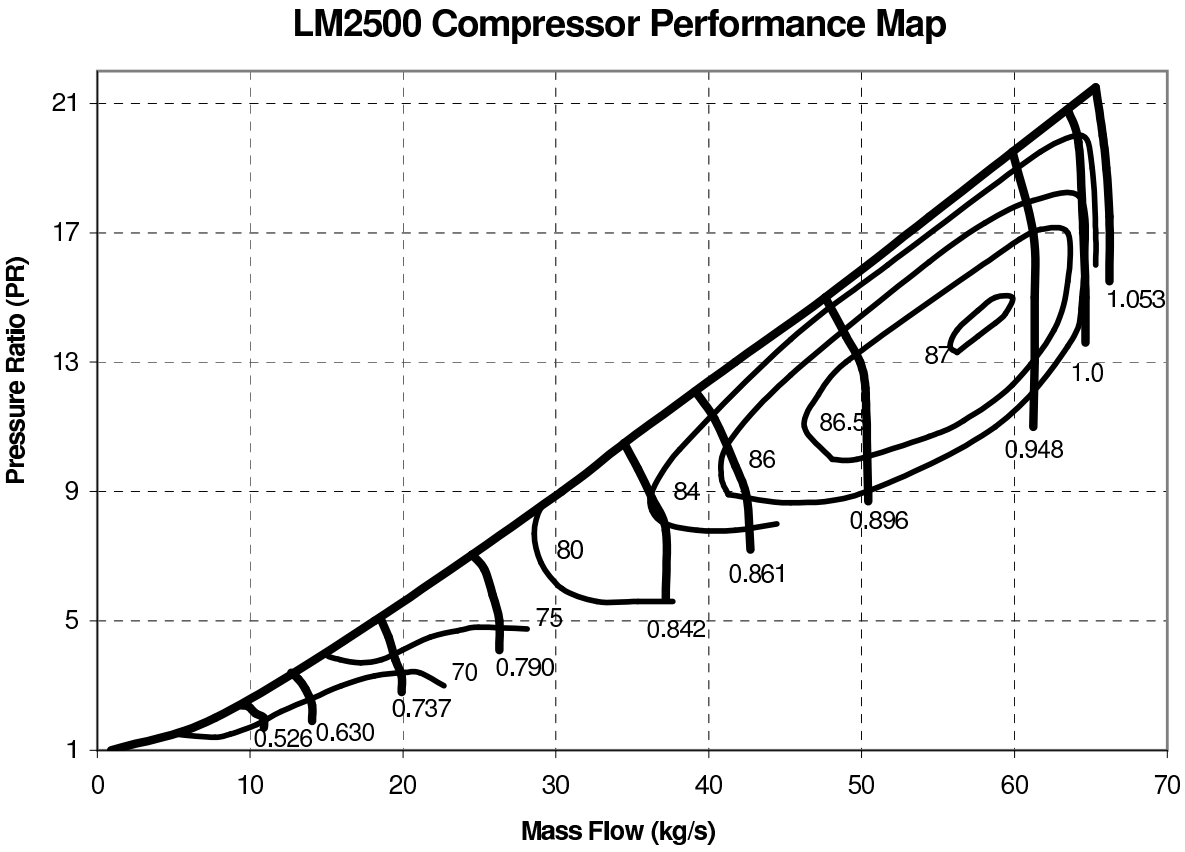

Figure 4.1: Compressor Performance Map [30]

Performance modeling of gas turbines must be established based on thermodynamic relationships between major components in gas path and its component maps. The compressor performance map is also a very useful diagnostic tool that lends itself to engine performance monitoring with the most readily available measurements. When the engine customer purchases the engine, most engine makers provide a performance deck which can calculate only the engine performance output with input data but cannot see the context of the program. One can construct a compressor map, from the operational data. However this would require a reliable set of historic distributed control system (DCS) data that is usually not the case. In generating component maps, several methods exist and are briefly described in this section.

A scaling method has been proposed by Kong [31] under the condition that each engine performance must follow its own component performance. This scaling method is applicable only if it may use similar maps to the actual engine maps which implies

scaling factor close to 1.0 hence similar performance behavior between original component and scaled component. This agrees with the measured performance if the analysis is performed near the design operating point of the engine. Another method called system identification method proposed by Kong [32] builds a math model between scaling factors at some given conditions (input) and Pressure Ratio, Mass Flow and Efficiency (output) with polynomial equations up to 3rd order and finally analyzing the engine performance with the identified maps.

A different approach to input output relationship for the engine/component performance with the use of neural networks has been developed by Yu[33] through a trilinear back propagation network. Again this method relies heavily on the quantity of engine data from the engine manufacturer, which is not always a realistic case scenario, and has a low precision. A combined hybrid approach developed by Kong[34] takes advantage of genetic algorithms to determine the coefficients of the polynomial equations of the system identification method. This method provides higher accuracy than the traditional scaling method at operating points far away from the design point of the engine. Other approaches include fuzzy expert systems along with engine deck data for compressor performance map estimation [35, 36]

These methods and approaches to compressor map generation techniques and their effect to off-design adaptation have limited applicability due to their case specific nature which is obvious from both the consideration of engine deck data used for constructing the performance map and by the high order polynomials which add complexity and decrease significantly the computation time.

Therefore the novel compressor performance method developed not only provides a useful performance, adaptation and diagnostic tool but also tackles the aforementioned issues by being generic, simpler and efficient in terms of computation.

The aim of this method is to analyse the shape of a default compressor map mathematically so that this shape could then be controlled by an optimiser and therefore match the off design operating points of a gas turbine. The original LM2500 compressor performance map published in [30] is taken as the default map for this analysis. This map has been digitised from the article published by Klapproth and it can be seen in figure 4.1.

Each compressor map comprises of the lines of constant speed and the efficiency contours. The LM2500 gas turbine engine is very similar to the the LM2500+ with their only difference been the zero stage at the latest version which enables the engine to have a 23% increase in mass flow rate. In this method the speedlines are analysed

first mathematically and then a similar analysis will follow for the efficiency contours.

4.2 Methodology

4.2.1 Speedlines

Mathematical Analysis

The compressor map is first analysed by expressing the lines of constant speed in the Pressure Ratio- Mass Flow plane as a function of the compressor's rotational speed which is the most reliable measurement from a gas turbine instrumentation set.

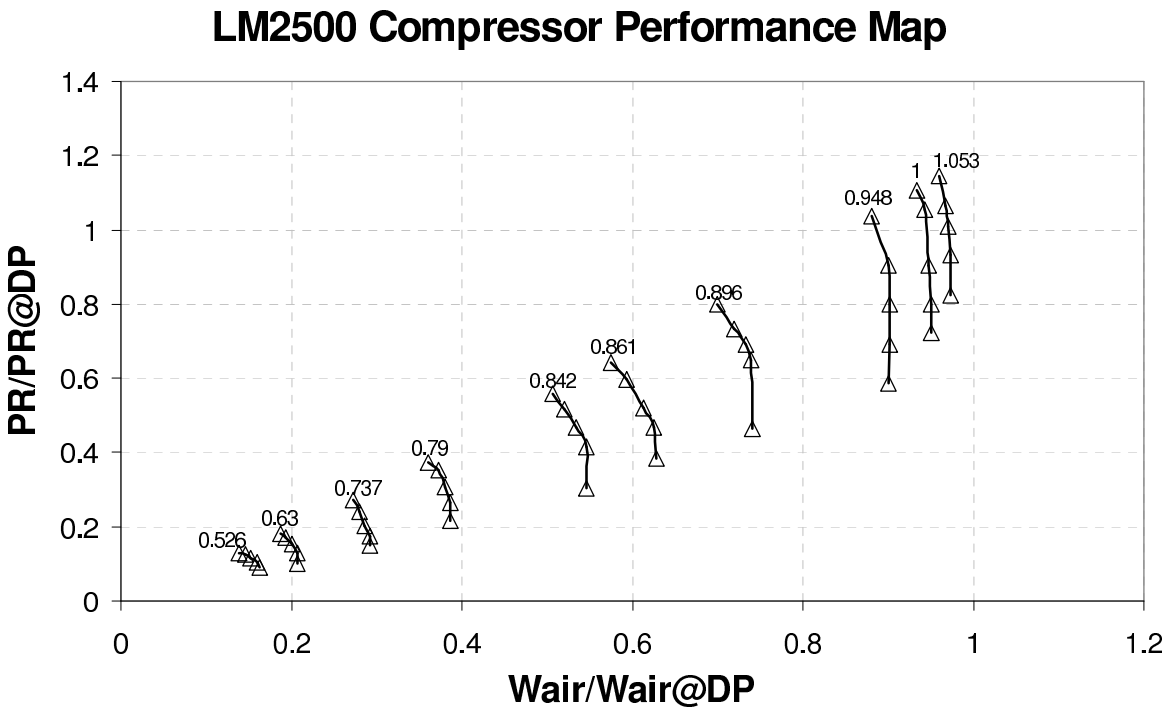

Figure 4.2: lm2500 compressor map

Each speedline can be expressed by a mathematical equation. Amongst a variety of different mathematical approaches that have been explored the equation that accurately captures the shape of each speedline is that of an ellipsis.

An ellipsis is described by the equation

$$\left(\frac{x-x_c}{a}\right)^2+\left(\frac{y-y_c}{b}\right)^2=1 \tag{4.1}$$

where (x_c, y_c) are the coordinates of the center of the ellipsis. Assuming the center at $(0,0)$ then equation 4.13is simplified to the following form

$$\left(\frac{x}{a}\right)^2+\left(\frac{y}{b}\right)^2=1 \tag{4.2}$$

$$\left(\frac{W}{a}\right)^2+\left(\frac{PR}{b}\right)^2=1 \tag{4.3}$$

In order to define an ellipsis accurately it is essential to find the constants a and b, which determine where the ellipsis is going to meet the x and y axis when PR=0 and W=0 respectively. Since this is the case, an extrapolation took place to find out where each curve meet the x axis. As these points have been determined then the equation 4.13 was solved for coefficients a and b.

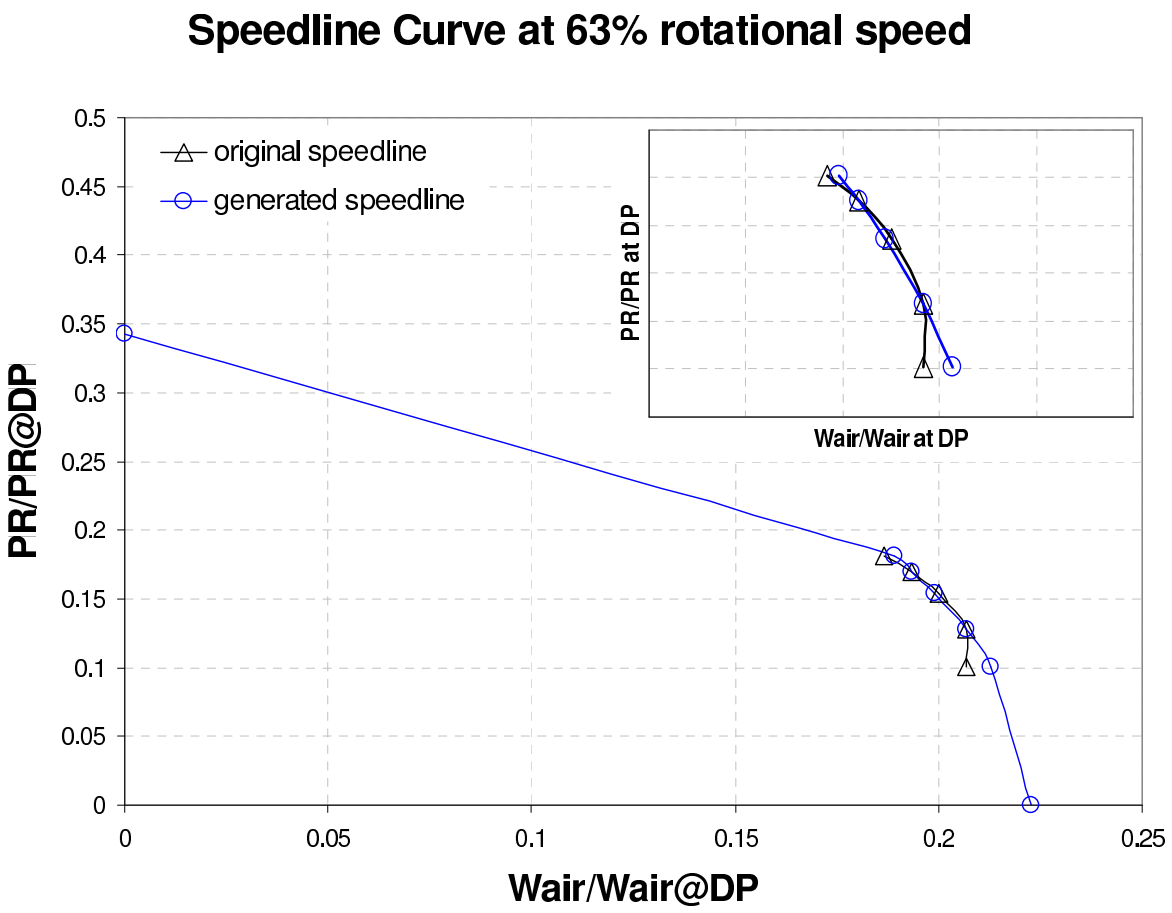

Figure 4.3: Speedline curve at 63% rotational speed

$$a = \frac{W}{\sqrt{1 - \left(\frac{PR}{b}\right)^2}} \tag{4.4}$$

since Wmin and PRstop are known then

$$b = \frac{PR}{\sqrt{1 - \left(\frac{W}{a}\right)^2}} \tag{4.5}$$

so a and b of the ellipsis are known therefore we can plot this speedline starting from Wmin to Wmax and from PRstop to PRlow by the use of equation 4.14 and the speedline can be seen from **??**

This process is performed for every speedline and the result can be seen in the following figure

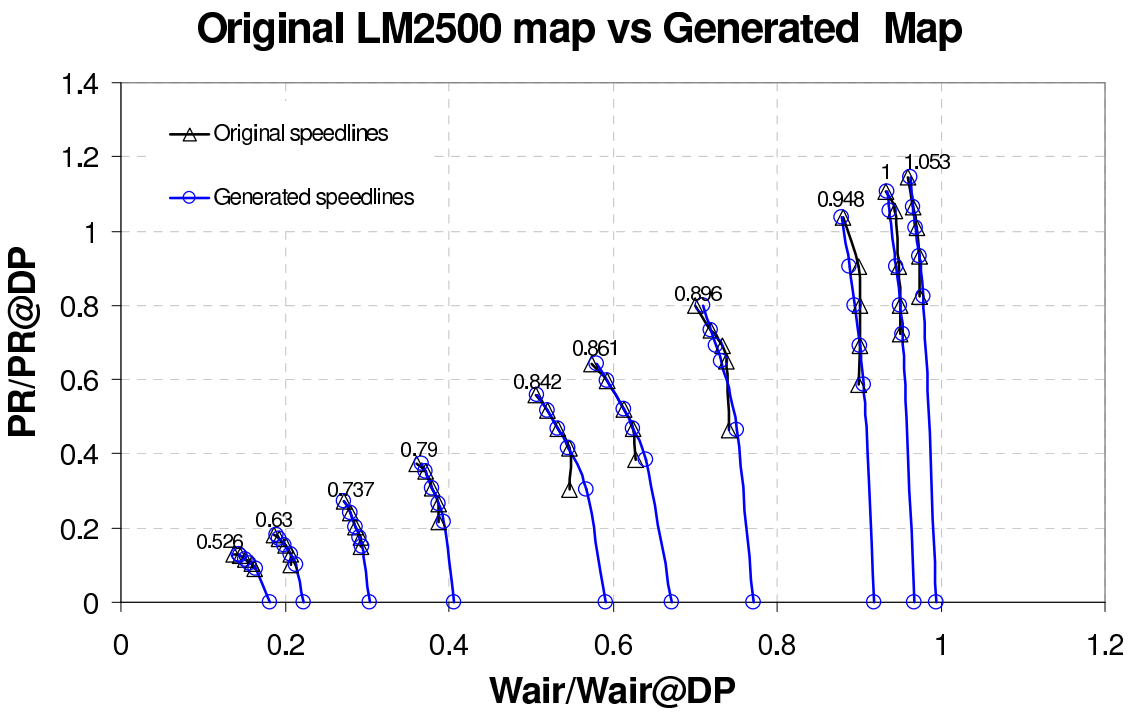

Figure 4.4: Speedline compressor performance map

Control Analysis

The objective of this analysis is to see which are the parameters that control the shape and the size of each speedline. Its important at this point to emphasize the fact that each speedline has the following variables a,b,Wmin and PRstop . Those parameters are the ones that are going to be analysed in order to initialise optimization's procedure.

Each of these parameter should be expressed as a function of speed since speed is the most reliable measurement from a family of measurements of a gas turbine

$$a, b, Wmin, PRstop = f(N)$$

taking each parameter individually it is concluded that each constant can be expressed by an equations as seen here

The coefficient a of the ellipsis is an exponential function of speed and coefficients a1,a2

$$a = a_1 * N^{a_2} \tag{4.6}$$

The coefficient b of the ellipsis is an exponential function of speed and coefficients b1,b2 and PRdp, where PRdp is the design point pressure ratio.

$$b = PRdp * (b_1 * N^{b_2}) \tag{4.7}$$

The coefficient PRstop determines where each speedline should stop to be plotted and this can be seen from the following figure. Generally the boundaries of a compressor map can be expressed by a simple linear equation where PRstop is a function of a and PRdp as expressed here

$$PR_{stop} = ((PRdp * 1.2) - 1) * a + 1 \tag{4.8}$$

The mass flow rate corresponding to the point where the compressor map stops to be plotted ie.PRstop can be expressed based on the ellipsis equation.

$$a_{min} = \sqrt{a^2 * (1 - (PR_{stop}/b)^2)} \tag{4.9}$$

Each speedline will consist of five points since PYTHIA's default compressor maps have five points per speedline curve therefore astep is expressed in terms of coefficients amin and a.

$$a_{step} = (a_{min} - a)/4 \tag{4.10}$$

Now mass flow can be determined by the following equation as a function of amin and astep

$$W = a_{min} + j * a_{step} \tag{4.11}$$

Since mass flow W is calculated for each speedline then Pressure Ratio PR can be determined by the elliptic coefficients a,b and mass flow rate W.

$$PR = \sqrt{b^2 * (1 - (W/a)^2)} \tag{4.12}$$

Totally there are 4 coefficients that enable the process to determine as accurately as possible the speedlines from 50% up to 115% of compressor shaft speed. These coefficients are going to be determined by the genetic algorithm optimiser in order to match the operating points targeted. A graph showing the 2 parameters of this ellipsis expressed with respect to the constant speed is seen from figures 4.5 and 4.6.

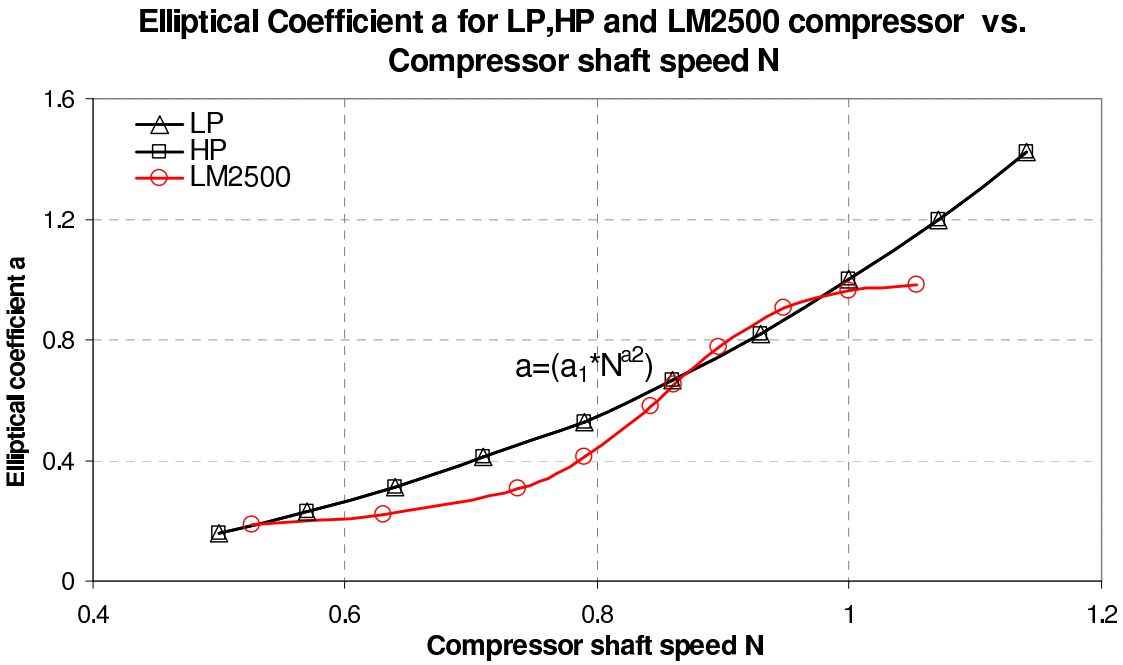

Figure 4.5: Elliptical coefficient a for LPC, HPC and LM2500 vs shaft speed

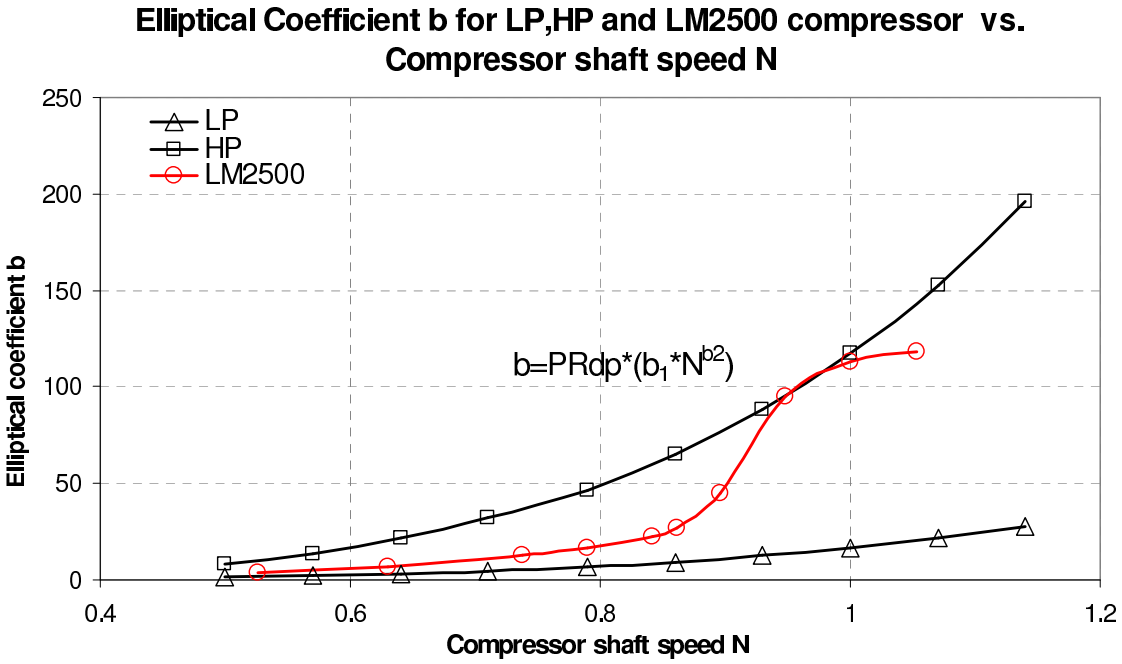

Figure 4.6: Elliptical coefficient b for LPC, HPC and LM2500 vs shaft speed

4.2.2 Efficiency

Mathematical Analysis

The efficiency contours are describing the regions of constant isentropic compressor efficiency. As seen from figure 4.8 the contours can be described by the cutaway of a three dimensional ellipsoid shape in the PR-W plane. However there is no analytical solution for determining the points of intersection between an ellipsoid and an ellipsis therefore this approach is limited by its complex mathematical nature which in turn makes the objective of determining the efficiency wrt compressor shaft speed not feasible. After an extensive review of mathematical methods for expressing the efficiency contours analytically as a function of pressure ratio, mass flow and speed the most straight forward and generic approach was to extrapolate the intersection points between the speedlines and the efficiency contours and plot them against mass flow rate as seen from figure 4.7.

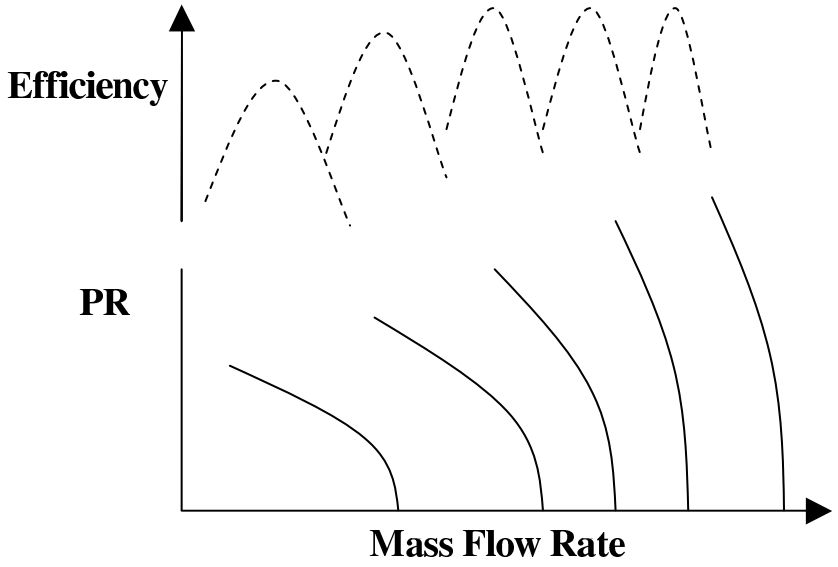

Figure 4.7: Typical compressor efficiency map

It can be assumed that each efficiency line belongs to an elliptic curve with the following equation

$$\left(\frac{x - x_c}{a}\right)^2 + \left(\frac{y - y_c}{b}\right)^2 = 1 \tag{4.13}$$

where (x_c, y_c) are the coordinates of the center of the ellipsis. Assuming the center at $(xc, 0)$ then equation 4.13is simplified to the following form

$$\left(\frac{W - xc}{a}\right)^2 + \left(\frac{ETA}{b}\right)^2 = 1 \tag{4.14}$$

In order to define this ellipsis accurately it is essential to find the parameters a and b, which determine where the ellipsis is going to meet the x and y axis when ETA=0 and W=0 respectively. The ellipsis that describes the efficiency lines has the x axis center at the middle of the speedline's mass flow rate range and the y axis center at y=0 as seen from the next figure. As the mass flow rate range, for which efficiency has to be determined, is known from the speedline generation procedure the only unknown parameter that has to be defined is the the coefficient b of the efficiency.

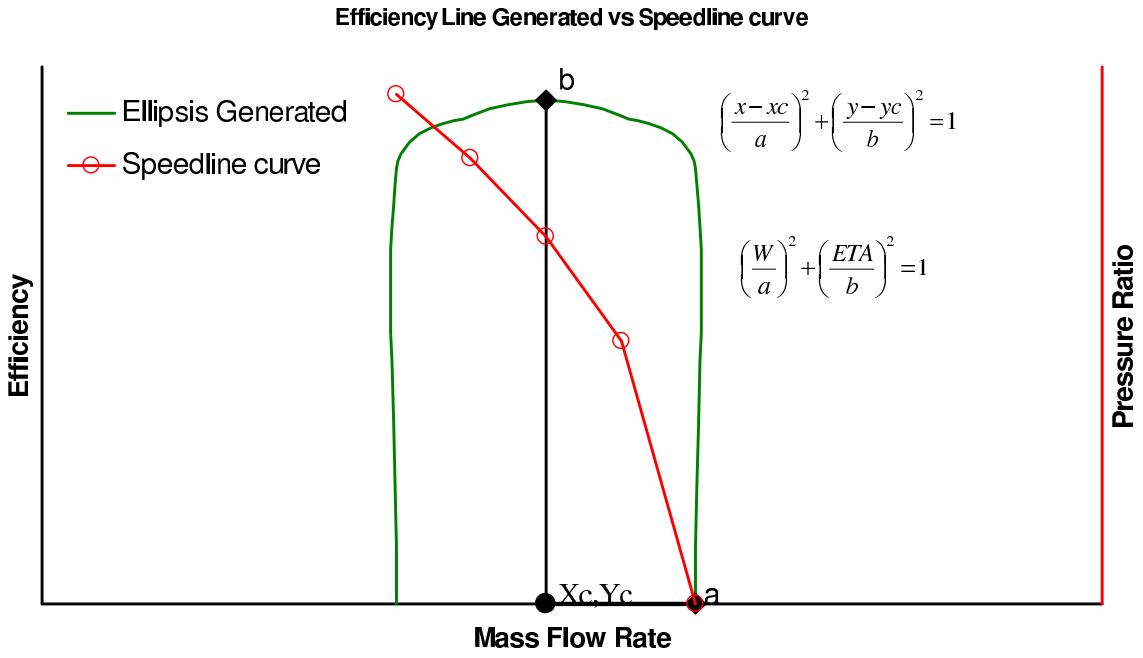

Figure 4.8: Efficiency curve at 63% rotational speed

Elliptical coefficient a is the middle point of the speedline curve and given by the following equation where Wmax is the

$$a = (Winitial - Wfinal) \tag{4.15}$$

Since a and xc are known then the isentropic efficiency ETA can be determined by the following equation

$$b = \frac{ETA}{\sqrt{1-\left(\frac{W}{a}\right)^2}} \tag{4.16}$$

Control Analysis

The objective of this analysis is to see which are the parameters that control the shape and the size of each efficiency line. Each efficiency line is dependent upon the elliptical coefficients a and b . Those parameters are the ones that are going to be analysed in order to initialise optimisation procedure.

Each of these parameter should be expressed as a function of speed since speed is the most reliable measurement from a family of measurements of a gas turbine

$$a, b = f(N)$$

taking each parameter individually it is concluded that each constant can be expressed by an equations as seen here

The coefficient a of the ellipsis is determined by the 4.15

The coefficient b of the ellipsis is a polynomial function of speed and coefficients ETAb1,ETAb2 and ETAb3

$$b = ETAb1 * (N^2) + ETAb2 * (N^1) + ETAb3 \tag{4.17}$$

Each efficiency line will consist of five points since PYTHIA's default compressor maps have five points per efficiency curve therefore astep is expressed in terms of coefficients amin and a.

$$a_{step} = (a_{min} - a)/4 \tag{4.18}$$

Since mass flow W is determined from the earlier speedline procedure then compressor isentropic efficiency ETA can be calculated by the following equation.

$$ETA = b * \sqrt{1 - \left(\frac{W}{a}\right)^2} \tag{4.19}$$

There are three coefficients that enable the process to determine as accurately as possible the compressor efficiency from 50% up to 115% of compressor shaft speed. These coefficients are going to be determined by the genetic algorithm optimiser in order to match the operating points targeted. A graph showing the efficiency distribution against the compressor shaft speed N is seen from the next figure.

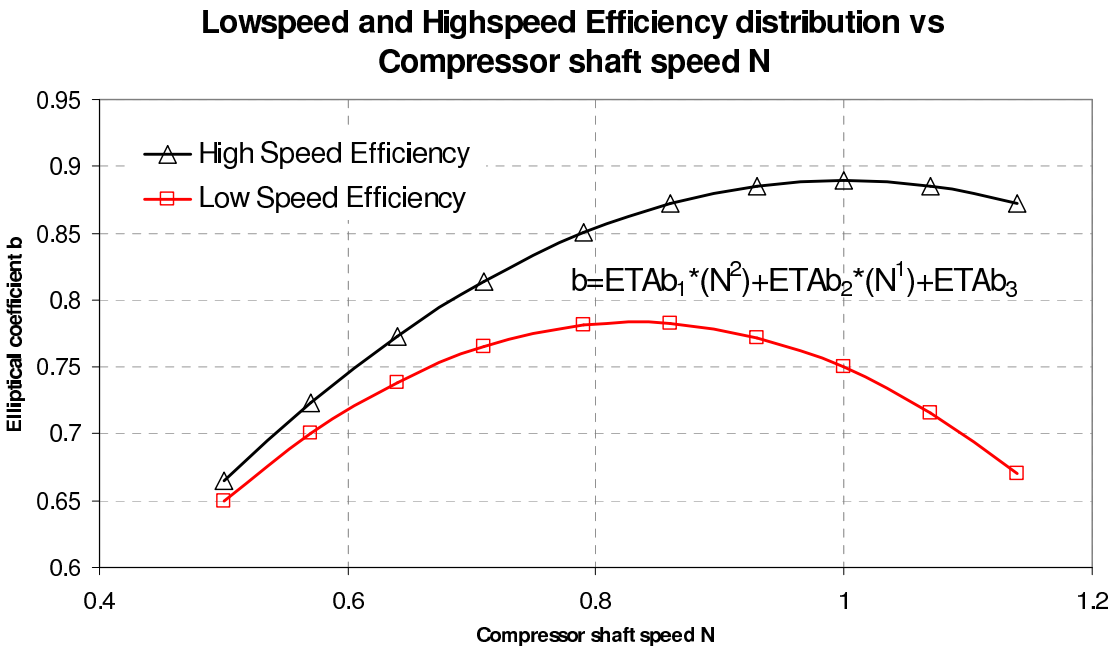

Figure 4.9: Elliptical coefficient a for LPC, HPC and LM2500 vs shaft speed

It is noticed that there are two different elliptical coefficient b curves denoted as high speed and low speed efficiency. This distinction is based upon the fact that the peak efficiency of a compressor doesn't necessarily coincide with the maximum speed. Therefore the efficiency equation can capture this peak efficiency characteristic varying from 80% up to 100% of compressor shaft speed.

4.3 Sensitivity analysis

At this point it is crucial to perform a sensitivity analysis for the coefficients that are responsible for the generation of the compressor performance map under the developed method. This novel compressor generation method employs 7 coefficients in order to mathematically express a compressor map. A sensitivity analysis has been performed where the effect that a -10% drop in each of theses coefficients had in the pressure ratio PR, mass flow W and the isentropic efficiency ETA of the compressor.

In order to capture the trend of such changes in a compressor map structure three lines of constant speed have been selected from the total number of 10 lines that each

map has. The first line at the lowest speed where its parameters like PR,W and ETA are denoted with number 1, the second line being located at the middle of the compressor map noted as 2 and the final line at the maximum speed as 3. Thus by selecting this representative sample of the compressor map, the effect that each coefficient modification implies to the engine performance parameters as PR,W and Efficiency for these lines is shown in figure 4.10

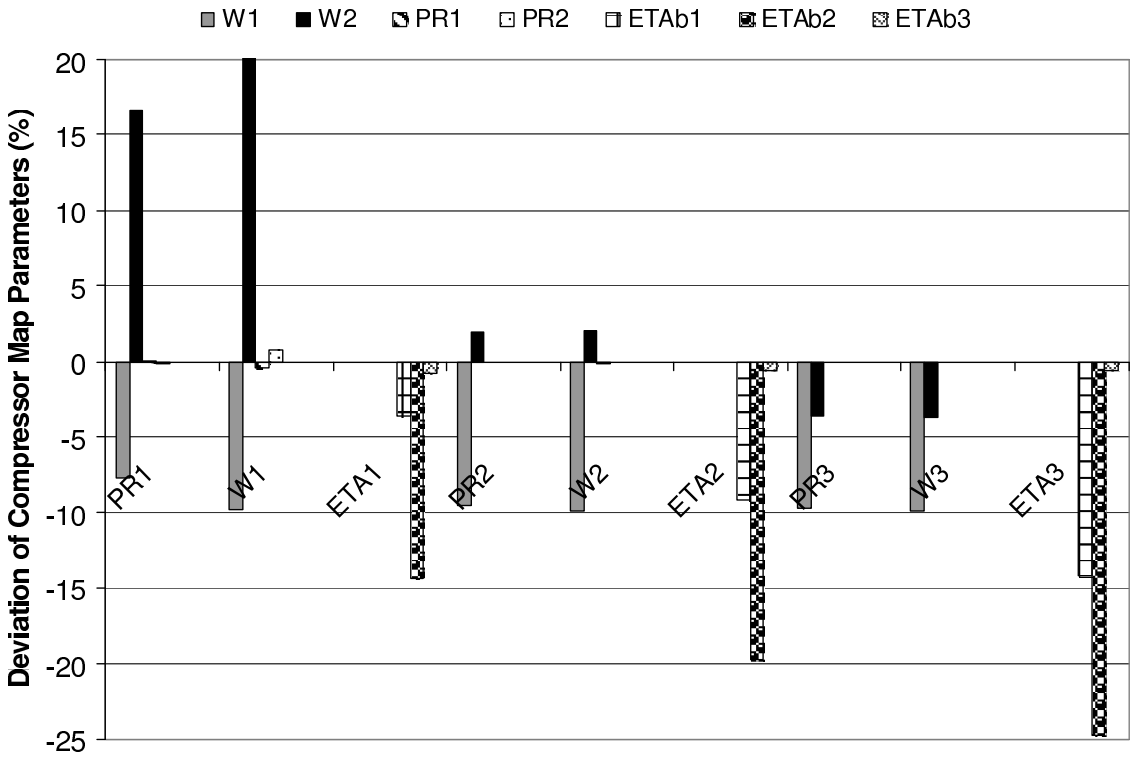

Figure 4.10: Sensitivity Analysis of Compressor Map Coefficients

It is noticed that for the first line of constant speed of the compressor map the coefficient that has the highest effect is the coefficient W2 followed by W1. These two factors are included in the equation 5.7

$$a = a_1 * N^{a_2} \tag{4.20}$$

which after the appropriate substitution is

$$W = W_1 * N^{W_2} \tag{4.21}$$

The power coefficient of this equation W2 affects the low speed region of the compressor map, which starts from 0.5, more than the high speed region of the map, where constant speed is nearly 1 and the N^{W_2} part of the equation is close to unity. The coefficients W1 and W2 of equation 4.21 are only affecting the pressure ratio and the mass flow of the compressor map as the value of isentropic efficiency is determined by the coefficients ETAb1,ETAb2 and ETAb3 which are independent of W1 and W2. For a -10% drop of W1 the pressure ratio and mass flow rate decrease by -7.5% and -10% respectively. On the other hand by a -10% drop in W2 the pressure ratio and mass flow rate increase by 16% and 20% respectively and the reason for this increase is that the value of constant speed is less than 1. For the line of the compressor map which is at a constant speed value higher than 1, the same drop would produce a decrease of pressure ratio and mass flow rate PR3 and W3 respectively.

The isentropic efficiency of the compressor map's low speed region more sensitive to the coefficient ETAb2. As the efficiency lines are expressed as an elliptical equation the b constant of the ellipsis, which lies in the y axis, is determined by the quadratic equation 5.6

$$b = ETAb1 * (N^2) + ETAb2 * (N^1) + ETAb3 \tag{4.22}$$

It is concluded that the effect of changing the ETAb2 while keeping everything else the same shifts the curve along the x-axis, and moves it up and down. Specifically a -10% drop in ETAb2 results in a -14% decrease in isentropic efficiency.

For the second region of the compressor map W1 and W2 are the coefficients affecting the pressure and mass flow rate and ETAb1 and ETAb2 the efficiency of the compressor. A -10% drop in W1 decreases PR2 and W2 by -8% and -10% respectively. The effect of W2 drop in this region is smaller that the first region for the compressor map as the value of constant speed in close to unity and its effect is a small increase of 2% for both the pressure ratio PR2 and mass flow W2. The efficiency drops by 20% and 10% when decreasing the coefficients ETAb2 and ETAb1 respectively.

At the final region of high speed of the compressor map the decrease of W1 by -10% results in a -10% drop in pressure ratio PR3 and mass flow rate W3. Coefficient W2 has a smaller effect in PR3 and W3 than W1 which is translated in -4% drop for both PR3 and W3. Finally the efficiency of this compressor map's region is decreased by -14% and -26% when dropping by -10% the coefficients W1 and W2 respectively.

Summarising the most sensitive coefficients are enlisted here

1. For the low speed region
    - W2 for PR1 and W1
    - ETAb2 for ETA1
2. For the middle speed region
    - W1 for PR2 and W2
    - ETAb1 and ETAb2 for ETA2
3. For the high speed region
    - W1 for PR3 and W3
    - ETAb1 and ETAb2 for ETA3

The effect that these coefficients have in the shape of the compressor map can be seen analytically from the following figures. The initial compressor map and the one where each coefficient has been decreased, by the same amount as in the sensitivity analysis, are seen in the same graph in order to extract general trends and patterns that the map's shape follows for each coefficient.

Starting by the effect that a -10% drop in W1 has in the compressor map it can be seen from figure 4.11, where the modified map is in dotted lines, that the compressor map in the PR vs W plane shifts to the left.

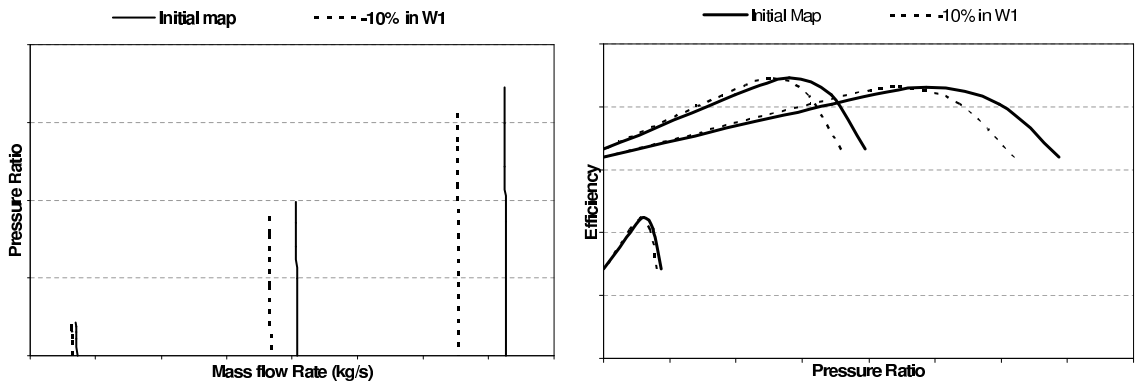

Figure 4.11: Effect of W1 coefficient to the compressor map

This is a result of the decrease in mass flow rate W1 and PR1 that this drop in W1 implies. On the efficiency map the value of the isentropic efficiency remains the same,

as there is no change in the y-axis coordinates, however the pressure ratio decreases which in turn displaces the curves along the x axis to the left.

The drop of -10% in W2 affects the compressor map as seen in figure 4.12, where the map in the PR vs W plane is "shrinked" and compressed in lower boundaries than the initial map.

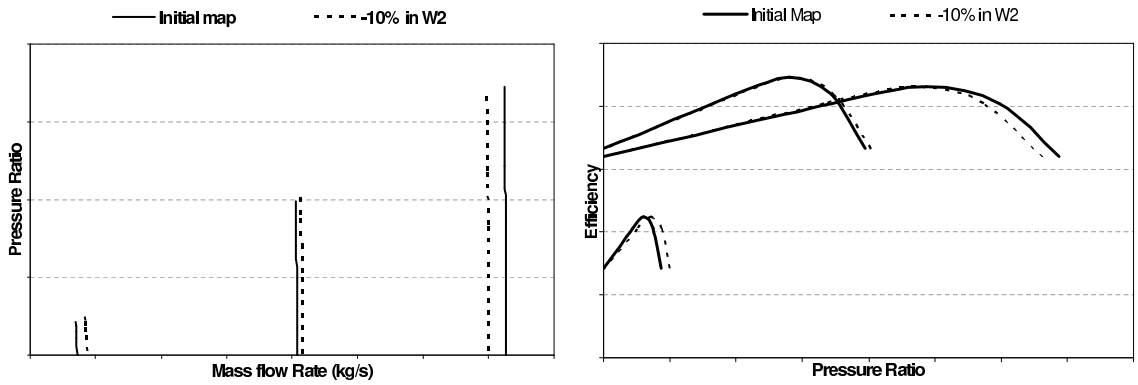

Figure 4.12: Effect of W2 coefficient to the compressor map

This is due to decrease in mass flow rate W3 and pressure ratio PR3 for the high speed region and increase in the low speed region of PR1 and W1. On the efficiency map the same effect is noticed, again with the isentropic efficiency values remaining uninterrupted.

Although the change in PR1 had a very small effect in the sensitivity analysis that has been earlier performed it is important to emphasize that this coefficient is crucial for the transition of the compressor map shape from high pressure to low pressure and vice versa. The maps of high pressure compressors have almost vertical lines at the high and middle speed regions where for the low pressure the curvature of the lines is significantly higher. The margin for the PR1 coefficient is is quite wide for compressor generation purposes so that a gas turbine user can customise the compressor map, but for optimisation purposes this margin will be narrowed based on the nature of the compressor under investigation ie. low, intermediate and high pressure. For this case where a high speed compressor is represented and in order to have a Representative modified compressor map the coefficients PR1 has been decreased by 70% and the effect of this change is seen in figure 4.13.

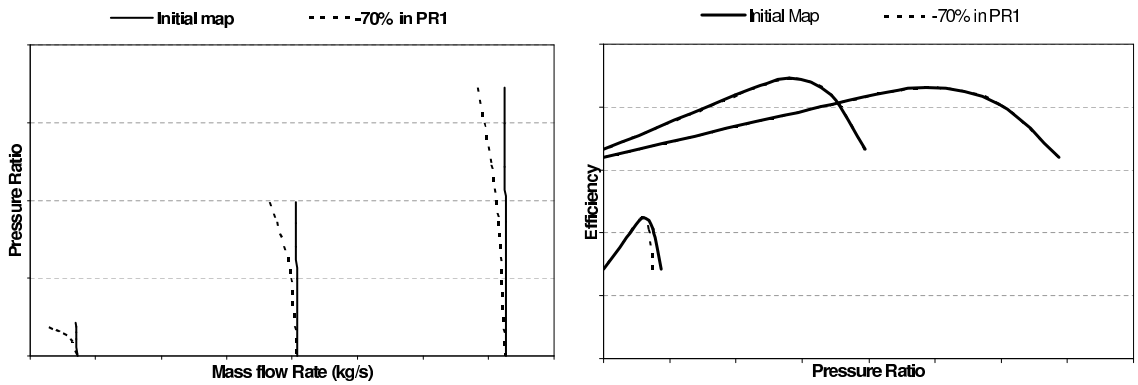

Figure 4.13: Effect of PR1 coefficient to the compressor map

As seen from the figure above the lines of constant speed in the PR vs W plane compressor map are not vertical as the initial map but present a curvature that characterises the low and intermediate pressure compressors. If the gas turbine user wishes to construct a compressor map that will satisfy a low pressure compressor criteria he has to decrease significantly the value of PR1 for a realistic representation of the compressor map.

The effect that a -10% drop in ETAb1 and ETAb2 have in the compressor map is seen in figure4.14. The drop in ETAb1 decreases in turn the isentropic efficiency as noticed from the shift of the compressor map along the y-axis . The high speed lines present a higher decrease that the middle and low speed lines as described earlier in this section. The pressure and mass flow rate are not affected by the change of ETAb1 coefficient.

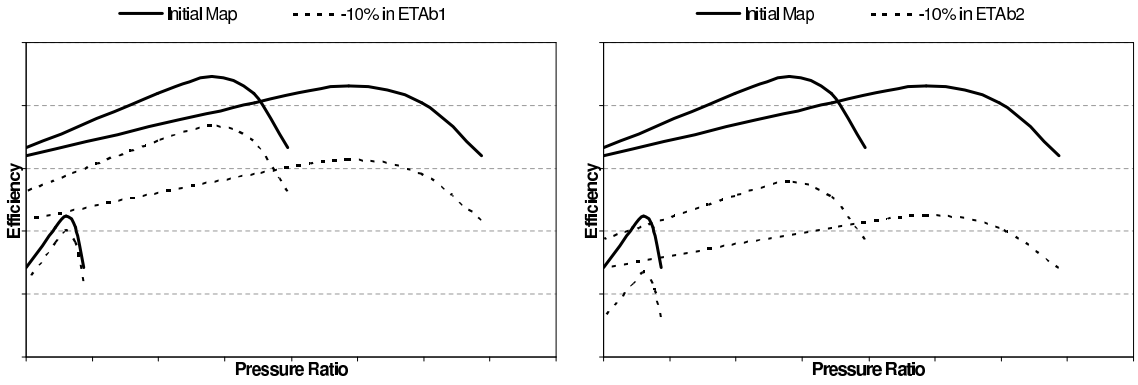

Figure 4.14: Effect of ETAb1 and ETAb2 coefficients to the compressor map

Finally the effect of the drop of -10% in ETAb2 coefficient has a similar to ETAb1,

effect to the compressor map. However the percentage of resulted decrease in the isentropic efficiency of the compressor is higher here which proves the increased sensitivity of this coefficient ETAb2 compared to ETAb1.

The analysis performed justifies the fact that the compressor performance map relies on the coefficients that can mathematically describe its shape. In addition it is also a matter of the appropriate selection of the range, in which each coefficient lies, for satisfying the design point criteria of the gas turbine and the nature of the compressor. This analysis is a useful tool that can guide the gas turbine user to construct a compressor performance map through a program that has been developed and integrated in PYTHIA's simulation and diagnostics software.

4.4 Demonstration

The program has been developed in visual basic that generates a compressor map based on the discussed method. The compressor map comprises of 10 speedline and efficiency curves. The output of this file is stored in a text file ready to be read by both PYTHIA and Turbomatch. The procedure for generating a compressor performance map can be seen from the next algorithm.

Algorithm 1 Compressor Map Generation Algorithm

1. Start from compressor shaft rotational speed N = Nminimum which is 0.5 and
   (a) with a step of Nstep=(Nmax-Nmin)/number of lines
   (b) then the parameters a1, a2, b1, b2, ETAb1, ETAb2, ETAb3 are known
2. Determine from the first speedline up the 10th the following parameters
   (a) Elliptical speedline coefficient a
   (b) Elliptical speedline coefficient b
   (c) Pressure ratio limit of the surge line PRstop
   (d) Starting point for mass flow amin
   (e) Plotting step astep
   (f) Elliptical efficiency coefficient ETAa
   (g) Elliptical center of efficiency curve xc
   (h) Elliptical center of efficiency curve yc
   (i) Efficiency efficiency coefficient ETAb
3. Determine the performance parameters from the first point of each line up to the 5th that a line contains
   (a) Mass Flow Rate W
   (b) Pressure Ratio PR
   (c) Isentropic Efficiency
4. Repeat step 3 until the performance paremeters of the 5th point of each line are determined
5. Repeat step 2 until the parameters of the 10th line are determined
6. End

A graphical representation of both low pressure and high pressure map can be seen from the program's graphical interface as seen in the next figure. The user has the ability to control the shape of the compressor map by modifying the associated coefficients in the textboxes and construct a new compressor map tailored to the engine specifications. Therefore this program provides a useful tool to the user for developing a engine model for simulation and diagnostic purposes in PYTHIA's environment.

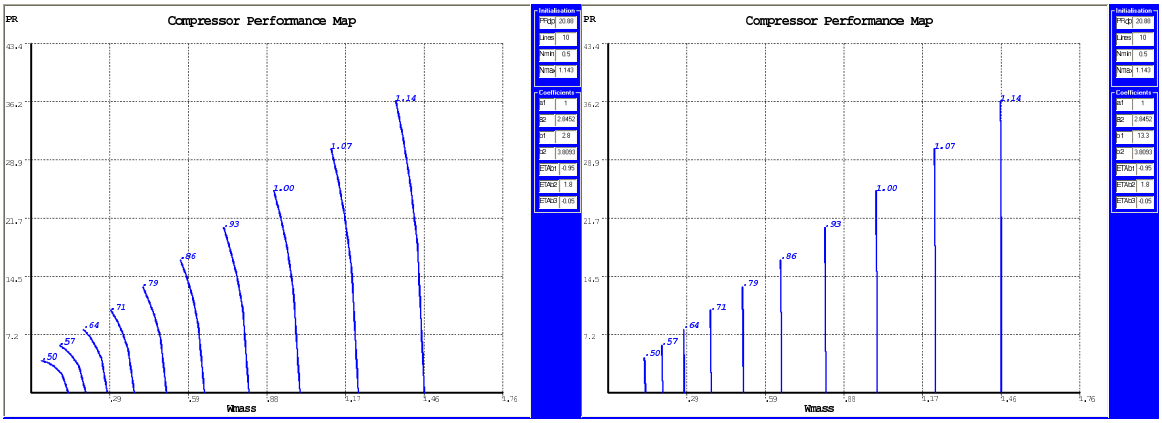

(a) LP Compressor Map PR vs W

(b) HP Compressor Map PR vs W

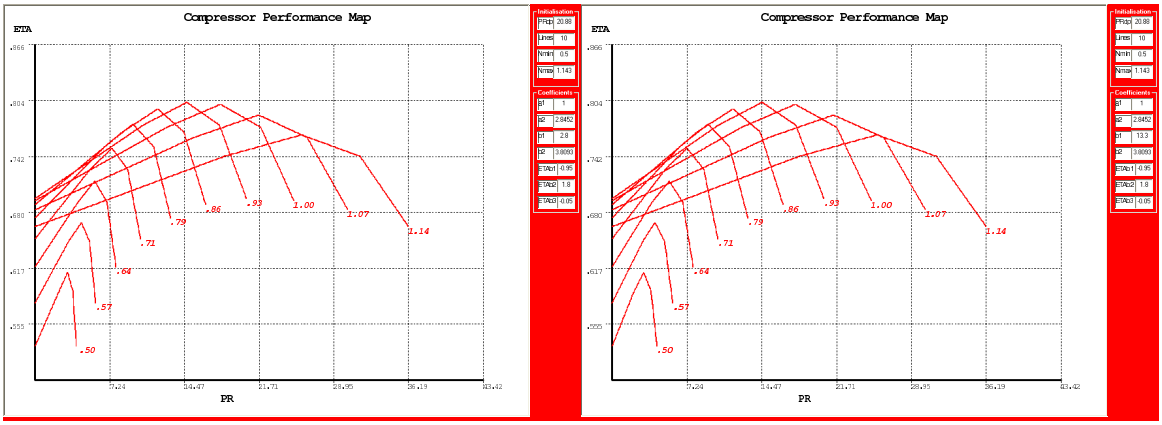

(c) LP Compressor Map ETA vs PR

(d) HP Compressor Map ETA vs PR

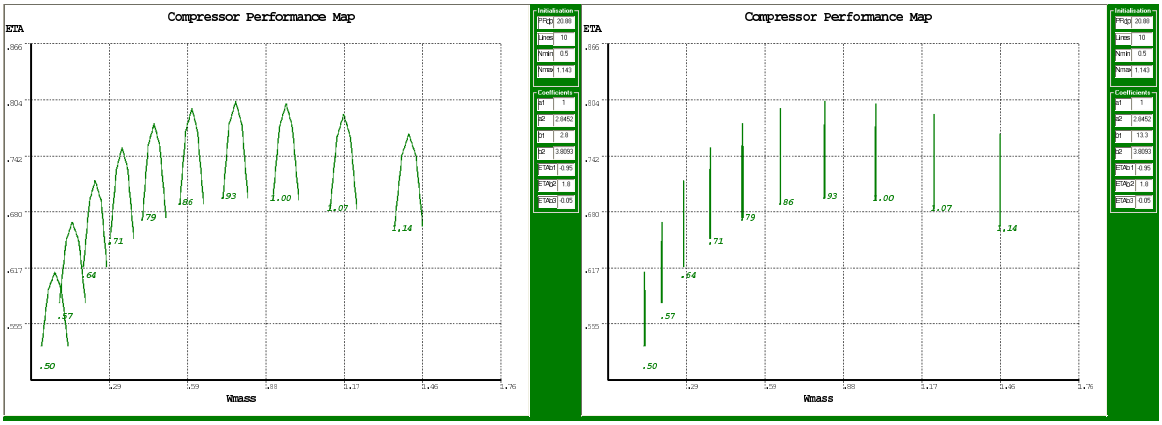

(e) LP Compressor Map ETA vs W

(f) HP Compressor Map ETA vs W

Figure 4.15: Generated Compressor Performance Maps

As seen from figure 4.15the distribution of speedlines in the PRvs W plane compressor map is exponential which means that as the compressor shaft speed increases the

gap between the speedlines increases as well. This effect can be mimimised by simply changing the type of mathematical equation which distributes the coefficient a of the ellipsis 4.5. Thus the generated compressor map will be able to capture that effect through a quadratic equation instead of an exponential.

The disadvantage of this process will be the addition of two extra coefficients that quadratic equation has to the genetic algorithm optimisation that is employed in the developed off-design adaptation. This will result in a further computation time penalty that can be avoided as the objective is to generate a compressor map that can be fully controlled mathematically and not to exhaust the accuracy limits by making a compressor map very case-specific. However for future modifications of the developed map generation method this could be explored as the program is modular and enables further development.

The crucial role that the compressor map has in the adaptation of an engine model to a service engine at off-design conditions and the use of genetic algorithms optimisation technique for achieving the former fundamental objective, follows in the next section.

Chapter 5

Off-Design Performance Adaptation

5.1 Introduction

Since effective gas turbine performance diagnostics is strongly dependent on accurate engine performance models near a chosen nominal diagnostic operating condition, such as design operating condition or full power condition, any noticeable performance prediction errors comparable to performance deviation due to engine degradation may lead to misleading diagnostic results. To produce an accurate engine model, the following conditions have to be satisfied.

- As described in design point adaptation chapter it is of paramount importance to adapt the engine model to the service engine in order to match the engines target measurements, by selecting a set of component performance parameters to be adapted.
- Construction of a compressor map that will meet the engine model specifications and at the same time capture as accurate as possible the compressor map for the specific engine. Although compressor maps are exclusive property of manufacturers and not available to gas turbine users it is well known that all the engines' compressor maps share some common characteristics and patterns with each other, that have been considered in the compressor generation method. Therefore a construction of an initial map from the design point characteristics of a gas turbine is quite a straight forward procedure from the compressor generation method that has been developed. The parameters affecting the shape of the performance map are at the user's disposal to modify for the aforementioned scope.

- Adaptation of the engine model to satisfy engine off-design performance by creating new engine component maps, as these maps play important role in off-design performance predictions. Through the use of genetic algorithms optimise the coefficients that mathematically express a compressor map, as in compressor generation method, in order to minimise the error between the simulated and target measurements..

Engine off-design performance represented by measurable parameters, such as gas path pressures, temperatures, shaft rotational speeds, fuel flow rate, thrust, etc., heavily depend on the characteristics of the compressors [37]. Therefore, the shape of the compressor characteristic maps plays an important role in determining the values of engine measurable parameters at engine off-design operating conditions. Thus, if a set of selected measurable off-design performance parameters is imposed as a target, the compressor characteristic maps can be modified in an "inverse" mode to match the target. Such an approach is called off-design performance adaptation.

Most gas turbine analytical models proposed in the literature are simply design models. Some others, however, are able to predict off-design behavior by means of zero-dimensional models [38, 8, 1, 17, 18], one-dimensional or more sophisticated models of the components [26]. The models are referred to as zero-dimensional if only the thermodynamic transformations across the component are considered without simulating the internal flow field.

Various methods have been developed for adapting an engine model to a service engine at part load conditions [39, 40, 8, 14, 25, 12]. The majority of the methods are using the deck data to construct a compressor map and then through thermodynamics performance simulation codes match a series of target measurements at part load conditions. This process has being improved over the years by the inclusion of optimisation techniques like neural networks and genetic algorithms [41, 42, 43, 38]. The limitation of these methods is the fact that they are very case specific. This is supported by the fact that compressor performance maps are exclusive property of the engine manufacturer and not always available for determining the performance of an engine at off-design conditions. In addition variable geometry compressor scheduling is not always known and the effect that the variable inlet guide vanes have in the shape of a compressor map shape can not be predicted accurately at a zero dimensional models.

The developed off-design adaptation method is a novel method that combines a novel compressor map generation technique with the optimisation capabilities of a genetic

algorithm. It is a generic method which covers all the types of compressors from low pressure and high pressure and has the capacity to adapt the engine model to a series of off-design operating points.

To improve the accuracy of gas turbine performance prediction in the vicinity of engine design point, the compressor map coefficients that have been established in the compressor generation method are employed and an adaptive searching approach for a best set of the coefficients using a Genetic Algorithm is described. The proposed adaptation approach is then applied to a model aero gas turbine engine to test the effectiveness of the approach with several case studies. Analysis of the adaptation results and discussion of the advantages and disadvantages of the method are provided accordingly.

The compressor map coefficients defined in compressor map generation method are the ones that will be optimised for the off-design adaptation. These factors are tuned through the adaptation process by the genetic algorithm in order to fit the predicted off-design performance to the observed off-design performance. In order to build the Objective Function (OF) as determined in equation and perform the off-design adaptation process, a set of observed off-design performance measurements must be chosen as a target. This set of measurements will be matched with an iterative optimization procedure by repeatedly adapting the set of compressor map's coefficients until the Objective Function reaches its minimum.

Several case studies have been carried out in order to validate the developed adaptation method and test its accuracy and limitations. In addition a comparison has been made between the newly developed off-design adaptation method with an earlier adaptation approach developed by Lo Gatto and Li[39], in order to emphasize the advantages and disadvantages of the new adaptation method in terms of accuracy, computation time and future capabilities.

From a series of service engine data the test cases that have been carried out for this purpose are presented here.

Case No	Power Output (MW)	Target Data	Op. Points	Method Used	Map No
1	30.0-29.0	Simulation	2	New Adaptation	3
2	30.0-29.0	Simulation	2	Older GA Method	4
3	30.0-28.0	Simulation	4	New Adaptation	3
4	30.0-28.0	Simulation	4	Older GA Method	4
5	30.0-28.0	MEA	4	New Adaptation	3
6	30.0-28.0	MEA	4	Older GA Method	4
7	29.1-25.0	MEA	5	New Adaptation	3
8	23.9-20.0	MEA	4	New Adaptation	3
9	19.0-17.0	MEA	3	New Adaptation	3

Table 5.2: Off-Design Adaptation Test Cases

The range of the gas turbine's power output, which is the handle of the engine, starts from 30 MW up to 28 for the first six test cases and reaches a minimum of 17.0 MW for the last two test cases. The number of operating points that the adaptation process handles extends from two points up to 4 The last two test cases are have in total 12 operating points but these are not completed in one adaptation process but its a sum of three different adaptations each one having 4 points. The reason for this artificial technique of extending the range of adaptation is that many gas turbines, which have variable stator vanes for improving their part load performance, have different shape of compressor maps from high power setting to lower power setting, as this is the case for test cases 7 and 8.

The source of target data is through simulation for the first group of test cases and Manx Electricity authority service engine data for the second group.

The compressor map used for Lo Gatto adaptation method is a default compressor map provided by PYTHIA labeled "4" . The compressor map used for the new developed adaptation is labeled number "3" as this is a customised compressor map that is created by the developed compressor generation method and altered by the gas turbine to satisfy the initial design point conditions of any gas turbine engine. 5.2

Accuracy, computation time and limitations of the adaptation is affected by the number of off-design operating points that the process has to satisfy. A single point adaptation process is more accurate and significantly faster than a multiple point process. In real case scenarios a gas turbine user would prefer to have a series of off-design operating points adapted and therefore have a spherical overview of the gas turbine's performance for the maximum range of operation envelope, that a software programme

like PYTHIA can handle. The multiple point adaptation implies a single compressor map that would satisfy the total number of operating points. Therefore the test cases presented here are multiple point test cases in order to exhaust the capabilities and limitations of the adaptation process.

The first group of cases studies refers to the first four cases, where the observed off design performance at different off-design conditions are simulated with Cranfield performance simulation software PYTHIA, by choosing a default compressor map from PYTHIA as 'real' map. The off design simulation provides simulated measurements that have been considered as real for validating the off-design adaptation. At the off-design performance adaptation the compressor map generation technique has been employed in order to construct a initial map that will by modified by the genetic algorithm optimiser. The Genetic Algorithm is used to tune the coefficients of the compressor map to fit the predicted off-design performance to the "real" off-design performance. The user can modify the range of compressor map's coefficients when setting up the off-design adaptation therefore specify the searching space of the optimiser. A similar process is involved for employing the older adaptation method developed by Lo Gatto and Li[39]with the differences that the compressor map shape is altered only through the GA optimisation process, the user can not customise a compressor map before the adaptation , and the shape of the compressor map isn't fully controlled mathematically as the new developed method. A detailed comparison between the two method will be amplified in the discussion section of this chapter.

In the second group of case studies, the observed off design performance at different off-design conditions are data provided by MEA. This set of data are obtained at steady state conditions, selected from a series of available data at similar ambient conditions and finally have been corrected before the adaptation process. At the off-design performance adaptation the compressor map generation technique has been employed as previously described in the first group of case studies. In addition the same target data have been used for the adaptation method by Lo Gatto.

The sets of compressor coefficients that ensure a better match for both case studies are provided during the iterations. Once the Objective Function reaches its minimum, the best set of compressor map coefficients is obtained and can be used to produce more accurate off-design performance predictions.

5.1.1 Genetic Algorithms

A Genetic Algorithm (GA) that follows the idea of Darwin's natural evolution is one of the optimization searching techniques that have a wide range of applications[44, 45, 46, 47, 48]. The genetic algorithms (GAs) is an adaptive heuristic search algorithm based on the evolutionary needs of natural selection and genetics. Genetic algorithms are model based methods which the use a searching and optimization technique [27]. The GAs have the following three operations

1. Selection: chooses the strings for next generation based on the "survival of the fittest" criterion

2. Crossover: allows info exchange between strings by swapping parts of the parameter vector in order to get fitter strings

3. Mutation: introduces new or prematurely lost info in the form of random changes applied to random chosen vector components

A real coded GA is used to ensure accurate representation of individuals, the map's coefficients, within a GA population. GA is chosen in the off-design adaptation process to obtain the best set of compressor map's coefficients although it is generally known to be computationally more expensive than conventional optimization methods.

The quality of each set of coefficients within the GA population is assessed by its Objective Function (OF) . Thus, a value of OF approaching 0 indicates a good set of coefficients while a high value of OF represents a poor set. Along with the three conventional GA operators mentioned above, an elitism operation is used in this process [27]. With this operation, the worse strings in GA population of any generation are replaced with better strings generated by the three conventional GA operations and a fitter GA population is produced in the next generation. With this process it is always ensured that the average fitness of the whole population will improve from one generation to the next. The numbers of crossovers and mutations in each generation of the GA search is determined by the probabilities assigned to these operators. The probability of crossover is set at 35% whereas the probability of mutation is set at 30%. The accuracy of the results and the speed of the search depend on the number of maximum GA generations used and the size of the population. The higher number of maximum generations with larger size of population the more beneficial to a more accurate solution with the drawback of higher computational costs.

5.2 Methodology

The characteristics of a compressor can be represented by 4 characteristic variables: the corrected mass flow rate (WAC), the pressure ratio (PR), the isentropic efficiency (ETA) and the non-dimensional shaft rotational speed (N) relative to its design-point value. These 4 variables are linked together in two characteristic maps: the PR-WAC map and the ETA-PR map such that the operating point of the compressor can be uniquely determined once any 2 out of the 4 variables are specified. More details of the compressor characteristic maps can be found in the compressor generation chapter. In engine off-design performance adaptation analysis, the dependent measurable performance parameter vector ($\vec{P}$) is a function of the ambient and operating condition vector ($\vec{u}$) and the independent component characteristics vector.

$$\vec{P} = f(\vec{X}, \vec{u}) \tag{5.1}$$

Off-design performance adaptation is directly linked to the modification of the compressor characteristics that is part of $\vec{X}$. When a set of observed measurable off-design performance vector $\vec{P}_M$ is imposed as a target of the adaptation, the difference between the predicted measurements ($\vec{P}$) and the observed measurements ($\vec{P}_M$) can be evaluated by means of an Objective Function (OF) defined as follows

$$OF = \sum_{j=1}^{l} \sum_{i=1}^{k} a_{i,j} \left| \frac{P_{i,j} - P_{M_{i,j}}}{P_{M_{i,j}}} \right| * 100 \tag{5.2}$$

where $P_{M_{i,,j}}$ are the values of the observed measurements and $P_{i,j}$ are the corresponding predicted measurements. $a_{i,j}$ are the weighting factors taking into account the uncertainty of the individual measurements. The uncertainty analysis of the measurements goes beyond the scope of this study and the weighting factors are set for simplicity, where the number k is the total number of measurable parameters and l the number of off-design operating points of the adaptation process.

Based on Equations 5.1 and 5.2, the Objective Function OF can be expressed as a function of the $\vec{X}$ and the $\vec{u}$ vectors:

$$OF = F(\vec{X}, \vec{u}) \tag{5.3}$$

Thus, for a given off-design operating condition, the Objective Function (OF) is used to assess the accuracy of off design performance prediction; i.e. small value of the

Objective Function indicates accurate off-design prediction and vice versa. To achieve a good adapted off-design engine performance model or obtain a minimum Objective Function, an optimization technique may be used in the off-design adaptation process.

The off-design point adaptation uses the design point scaled compressor maps and rescales them with compressor map coefficients to match the required performance target by keeping the same design point [25]. The compressor map coefficients are extracted from these equations:

$$a = a_1 * N^{a_2} \tag{5.4}$$

$$b = PRdp * (b_1 * N^{b_2}) \tag{5.5}$$

$$ETAb = ETAb1 * (N^2) + ETAb2 * (N^1) + ETAb3 \tag{5.6}$$

The following seven coefficients $W1, W2, PR1, PR2, ETAb1, ETAb2, ETAb3$ determine the shape of the compressor map and are the ones from which genetic algorithm selects the best set in ordet to perform the off-design adaptation.

So the compressor map parameters of the adapted map pressure ratio, mass flow rate and efficiency are:

$$W_{final} = W1_{final} * N^{W2_{final}} \tag{5.7}$$

$$PR_{final} = PRdp * (PR1_{final} * N^{PR2_{final}}) \tag{5.8}$$

$$ETA_{final} = ETAb_{final} * \sqrt{1 - \left(\frac{W_{final}}{ETAa}\right)^2} \tag{5.9}$$

where the coefficients of the performance map have been selected by the genetic algorithm. Then the compressor map is scaled by the design point scaling factors in order to match the design point performance of the engine under investigation. These scaling factors are listed here

$$SF_{N,DP} = \frac{N_{DP}}{N_{Map}} \tag{5.10}$$

$$SF_{PR,DP} = \frac{PR_{DP}}{PR_{Map}} \tag{5.11}$$

$$SF_{WAC,DP} = \frac{WAC_{DP}}{WAC_{Map}} \tag{5.12}$$

$$SF_{ETA,DP} = \frac{ETA_{DP}}{ETA_{Map}} \tag{5.13}$$

The compressor map scaling that is performed in this off-design adaptation process is shown in figure 5.1.

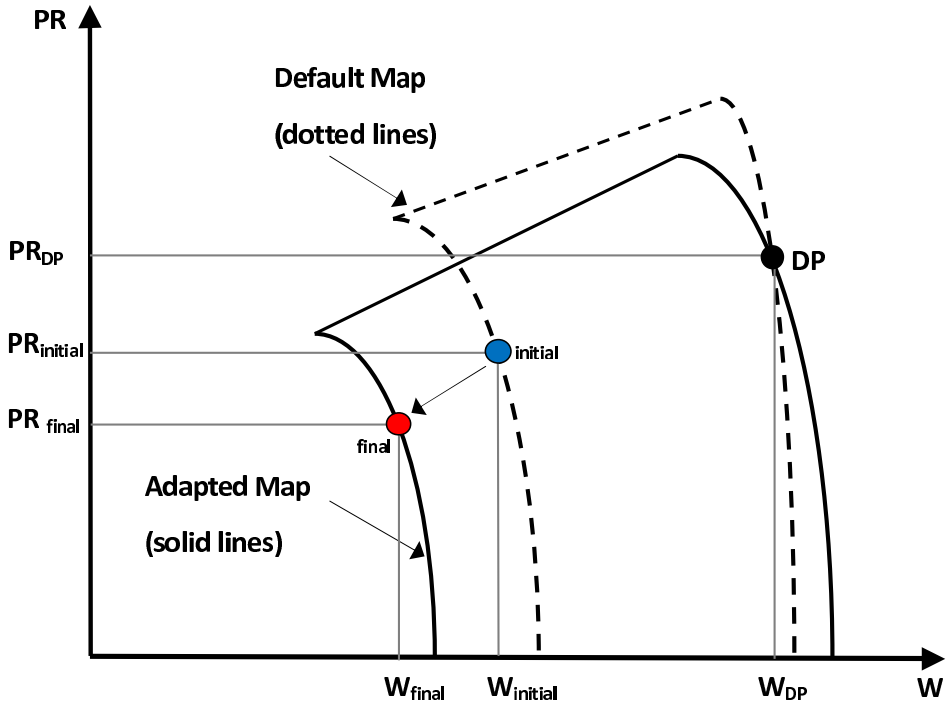

Figure 5.1: Off-Design Scaling of Compressor Map

The initial compressor map is in dotted lines and the adapted map in solid lines. The initial design point remains the same for both the initial map and the adapted map. The initially predicted off-design point lies in the default compressor map but doen't match the target measurements of the adpatation. Therefore by generating new compressor maps the speedlines are repositioned, through the modifications of the aforementioned map's coefficients, in order to match the target measuremenets. The final off-design operating point that satisfies these conditions is located in the adapted map.

The same process is followed for multiple off-design adaptation where a single

adapted compressor map has to satisfy accurately all the target data that each off-design operating point has. As seen in figure 5.2 the scaling takes into account two off-design operating points that their target measurments have to matched. Through compressor generation and the genetic algorithm optimiser the best set of coefficients is determined so as to generate a single compressor performance map for the aforementioned scope.

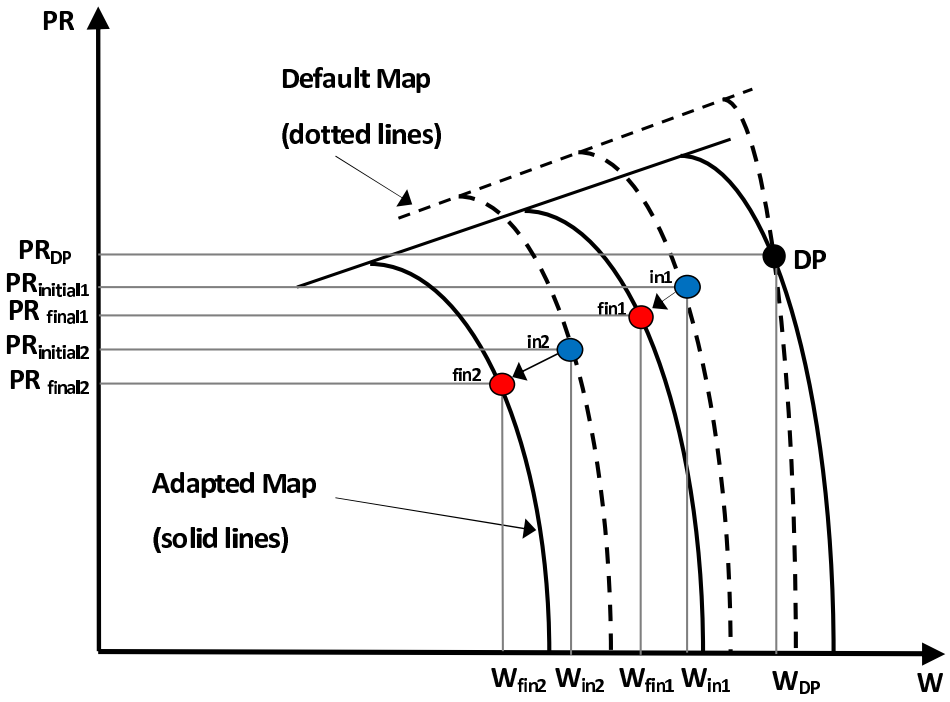

Figure 5.2: Multiple Operating Points Off-Design Scaling of Compressor Map

As noticed from figure 5.2 the distance of the second off-design operating point between the inital compressor map and the adapted map is greater than that of the first operating point. This is done intentionally in order to emphasize the fact that as the adaptation moves further away from the design point of the engine the accuracy of the prediction also drops.

Although this method incorporates genetic algorithms for adapting the performance of an engine at off design conditions, this optimisation procedure has various limitations. The accuracy of this adaptation method depends on the accuracy of the initial engine model, the quality of the compressor map used and on the distance, in terms of performance, that the pursued off-design point has with the nominal operating point.

The optimisation procedure for this adapatation mathod can be seen in figure 5.3.

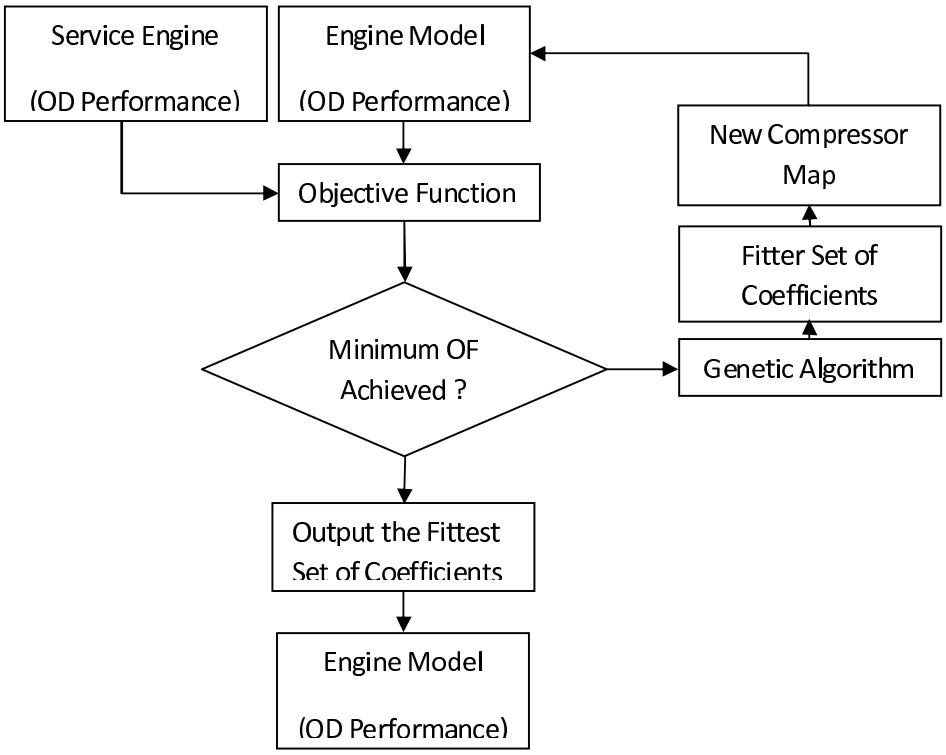

Figure 5.3: Procedure of Off-Design Adaptation

The objective function is the difference between the target measurments imposed by the service engine off-design performance and the off-design performance of the engine model developed. In order to minimise this objective function the genetic algorithm optimiser is employed. The genetic algorithm initially generates a, specified by the user, number of possible solutions by varying the values of the compressor map's coefficients over a specified range. It then calls Turbomatch code to get the off-design performance results of the initial population of compressor maps. The fitness of each set of coefficients is then determined. From a series of possible solutions the ones that present the best fitness are selected for the next generation that is going to occur though crossover and mutation. Finally this process of evaluation of each individual solution is repeated through all the processsess of the GA until the limitsa of population size and generations have been reached. Then the best set of compressor map coefficients that through turbomatch simulation present the lowest objective function, therefore the maximum fitness is provided to the gas turbine user.

5.3 Application

To demonstrate the effectiveness of the off-design performance adaptation, different cases have been tested by adapting different sets of maps of the developed engine model's compressor brick. Since an engine model, that simulates accurately the service engine under investigation, has been developed a set of to be adapted parameters has been selected in order to match the target measurements of the engine at off-design conditions. The list of the selected measurable parameters for the off design performance adaptation is given in table5.4. The nominal operating point for this configuration is at 30 MW with the power output set as the handle of the engine.

No	Symbol	Performance Parameter	Units
1	P3	Compressor Discharge Pressure	atm
2	T3	Compressor Discharge Temperature	K
3	P6	High Pressure Turbine Pressure	atm
4	T6	High Pressure Turbine Temperature	K
5	T8	High speed Power Turbine Temperature	K
6	ff	Fuel Flow	kg/s

Table 5.4: Measurable Performance Parameters

Test Cases 1 & 2

In the first test case the method has been validated by using as reference the simulations of turbomatch at off design conditions from 30 MW down to 29 MW with a step of 0.5 MW, with a default compressor map available from turbomatch labeled compressor map 4. Then the simulated results have been compared with the ones produced by the developed off-design adaptation method, which incorporates compressor generation ie. a different compressor map denoted map 3. The results of the new developed method indicate a very close match between the "real" and adapted measurements as seen from table 5.6.

Power Output (MW)	No	Parameter	"Real"	Earlier Adaptation	Developed Adaptation
30	1	P3	22.1	22.1	22.1
	2	T3	753.65	753.65	753.65
	3	P6	4.529	4.529	4.529
	4	T6	1119.15	1119.15	1119.15
	5	T8	789.55	789.55	789.55
	6	ff	1.752	1.752	1.752
29.5	1	P3	21.860	21.873	21.868
	2	T3	750.66	752.463	750.9695
	3	P6	4.488	4.4855	4.4885
	4	T6	1114.49	1116.44	1114.515
	5	T8	787.30	788.871	787.325
	6	ff	1.7273	1.72865	1.727301
29	1	P3	21.62	21.655	21.636
	2	T3	747.65	749.2665	748.225
	3	P6	4.448	4.4465	4.4485
	4	T6	1109.77	1110.567	1109.785
	5	T8	785.03	785.675	785.075
	6	ff	1.7025	1.70275	1.70254

Table 5.6: Test Cases 1 & 2: Off-Design Adaptation Results for "Real" data with Developed Adaptation Method and Earlier Adaptation by Lo Gatto

In the second test case again the simulations results from turbomatch off-design simulation, for the same power range and with compressor map 4, have been used as targets for the earlier adaptation method developed by Lo Gatto. In contrary to the first test case the engine model engaged the compressor map 4 in the adaptation process. The comparison between the two adaptation methods, that have the same targets and the same engine models, provides a good insight in the effect that the compressor map generation method has in the off-design adaptation.

The accuracy of the new developed adaptation is higher than the older method as seen from figure 5.4 where each targeted measurement is plotted against the power output of the engine for the whole range of simulation.

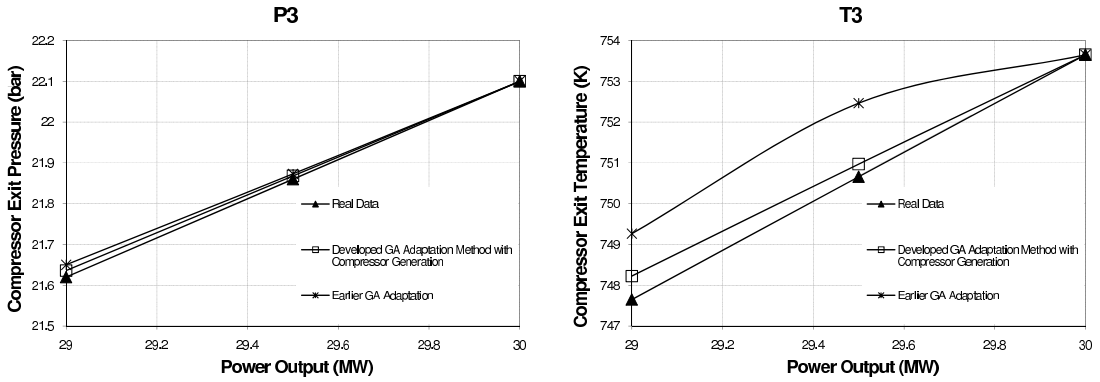

(a) P3

(b) T3

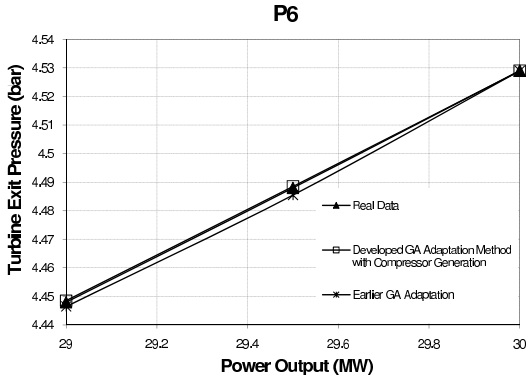

(c) P6

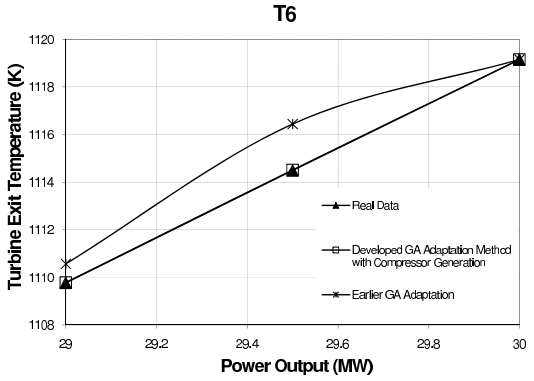

(d) T6

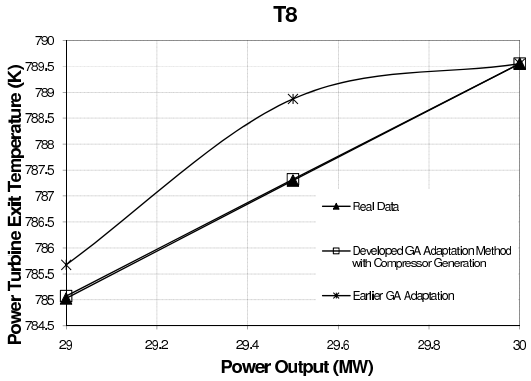

(e) T8

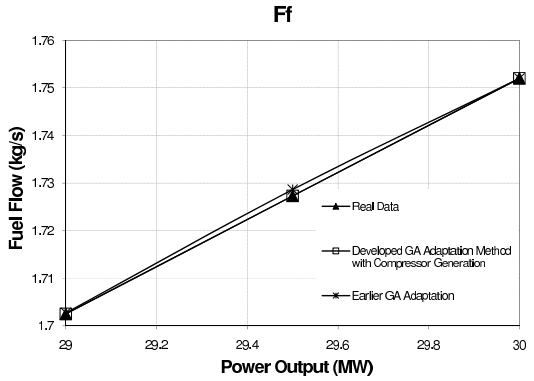

(f) Ff

Figure 5.4: Prediction of Test Case 1 and 2 Measurable parameters after adaptation vs "Real" data

As seen from the figure above the adaptation process by Lo Gatto presents a significant fluctuation, especially at the temperature measurements, at the first off-design

operating point and smoothes after that. This is mainly because the scaling of the compressor map in this method is rather linear, as every point of the compressor map is multiplied by the same scaling factor, which is in contrast to the, analytically expressed and controlled, compressor map that is employed in the new developed adaptation.

For these two operating point adaptation the developed method is capable of matching the target measurements quite accurately with the highest error being less than 10^{-1} %. In addition the developed adaptation, which incorporates compressor generation, follows the same trend with the target measurements which justifies the validity of the method. From the next figure the error that each target parameter has in the adaptation for test cases 1 and 2 against the power output of the engine can be seen.

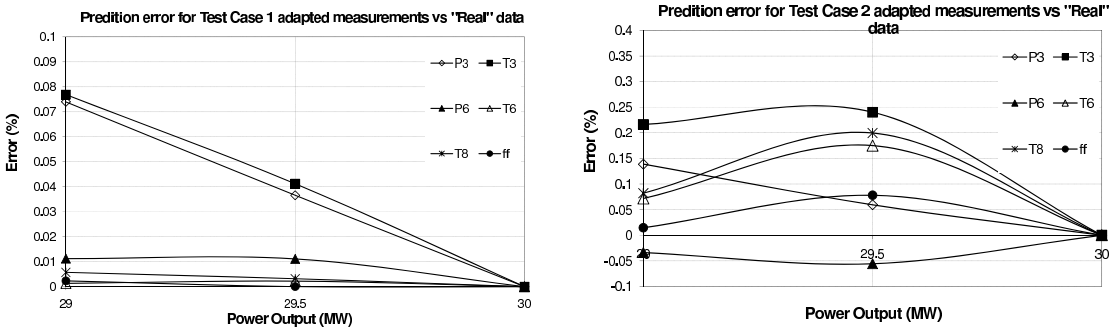

(a) Test Case 1: Developed Adaptation

(b) Test Case 2: Earlier Adaptation

Figure 5.5: Prediction error for Test Case 1 and 2 adapted measurements vs. "real" data

These initial test cases proved the validity of the new developed adaptation method and its superiority over the earlier adaptation. In the next test cases more operating points have been selected as targets as by increasing the number of points the accuracy of the adaptation is going to be affected.

Test Cases 3 &4

In the third test case which is in other words an expanded version of test case 1 the method has been tested from 30MW down to 28MW with the same step and compressor map as before. Then the simulated results have been set as the targets of the developed adaptation, that used compressor map map 3. The measurement targets have been matched successfully by the adapted engine model, as seen in table 5.8.

Power Output (MW)	No	Parameter	"Real"	Earlier Adaptation	Developed Adaptation
30	1	P3	22.1	22.1	22.1
	2	T3	753.65	753.65	753.65
	3	P6	4.529	4.529	4.529
	4	T6	1119.15	1119.15	1119.15
	5	T8	789.55	789.55	789.55
	6	ff	1.752	1.752	1.752
29.5	1	P3	21.860	21.886	21.876
	2	T3	750.66	754.266	751.279
	3	P6	4.488	4.483	4.489
	4	T6	1114.49	1118.39	1114.54
	5	T8	787.30	790.442	787.35
	6	ff	1.7273	1.73	1.727302
29	1	P3	21.62	21.68	21.652
	2	T3	747.65	750.883	748.8
	3	P6	4.448	4.445	4.449
	4	T6	1109.77	1111.363	1109.8
	5	T8	785.03	786.32	785.12
	6	ff	1.7025	1.703	1.70258
28.5	1	P3	21.379	21.452	21.4277
	2	T3	744.62	747.71	746.466
	3	P6	4.407	4.406	4.408
	4	T6	1104.97	1105.68	1105.16
	5	T8	782.71	783.3	782.87
	6	ff	1.6777	1.678	1.6778
28.0	1	P3	21.138	21.209	21.202
	2	T3	741.55	744.667	744.023
	3	P6	4.366	4.3651	4.367
	4	T6	1100.1	1100.94	1100.36
	5	T8	780.35	781.051	780.56
	6	ff	1.6528	1.6535	1.653

Table 5.8: Test Cases 3 & 4: Off-Design Adaptation Results for "Real" data with Developed Adaptation Method and Earlier adaptation by Lo Gatto

The fourth test case again is similar to test case 2 with the only difference being

the addition of two extra operating points and everything else being kept the same as before. This earlier adaptation process presents is tabulated in the table 5.8 and the comparison remarks remain the same for this test case as well.

The measurements are plotted against power as before and it can be noticed from figure 5.6 that the developed adaptation follows a the similar linear trend with the off-design simulated measurements. As the power drops, ie moving further away from the design point of the engine model the adaptation error increases. The earlier adaptation method although it presents the same fluctuation in temperatures it eases out in the final operating points.

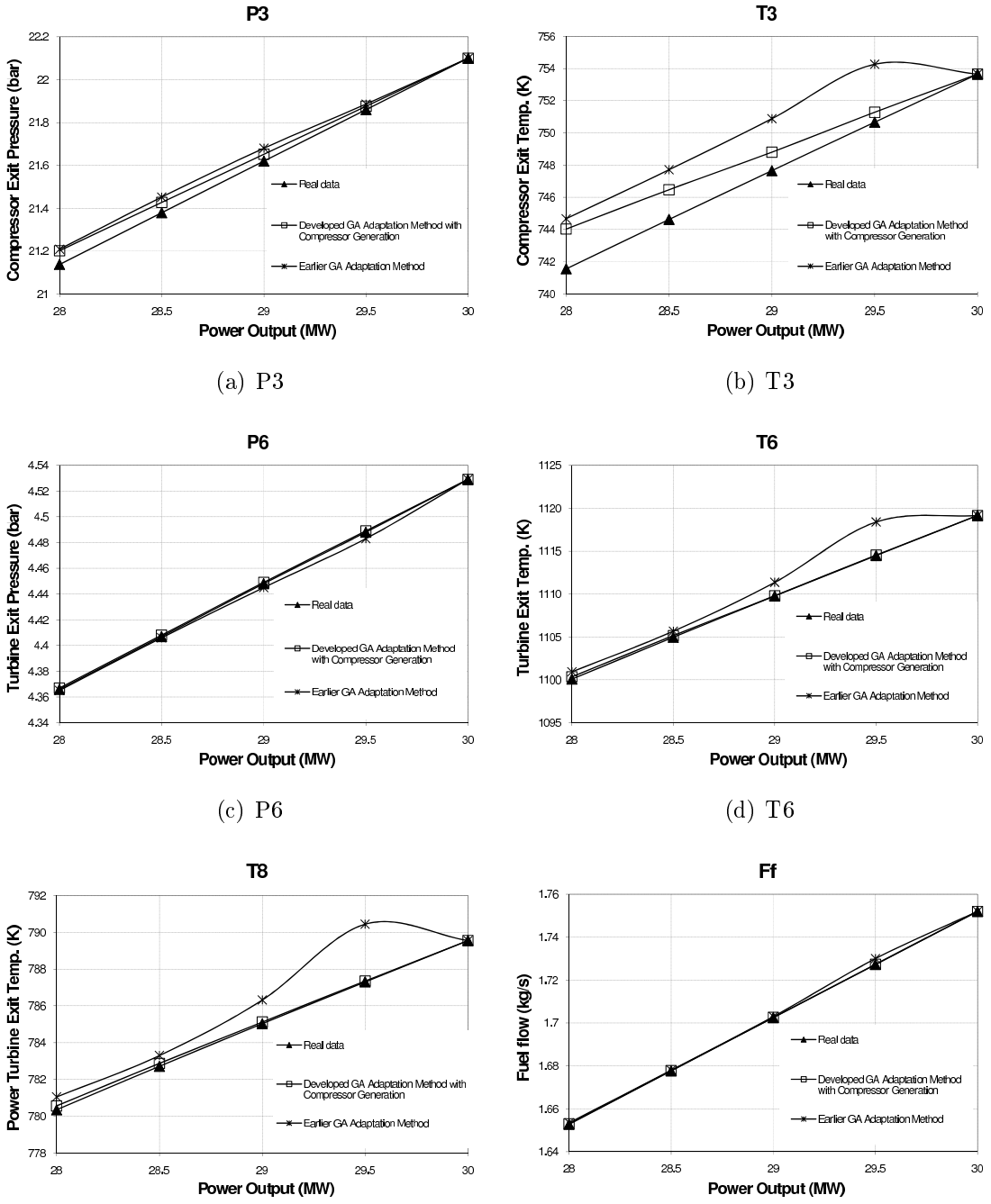

(a) P3 (b) T3

(c) P6 (d) T6

(e) T8 (f) Ff

Figure 5.6: Prediction of Test Case 3 and 4 Measurable parameters after adaptation vs "Real" data

Taking into consideration the linear compressor map scaling of the earlier method it isn't capable of satisfying accurately all the operating points targeted. This behavior is

also due to the fact that the method has prioritised the matching of the last operating point of a multi point adaptation rather than an average distribution of qualitative adaptation.

For these four point test cases the developed method has a maximum adaptation error almost 5 times bigger than the test case 1, but it is still in the region of less than 1% as seen in figure 5.7.

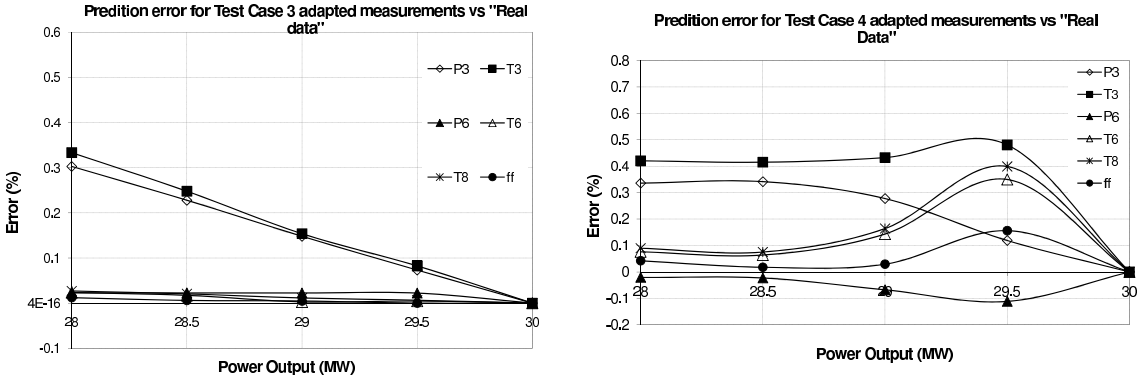

(a) Test Case 1: Developed Adaptation

(b) Test Case 2: Earlier Adaptation

Figure 5.7: Prediction error for Test Case 3 and 4 adapted measurements vs. "real" data

It is also noticed that the pressure and the temperature at the exit of the compressor present the highest error compared to the other measurements and this is due to the fact that lines of high rotational speed of the compressor map are almost vertical. Therefore the pressure of the compressor exit that will be extracted from the compressor map is dependent upon the number of points that each line is able to contain.

In the compressor map generation process each speedline has 5 points that are evenly distributed along the speedline. It is obvious that this affects the prediction of the pressure and temperature parameters of the compressor exit, however it isn't affecting the adaptation process as the accuracy achieved is of high order. Although a higher number of points per speedline can resolve this issue, it will result in an undesirable computation time penalty.

The key characteristic of the new developed method, apart from the compressor generation, is its ability to handle multiple point adaptation successfully. The first four test case have tested and validated the new developed adaptation, and will be further tested in the following test cases where service engine data available from MEA will be matched.

Test Cases 5 & 6

In the fifth test case, the observed off design performance at different off-design conditions are data provided by MEA again from 30 MW down to 28 MW with a step of 0.5 MW. This set of data are obtained at steady state conditions, averaged at each power setting and corrected to the exact same ambient conditions for adaptation purposes.

At the off-design performance adaptation the compressor map generation technique has been employed as previously. The results show that there is a similar trend in the variation of the target measurements and the error between the actual MEA and the adaptation results are of the magnitude of 10^{-2}. The results for both set of data are tabulated in table 5.10. The maximum errors are observed as expected in the lowest power setting of the engine which is at 28MW.

Power Output (MW)	No	Parameter	MEA	Earlier Adaptation	Developed Adaptation
30	1	P3	22.1	22.1	22.1
	2	T3	753.65	753.65	753.65
	3	P6	4.529	4.529	4.529
	4	T6	1119.15	1119.15	1119.15
	5	T8	789.55	789.55	789.55
	6	ff	1.752	1.752	1.752
29.5	1	P3	21.9	22.01	21.91
	2	T3	749.95	756.55	749.88
	3	P6	4.49	4.502	4.495
	4	T6	1111.15	1119.48	1111.31
	5	T8	785.65	791.92	785.33
	6	ff	1.728	1.737	1.725
29	1	P3	21.71	21.81	21.72
	2	T3	746.55	751.27	746.46
	3	P6	4.441	4.446	4.45
	4	T6	1104.15	1107.94	1104.45
	5	T8	781.75	784.59	781.17
	6	ff	1.704	1.707	1.699
28.5	1	P3	21.51	21.64	21.52
	2	T3	744.45	749.54	744.35
	3	P6	4.400	4.410	4.416
	4	T6	1099.15	1102.82	1099.75
	5	T8	780.45	783.14	779.60
	6	ff	1.680	1.684	1.674
28.0	1	P3	21.317	21.44	21.34
	2	T3	742.95	747.93	742.75
	3	P6	4.342	4.351	4.3664
	4	T6	1095.15	1098.72	1095.91
	5	T8	778.65	781.29	777.37
	6	ff	1.672	1.679	1.665

Table 5.10: Test Cases 5 & 6: Off-Design Adaptation Results for MEA data with Developed Adaptation Method and Earlier adaptation by Lo Gatto

The predicted off-design measurable parameters which are the target measurements

of this adaptation process are plotted against the service engine data in figure 5.8. The service engine data follow a different trend than the first test case where the "real" data where actually off-design simulation results. The reason for this variation of target parameters against the power output setting of the service engine has to do with the data collection process from the MEA. It is fundamental at this point to explain the logic under which the power station operates. Since MEA has a 2 gas generators, 2 steam generators and one steam turbine configuration the operation of the power plant is driven by the island's demand for electricity and when applicable by the importing demand that UK mainland has from the island. Therefore MEA operates the power station by having 2 gas turbines running at part load conditions early in the day and reaching the nominal load at peak demand hours which are in the afternoon. At the end of the day one engine is shut down since demand has dropped, which leaves only the one engine operating at part load conditions before the next day comes and this is repeated.

It becomes clear that the data collected from the control systems have to undergo some preprocessing and corrections should be applied as steady state conditions data for such a wide operation regime and duration are extremely rare. The data used for this test case have been collected from single day of operation at the same operating conditions and very similar ambient conditions, in order to minimise uncertainties through corrections. As long as a good sample of data for each power setting has been averaged it was then corrected back to the original nominal point ambient conditions and then a single operating point was assigned to each power setting. The PYTHIA software has a parameter correction utility at the at the main window. However the off-design adaptation has the capacity to include different ambient conditions at each operating point apart from the handle of the engine model which is compulsory for this process.

The sixth test case employs the older adaptation method by using a default compressor map of PYTHIA as in test cases 2 and 4. The results indicate the same fluctuations as discussed before and as seen through figure 5.8 .

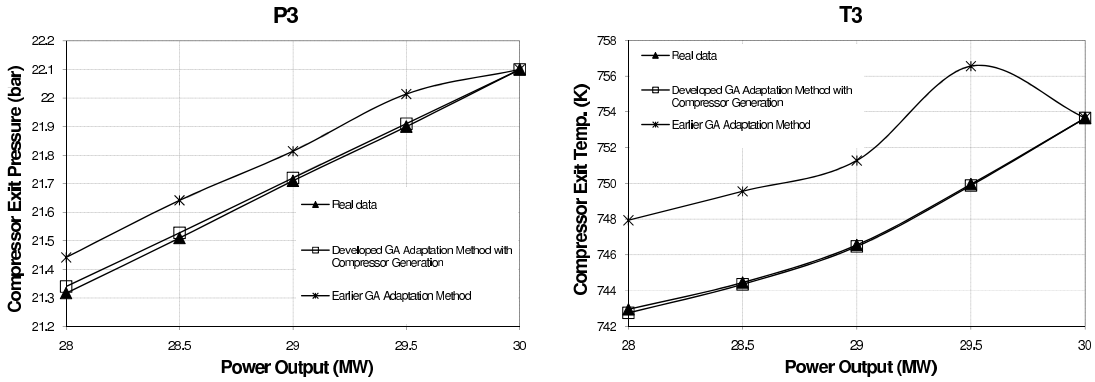

(a) P3

(b) T3

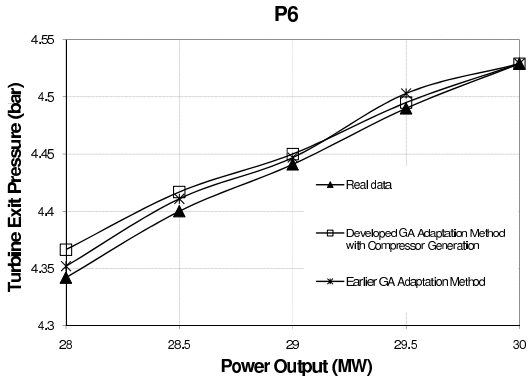

(c) P6

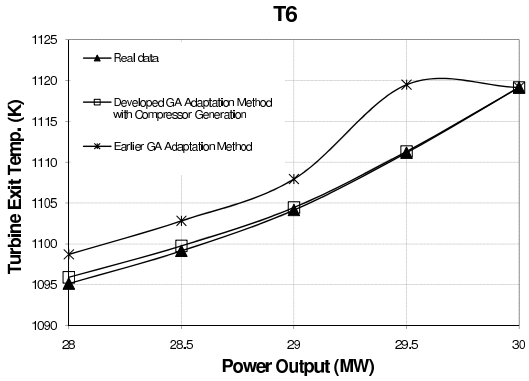

(d) T6

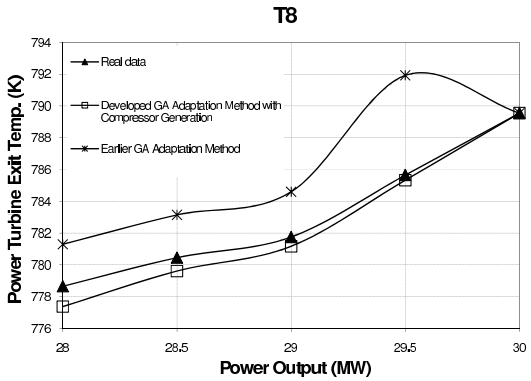

(e) T8

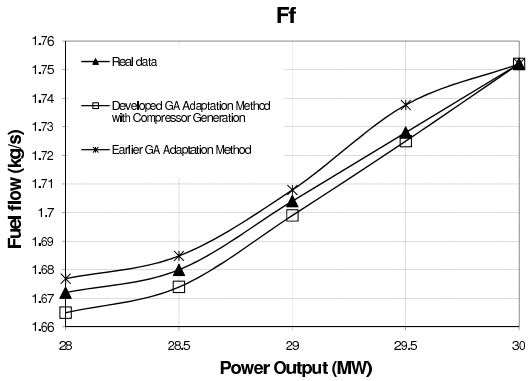

(f) Ff

Figure 5.8: Prediction of Test Case 5 and 6 Measurable parameters after adaptation vs MEA data

The error of the new developed adaptation is kept at the same levels as before with the highest error observed at the compressor exit temperature and pressure as seen in

figure 5.9. The older adaptation method has a maximum error of 1% which in terms of temperatures is translated in 8 to 9 deg. K. Although 1% error is quite normal, in terms of performance prediction of a gas turbine which is very sensitive on the gas path measurements this error is significant which in turn affects the accuracy of any diagnostic analysis.

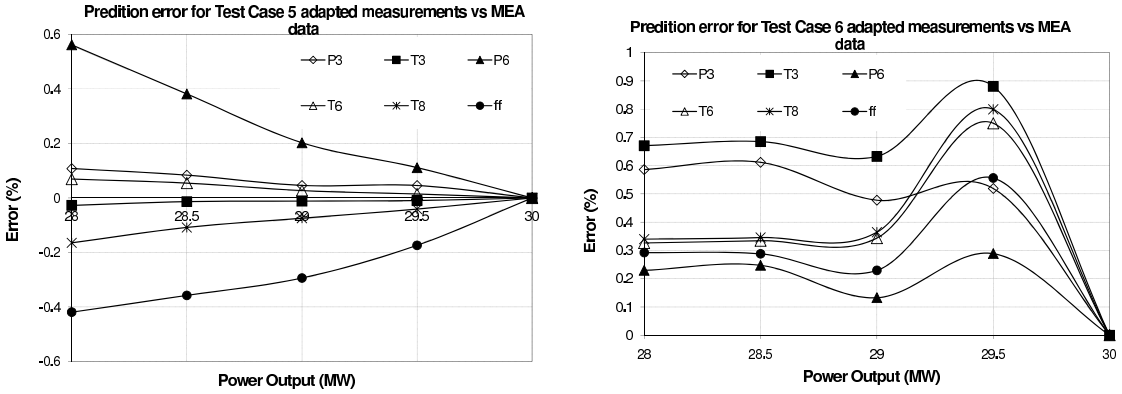

(a) Test Case 1: Developed Adaptation

(b) Test Case 2: Earlier Adaptation

Figure 5.9: Prediction error for Test Case 5 and 6 adapted measurements vs. MEA data

Test Cases 7, 8 & 9

In this group of test cases the part load performance of the service engine from 29 MW to 17 MW has been adapted. During the operation of the gas turbine a performance test has been carried over. At the shutdown of one gas turbine of MEA, which normally takes 10 min, this process has been expanded for 3 hours and a useful set of data have been collected. The gas turbine would reduce the power output in several steps and would operate at each power setting for at least 15minutes in order for the engine to stabilise its operation. This process has been repeated for several power levels before reaching a minimum which in this case is 17MW. The bunch of data collected requires further preprocessing before being set as targets for the adaptation process.

The adaptation process is not able to handle the whole range of this off-design operating points in one go. The reason for this is that the adaptation cannot handle operating points that are at least 7% higher or lower than the operating point of the gas turbine at which the engine model has been initially adapted through design point adaptation. This happens because the design point adaptation makes the model extremely accurate and tight in terms of flexibility in order to satisfy all the target measurements.

The result of this limits the off-design adaptation to reach much lower or higher than design point conditions power levels, speed levels or turbine entry temperature levels depending on what is the handle of the engine.

Turbomatch, which is the core code of performance simulation of PYTHIA, doesn't converge at such cases as a single compressor map cannot capture the operation of a gas turbine for such a range. This is mainly due to the fact that component characteristics especially the ones of the compressor change significantly for a variable geometry compressor. Although the assumption that a fixed compressor geometry map allows for successful performance adaptation close to design point conditions or in other word close the point at which the engine model has been initially adapted this is not the case for adaptation of the engine model at operating points far away from this benchmark. The off-design simulation has the capacity to run at the lowest power levels as its an iterative procedure which takes into account the operating conditions of the earlier step from the one it simulates. For example when simulating the off-design performance of an engine from 30 MW to 20 MW the simulation code will start at 30MW which is the design point and with a, predetermined by the user, step will then run the 29 MW case if the step is 1MW. Having completed the first step it will then start from 29 MW in order to reach the 28MW setting. This is not the case for the off-design adaptation where the starting point will always be the design point and therefore the program is not capable of handling large gaps in terms of performance.

Therefore in this test case the adaptation of the engine model occurs in three different steps. In order to have as less steps as possible the design point adaptation was performed at the middle operating point of each power output setting. In other words in the 29 -25 MW power output range the engine model has been adapted at 26.79 MW in order to allow for the +/- 7% allowance limit that off-design adaptation can perform in one simulation. The same applies to the other two test cases 8 and 9.

The results of test cases 7, 8 and 9 can be seen from tables 5.12, 5.14 and 5.16 respectively.

Power Output (MW)	No	Parameter	MEA	Developed Adaptation	Error (%)
29.15	1	P3	22.31	22.41	0.412
	2	T3	770.81	770.71	-0.013
	3	P6	4.491	4.499	0.168
	4	T6	1116.02	1115.09	-0.083
	5	T8	800.11	805.90	0.723
	6	ff	1.733	1.755	1.259
28.05	1	P3	21.85	21.91	0.240
	2	T3	765.01	764.99	-0.002
	3	P6	4.401	4.405	0.090
	4	T6	1103.07	1102.61	-0.043
	5	T8	795.62	798.70	0.386
	6	ff	1.684	1.695	0.679
26.79	1	P3	21.33	21.33	0
	2	T3	758.36	758.36	0
	3	P6	4.297	4.297	0
	4	T6	1088.24	1088.24	0
	5	T8	790.48	790.48	0
	6	ff	1.627	1.627	0
26.03	1	P3	21.01	20.96	-0.265
	2	T3	754.35	754.40	0.006
	3	P6	4.234	4.23	-0.117
	4	T6	1079.29	1080.26	0.089
	5	T8	787.37	786.15	-0.156
	6	ff	1.593	1.587	-0.386
25.08	1	P3	20.61	20.49	-0.625
	2	T3	749.33	749.37	0.004
	3	P6	4.156	4.145	-0.285
	4	T6	1068.11	1070.03	0.179
	5	T8	783.50	780.62	-0.367
	6	ff	1.550	1.536	-0.890

Table 5.12: Test Cases 7 : Off-Design Adaptation Results for MEA data with Developed Adaptation Method

Power Output (MW)	No	Parameter	MEA	Developed Adaptation	Error (%)
23.98	1	P3	20.15	20.36	0.994
	2	T3	743.53	744.26	0.097
	3	P6	4.066	4.090	0.578
	4	T6	1055.16	1054.96	-0.019
	5	T8	779.01	784.22	0.668
	6	ff	1.500698	1.522	1.419
23.10	1	P3	19.79	19.90	0.546
	2	T3	738.89	739.30	0.055
	3	P6	3.994	4.009	0.372
	4	T6	1044.81	1044.69	-0.011
	5	T8	775.41	778.19	0.358
	6	ff	1.461	1.472	0.800
22.05	1	P3	19.35	19.35	0
	2	T3	733.35	733.35	0
	3	P6	3.907	3.907	0
	4	T6	1032.45	1032.45	0
	5	T8	771.13	771.13	0
	6	ff	1.413	1.413	0
20.05	1	P3	18.51	18.22	-1.603
	2	T3	722.79	721.96	-0.115
	3	P6	3.743	3.707	-0.972
	4	T6	1008.90	1010.93	0.200
	5	T8	762.97	759.58	-0.443
	6	ff	1.323	1.303	-1.492

Table 5.14: Test Cases 8: Off-Design Adaptation Results for MEA data with Developed Adaptation Method

Power Output (MW)	No	Parameter	MEA	Developed Adaptation	Error (%)
19.04	1	P3	18.09	18.18	0.519
	2	T3	717.46	717.84	0.052
	3	P6	3.660	3.673	0.353
	4	T6	997.01	996.91	-0.010
	5	T8	758.84	761.42	0.340
	6	ff	1.277	1.287	0.760
18.03	1	P3	17.67	0.045	0
	2	T3	712.13	-0.009	0
	3	P6	3.577	0.111	0
	4	T6	985.13	0.014	0
	5	T8	754.72	-0.040	0
	6	ff	1.232	-0.173	0
17.01	1	P3	17.24	17.20	-0.251
	2	T3	706.75	706.79	0.005
	3	P6	3.493	3.489	-0.111
	4	T6	973.12	973.94	0.084
	5	T8	750.56	749.44	-0.148
	6	ff	1.186	1.181	-0.366

Table 5.16: Test Cases 9: Off-Design Adaptation Results for MEA data with Developed Adaptation Method

What can be easily noticed from the previous tables is that the error is highest at the boundaries of each power range since the engine model has been adapted initially at the middle operating point of each test case. This could be avoided by always adapting the operating point of each test case at its maximum power output. However this would reduce the margin of adaptation, therefore this approach would require extra test cases to be simulated in order to cover the same range of operation. The maximum average error is noticed in fuel flow which is 0.89% followed by the one in pressure at the exit of the compressor which is 0.6 %. The general trend that the adapted measurements follow in relation to the target parameters can be seen in figure 5.10.

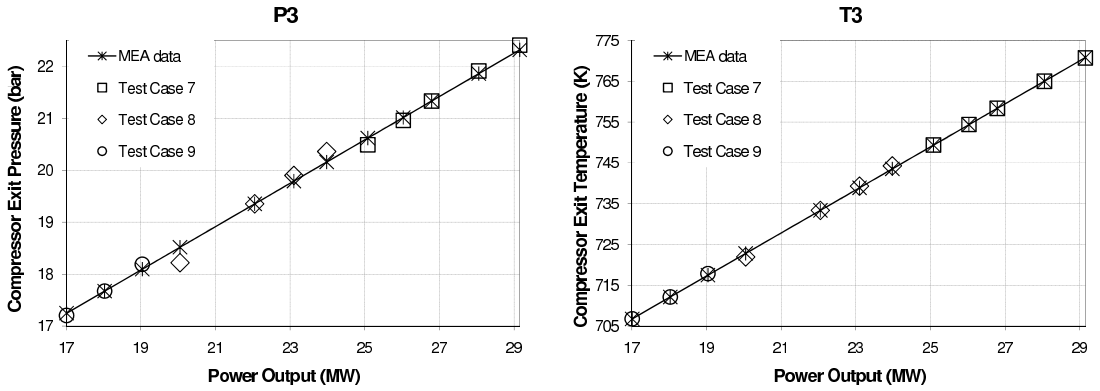

(a) P3

(b) T3

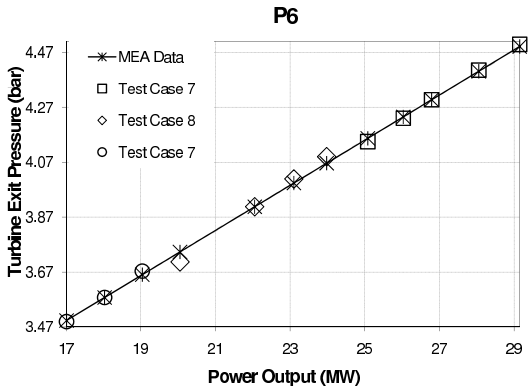

(c) P6

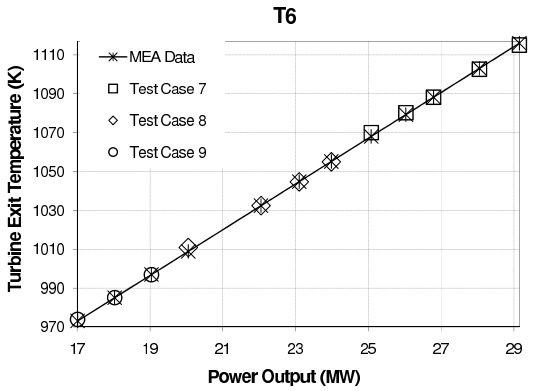

(d) T6

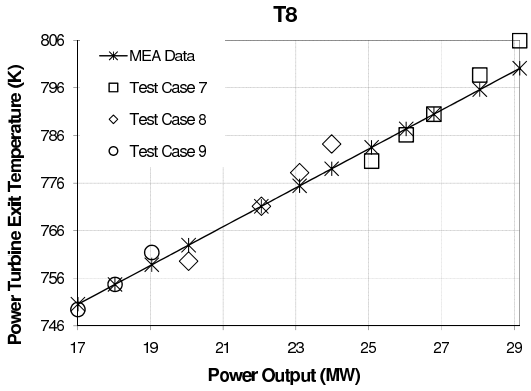

(e) T8

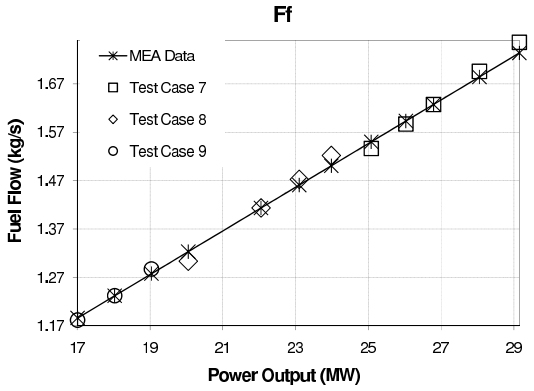

(f) Ff

Figure 5.10: Prediction of Test Case 7, 8 and 9 Measurable parameters after adaptation vs MEA Data

As expected the error of each parameter changes sign before and after the operating point, that the engine model has been initially adapted through the design point

Test Case	Operating Points	No of Gens	Size of Population	GA Fitness	Minimum OF	Computation Time (s)
1	2	1	20	0.81	0.23	24
2	2	1	20	0.65	0.52	20
3	4	1	10	0.54	0.84	60
4	4	1	10	0.36	1.81	30
5	4	1	20	0.79	0.26	100
6	4	1	20	0.55	0.82	60
7	5	2	20	0.71	0.27	140
8	4	2	20	0.78	0.25	120
9	3	2	20	0.80	0.24	110

Table 5.18: Multiple Point Off-Design Adaptation Simulation Properties

adaptation capability of PYTHIA. These test cases have given rise to the limitations that the developed adaptation has. The strong features of the developed adaptation and its limitations are discussed in the next section of the chapter.

5.4 Discussion of Results

A group of key parameters that have to be taken into consideration for all the test cases is the computation time in relation to the genetic algorithm properties and the number of operating points adapted.Typically for a single point adaptation with 5 generations and 50 being the population size the process takes almost a minute. The multiple point adaptation takes considerably longer to converge with the time being almost 6 minutes for 5 generations each one having a population size of 50. The maximum fitness achieved for the multiple point adaptation test cases, that have been presented, is in the range of 70 to 80% with the minimum objective function lying between 0.2 and 0.4. The table 5.18 summarises the simulation properties for all the test cases.

The developed adaptation takes slightly longer than the older adaptation method to converge as seen in Test case 1 and 2 respectively. However its accuracy is superior to the earlier method as seen from the fitness of the genetic algorithm which is 16% more accurate. The minimum objective function is at also improved in comparison with the earlier method.

In test cases 3 and 4 the size of population is a limiting factor for the accuracy of the adaptation and this is justified by the fitness values and minimum objective function,

which for the earlier adaptation method is unacceptable as it is greater than 1.0. The time for the developed adaptation to converge is double that of the older adaptation method and this occurs due to the compressor generation method that is integrated into the adaptation process. Although the compressor map generation itself is quite fast in terms as it is an analytical process it is called multiple times from the genetic algorithm subroutine which requires extra time, especially the intermediate steps of reading and writing the textfile of the map, before the program converges .

In test cases 5 and 6 where the population size has been increased so did the accuracy and the computation time of the adaptation. The fitness of the developed adaptation reaches a level of 0.79 which is very accurate for a multiple point adaptation and supported by the minimum objective function which is kept as low as possible with a value of 0.26. The extra time required for this test case cannot be overweighted by the earlier adaptation method in test case 6 as it is not accurate enough.

In test cases 7, 8 and 9 the number of generations have been increased and this increased the computation time which exceeds the 2 minutes for test cases 7 which has 5 points. Even in these multiple point cases the accuracy of the developed method remains its strong feature. A collection of bar charts which summarises the aforementioned characteristics of the developed off-design adaptation method can be seen in figures 5.11, 5.12 and 5.13.

Figure 5.11: GA Fitness for Adaptation Test Cases

Figure 5.12: Minimum Objective Function for Adaptation Test Cases

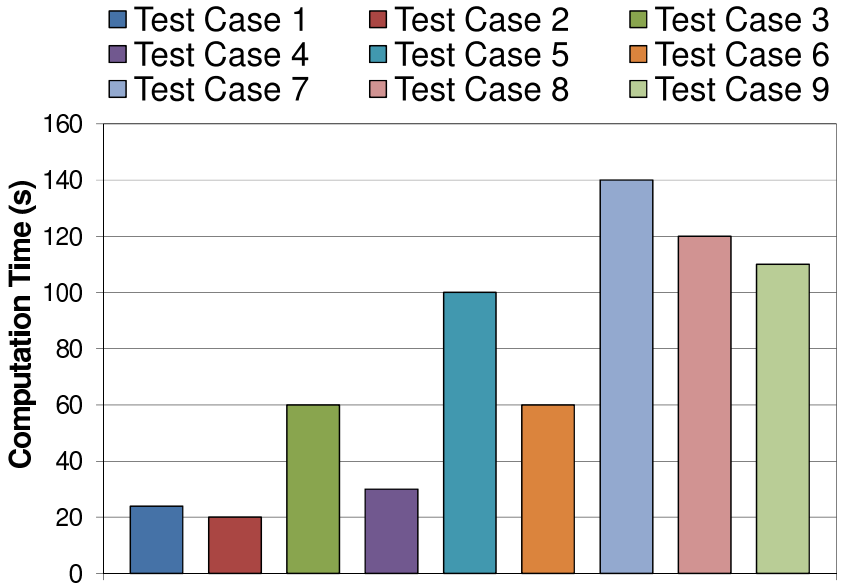

Figure 5.13: Computation Time for Adaptation Test Cases

The setting window of PYTHIA's off-design adaptation along with the adaptation result can be seen from figure 5.14.

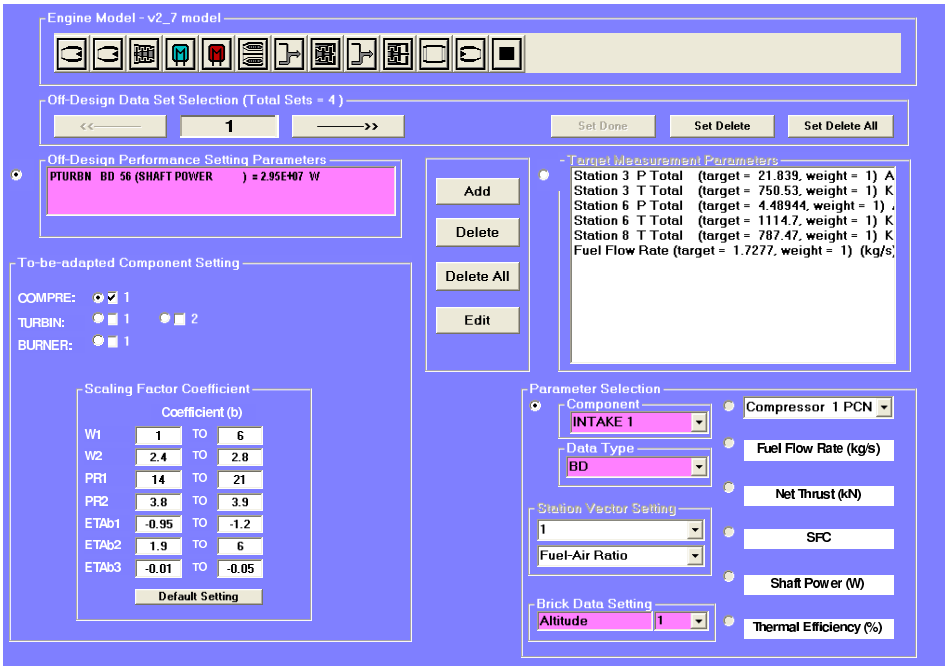

(a) Adaptation Setting

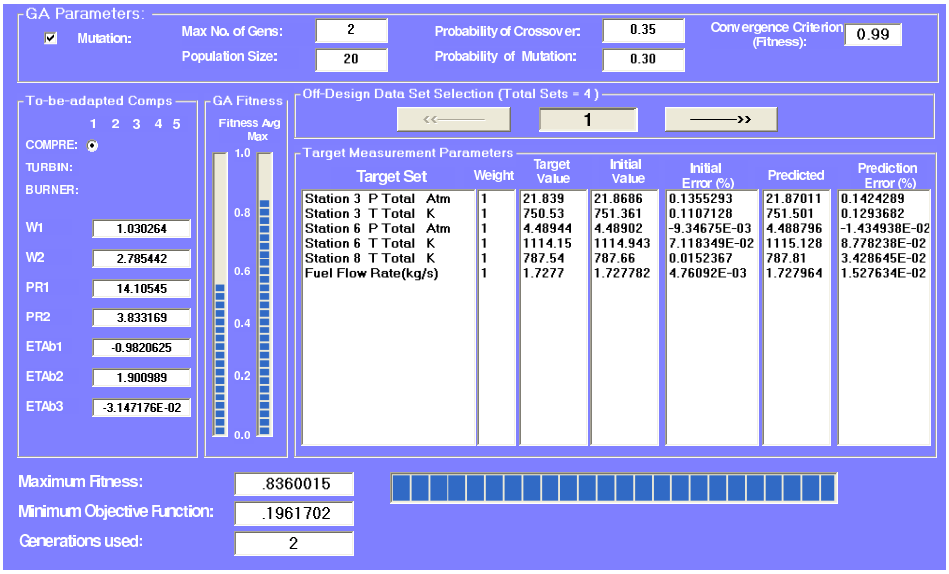

(b) Adaptation Result

Figure 5.14: Off-Design adaptation setting and Results window

The user has to set the operating conditions of the gas turbine, in the left pink framed window, which is the power output for this engine configuration and then select the target measurements from the right window as seen in figure 5.14a. The result window provides the user with the coefficients of this adaptation process, which are then used

for representing the adapted compressor map, the properties of the genetic algorithm optimiser along with the simulated measurements results and their corresponding errors as in figure 5.14b.

Since the adaptation has converged the programme provides the user with a comparison graph of the compressor map before and after the adaptation process, in black and red colour respectively, in order to aid the user determine the direction at which the compressor map has been shifted to match the off-design operating point as seen in figure 5.15.

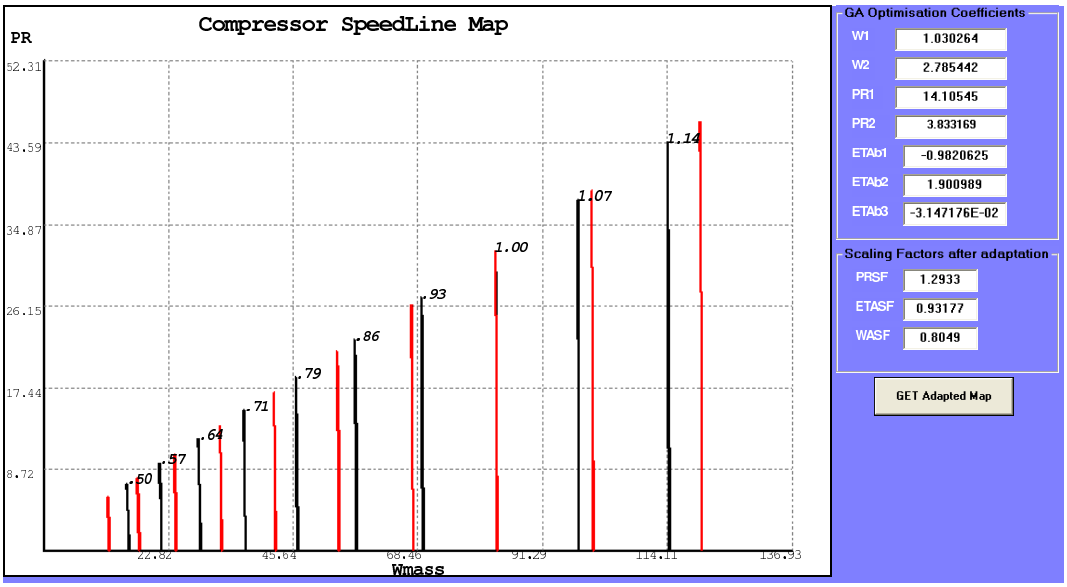

(a) Compressor Pressure Map before and after Adaptation

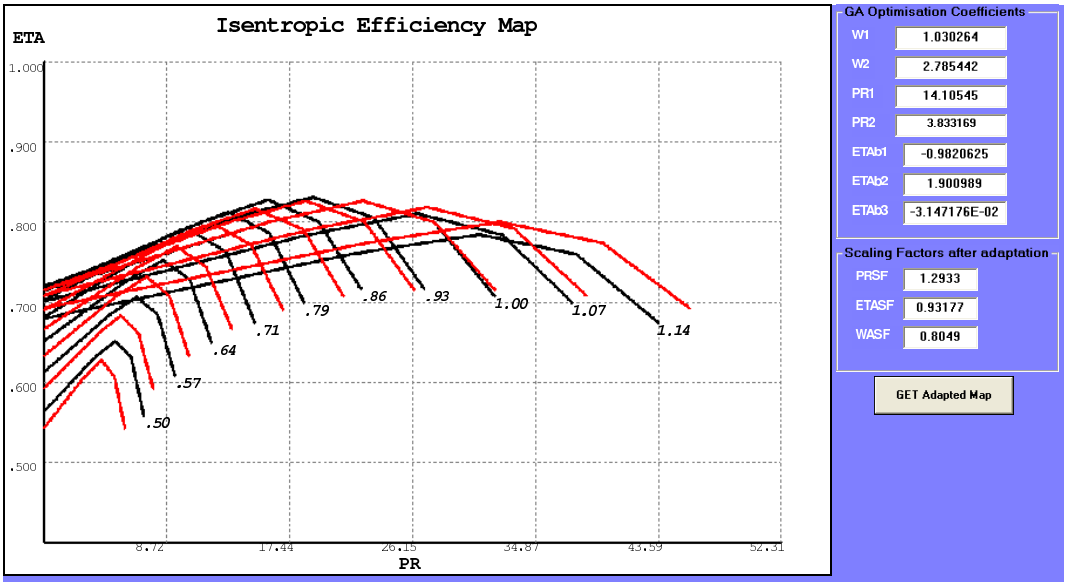

(b) Compressor Efficiency map before and after adaptation

Figure 5.15: Compressor Performance maps before and after adaptation

The range of the off-design operation that the adaptation process is able to cover is heavily dependent upon the engine model capabilities that Turbomatch simulation code allows PYTHIA off-design adaptation to handle. The off-design adaptation that has been developed in visual basic and integrated in PYTHIA software has strong features as its accuracy and its ability to generate a compressor map that captures the engine performance for the operating points targeted. The programme is robust, modular that

allows for further development of both the map generation code and the adaptation code and user friendly that enables the user to have a complete overview of the off-design adaptation.

However the major limitation of the developed adaptation has to do with the margin that this process is capable of converging successfully. When constructing an engine model and adapting it through design point adaptation the result of this process is very case specific engine model that meets the target measurements. The side-effects of this process are reflected in the off-design adaptation where the off-design adaptation isn't allowed to run at off-design points far away from the point that has been initially adapted. This isn't a responsibility of Turbomatch as its simulation code is able to cover a wide range of off-design operation. The disadvantage is that all the features of PYTHIA program, which is built in visual basic, are calling the turbomatch code and extract, required for each case, information without having the ability to modify the Turbomatch core code and have full control of it. This has limited the adaptation as its logic is different than the off-design simulation. The earlier off-design adaptation developed by Lo Gatto justified this difference as shown in the prediction error figures of the previous section.

The new developed off-design adaptation method narrows this gap between the off-design simulation as the behavior of the developed adaptation resembles the simulation's one as seen from figures 5.5, 5.7, 5.9. The reason for this lies solely in the compressor map generation method which facilitates the off-design adaptation. This is accomplished by the analytical nature by which the compressor map is expressed in first place and the wide margin for which a user can modify its shape.

The computation time of adaptation depends on the number of operating points, generations, and the population size of the genetic algorithms. The developed off-design adaptation is taking longer than the older adaptation method as its operation includes extra subroutines that add to the total time for convergence. However the improved accuracy is of major importance at this point and advantageous to the new developed off-design adaptation method. Another advantage of this method is its unique feature of the compressor map generation that has the potential for a wide range of applications. The limitations that the adaptation process has doesn't take full advantage of the novel map generation method that is integrated in it.

The initial adaptation of the engine model, although it is called design point as it refers to the line speed of 1.0 in the compressor map, is actually an artificial design point that satisfies the target parameters. In test cases 7,8 and 9 where for a wide range of

operation three different adaptations have been performed, three different compressor maps satisfy the targeted operating points. Each compressor map is significantly different from each other but something that allows future exploration and is rec commended is the combination of these 3 maps. This will produce a single adapted compressor map that would allow the adaptation to occur in a single simulation.

Another suggestion for this limitation would be the transfer of features from the design point adaptation to the the off-design adaptation developed. In other words the off-design adaptation should always refer to the previous operating point in a multi-point adaptation rather than the initial design point. The engine model developed has a single compressor brick in the off-design adaptation. However there are gas turbine configurations that have bleed cooling flows from the compressor that cannot be modeled as accurately with a single compressor brick in the engine model. The capability of off-design adaptation to accommodate more than one compressor brick would improve the flexibility of the model. The software code is modular enough that allows further development. A developer's guide has been prepared for assisting the aforementioned scope. A user's guide has been also written which will assist the MEA's personnel and any prospective students that will use the developed features of the PYTHIA.

Chapter 6

Gas Turbine Diagnostics

6.1 Introduction

The degradation that an engine experiences during its lifespan operation is classified into two categories. The first one being called "recoverable" referring to compressor fouling, inlet clogging etc and the other one "non-recoverable" is associated with the engine's hot end components and parts. Some of the most common degradation occurring in a gas turbine are the following:

1. Compressor fouling
2. Blade tip clearance increase due to wearing erosion
3. Labyrinth seal damage
4. Foreign and Domestic Object Damage (FOD,DOD)
5. Hot end component damage
6. Corrosion

The effect that each type of degradation has in the performance of the gas turbine components is oftenly expressed in terms of mass flow capacity and isentropic efficiency as summarised in table 6.2

Degradation Fault	Represented by	Range
Compressor Fouling	$\downarrow \Gamma_c$	0.0 –(-5.0%)
	$\downarrow \eta_c$	0.0 –(-2.5%)
Compressor Erosion	$\downarrow \Gamma_c$	0.0 –(-5.0%)
	$\downarrow \eta_c$	0.0 –(-2.5%)
Turbine Fouling	$\downarrow \Gamma_t$	0.0 –(-5.0%)
	$\downarrow \eta_t$	0.0 –(-2.5%)
Turbine Erosion	$\uparrow \Gamma_t$	0.0 –(+5.0%)
	$\downarrow \eta_t$	0.0 –(-2.5%)
FOD	$\downarrow \eta_c$	0.0 –(-5.0%)
	$\downarrow \eta_t$	0.0 –(-5.0%)

Table 6.2: Component Degradation Table

The performance degradation attributed to the compressor fouling is mainly due to deposits formed on the compressor blades by particles carried in by the air that are not large enough (typically a few microns diameter) to be blocked by the inlet filter [49]. These deposits result in a reduction of compressor mass flow rate, compressor efficiency and pressure ratio which in turn causes a drop in gas turbine's power output while increasing its heat rate. This type of degradation is by far the dominant mode. This degradation can be recovered by regular online and off-line compressor washing. Although online washing is not as effective as the off-line washing it is quite common for peak load configurations or single shaft power plants where operation cannot be interrupted. In combined cycle power plants that have more than one gas turbine and therefore the flexibility to shut down a gas turbine like MEA and leave only one engine operating at the end of the day, off-line washing is preferred. The net financial impact however, is almost always negative unless the fuel purchase price is extremely high and/or power sale price is too low. Some types of degradation of the LM2500+ engine's hot end components are shown in the figure below.

The performance degradation associated with hot gas path components is influenced by myriad factors such as fuel quantity, number of starts, amount of water/steam injection etc. Typically for a base load machine this type of degradation can be 0.2-0.3 percent of the nominal (when new and clean) rating after a months operation[14]. The

only remedy for non recoverable degradation is an engine overhaul. The degradation that hot end components like the nozzle guide vanes, of one GE LM2500+ gas turbine, have experienced in the MEA's power station after 25,000hrs before the engine was overhauled can be seen in figure 6.1.

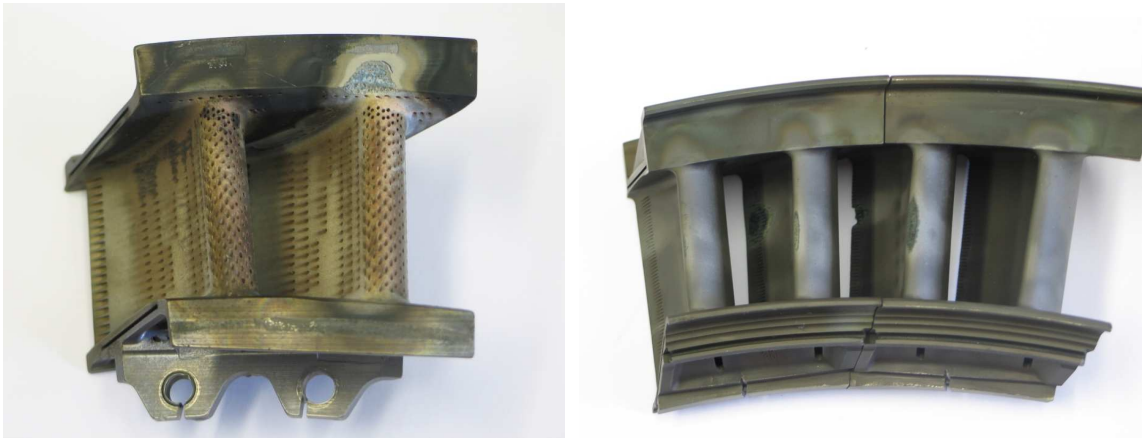

(a) 1st stage NGV Erosion (b) 2nd stage NGV Erosion

Figure 6.1: LM2500+ Nozzle Guide Vane degradation after 25,000hrs

The diagnostic process is modular and begins with gas turbine data, and applies data validity analysis to convert the data to more usable information. It then extracts the knowledge of performance and mechanical trends from the information through thermodynamic analysis. Then it compares the extracted knowledge to several knowledge bases, and completes a diagnosis or prognosis of the gas turbine's health [50]. Finally it alerts the operator to any important findings, and constructs a hierarchy of potential actions to correct any problems if uncovered. Whatever its specific contents and execution may be, any diagnostic system must rely on discernible changes taking place in observable parameters in order to detect physical faults [51].

6.1.1 Gas Turbine Diagnostic Schemes

Urban [52] triggered the evolution of gas path diagnostics in the form that is widely known nowadays, as the nonlinearity of the thermodynamic model has been considered. The objective function established represents the difference of the real and predicted measurements. Various optimization techniques have been developed to deal with the minimization problem. This objective function has been minimised by conventional algorithm which stopped at local minimum [27, 53, 54] . Then Zedda and Singh solved

this problem by using the sum of absolute values, minimized through genetic algorithms [55]. Genetic algorithm optimizer by using information from individual point to assess engine state have been also used [56]. Escher and Singh [7]considered Jacobian matrix updates where the solver is nonlinear consisting of successive applications of a linear one. Mathioudakis et al [50] constructed a composite objective function consisting of sum of squares and absolute values. A statistical approach has been also explored [38, 57]where the objective function is a combination and quadratic and a modulus function.

One of the main reasons for the development of many different methods is the fact that gas path measurements are difficult and costly to perform and are thus very limited in number, in contrast to the large number of parameters needed to be known for engine health assessment [50]. Methods associated with the diagnosis of gas turbine health are briefly described in this subsection.

Kalman Filters

One of the most published methods involve the use of Kalman filters as the primary vehicle for fault isolation process. Kalman filter methods were introduced as a fault isolation and assessment technique for relative engine performance diagnostics in the late 1970s and early 1980s. The general approach taken for engine fault diagnosis typically involves the use of a linearized model approximation evaluated at a selected engine operating point as proposed by Volponi [58, 43]. This provides a matrix relationship between changes in engine component performance (independent parameters) and the attendant changes in typically measured engine parameters such as spool speeds, internal temperatures and pressures, fuel flow, etc. (dependent parameters).

Neural Networks

Neural networks represent a powerful pattern recognition technique and have been applied for fault detection of complex systems such as aerospace vehicle, nuclear power plants and chemical process facilities among others [27, 59]. A key advantage of neural networks over other methods is their ability to recognize relationships between patterns despite the presence of noise contamination and/or partial information. More than 85% of published applications have used the feed forward back propagation network (FFBPN) [50]. A three layer feed-forward network has been used by Volponi [58]. The feedforward network is trained using supervised learning, which involves presenting

input output pairs to the ANN and then using the back propagation (BP) algorithm to learn the relationships between the inputs and outputs. The input data has been normalized and the data data used for training was not used for testing the neural network.

The neural network proposed by Depold [59] acts as templates to eliminate bad data much the same as analysis would with their rules of thumb. These templates identify spurious input errors . The first two ANN templates identify errors that result in all output parameters being either high out of statistical limits or low out of statistical limits. The remaining four ANN templates detect single parameter limit exceedences that are not physically possible. In the former study when five key jet engine parameters $(EPR, EGT, Wf, N2, N1)$ are considered, six basic templates can be defined which corrects approximately 9% of typical data. The neural networks disadvantage is the time required for their training but since this training is completed the computation is very fast and they can also deal with measurement noise and bias.

Bayesian Belief Networks

Bayesian belief networks (BBN) have been described by Romessis [60] . BBN represents the relation among variables of aerothermodynamic nature of an engine, component faults can be detected anytime measurements of gas path variables are available. Measurement noise, bias and changing operating condition affect the accuracy of the BBN since the thermodynamic relations are altered and the operating points shifted . Lee and Mavris [61] maintained the generality and the accuracy together, by multiple Bayesian models tailored to various fault situations where the have been implemented in one hierarchical mode

Gas Path Analysis

Gas path analysis (GPA) is a powerful diagnostic technique that has been extensively used to predict the health of a gas turbine, by using the variety of measurements located in the engine's gas path. This technique enables the gas turbine user to construct a reliable and robust maintenance strategy. Therefore the highly considerable maintenance and operational costs of gas turbines are reduced. Comprehensive reviews of gas path diagnostics techniques have been provided by Li [50] and Singh [37]. The gas path analysis initiated as a linear approach introduced by Urban [52] and followed by Stamatis et al [26] approach which considered the non-linearity effects of the problem.

However the limitations addressed by the repeatable uncertainties of the gas turbine system, motivated the development of various conventional and artificial optimisation techniques like neural networks [56], genetic algorithms [56], hybrid systems [60] and fuzzy expert systems [62]. Since the GPA is a model-based performance diagnostic technique thence the accuracy of the diagnostic analysis is dependent on extremely accurate performance simulation. The development of techniques to adapt a performance engine model to the measurements of a particular gas turbine engine is highly pursued. A design point performance adaptation method has been developed by Li [21]. The gas turbine's off-design performance adaptation is a more complex method which incorporates the development and the mathematical scaling of engine component maps as described in the previous chapter. Accuracy of such a prediction is highly dependent on the quantity of available engine design data and the quality of component characteristic maps. Many researchers have explored this topic for its catalytic role in the diagnosis since it increases the accuracy of engine performance model.

There are so many repeatable uncertainties involved during the operating life of a gas turbine like changes in ambient and operating conditions, noisy measurements and faulty instrumentation, all of which contribute to the added complexity of the diagnosis. Many performance software, that can handle a series of the aforementioned uncertainties, have been developed for academic and commercial use based on a family of diagnostic techniques [12]. The performance simulation and diagnostics software PYTHIA, that has been developed in Cranfield University and updated with a series of capabilities like the developed compressor generation method and the off-design adaptation, is the one used for this study. In this test case a gas path analysis method will be employed, through the use of PYTHIA software, in order to determine the actual degradation of an aeroderivative gas turbine. This application procedure commences with the development of an engine performance model, continues with the performance adaptation for matching the real engine measurements, pre-processes ambient and operating condition correction and concludes with the prediction of the engine component degradation using the concept of GPA index.

6.2 Gas Path Analysis Methodology

The basis of engine health monitoring schemes is to measure fundamental parameters such as speed, pressure, temperature, fuel flow and vibration levels and from these

measurements deduce the health of the plant by observing changes in the relationships between them [50]. Some monitoring may be carried out by observation of directly measured parameters but a deeper insight can be obtained by the use of gas path analysis which can determine critical performance parameter, such as airflow, turbine inlet temperature, and component efficiencies.

The estimation of health parameters is considered successful when the quantities measured on the engine are reproduced in the best possible way by, an engine performance model incorporating the health parameter [37]. To make the GPA successful the following criteria must be satisfied:

1. Performance adaptation improves the accuracy of the simulation
2. Selection of instrumentation set for better visibility analysis of engine health
3. Measurements data preprocessing to reduce the influence of measurement noise and deviated ambient and operating conditions
4. Sensor failure detection and engine component fault diagnosis

A linear and non-linear GPA approach developed at Cranfield [37] is an effective tool for inverse mathematical problems such a gas turbine performance adaptation and performance diagnostics. The idea of the method, which is similar as the design point adaptation process, is as follows. The thermodynamic relationship among performance parameters, component parameters and ambient, operating condition parameters can be represented with equation 6.1.

$$\vec{z} = h(\vec{x}, \vec{y}) \tag{6.1}$$

where $\vec{z} \in \Re^M$ is the measurable performance parameter vector and M is the number of performance parameters, and $\vec{x} \in \Re^N$ is the health parameter vector and N is the number of component parameters and $h(\,)$ is a vector valued function.

At an initially given design point which is denoted with subscript "0" equation x can be expanded in a Taylor series as:

$$\vec{z} = z_0 + \left.\frac{\partial h(\vec{x}, \vec{y})}{\partial x}\right|_0 \cdot (\vec{x} - \vec{x_0}) + \left.\frac{\partial h(\vec{x}, \vec{y})}{\partial y}\right|_0 \cdot (\vec{y} - \vec{y_0}) + HOT \tag{6.2}$$

HOT represent higher order terms which can be neglected. represents higher order terms of the expansion and can be neglected. Therefore, a linearised relationship gas turbine performance model can be expressed with equation 6.3.

$$\Delta\vec{z} = H \cdot \Delta\vec{x} + H^{'} \cdot \Delta\vec{y} \tag{6.3}$$

When there is no deviation from standard ambient condition and nominal operating condition, $\Delta\vec{y} = 0$. So

$$\Delta\vec{z} = H \cdot \Delta\vec{x} \tag{6.4}$$

For any expected deviation of $\Delta\vec{z}$ from its initial point, the deviation of to-be-adapted component parameters from its initial point can be predicted by inverting the influence coefficient matrix (ICM) H to a fault coefficient matrix (FCM) H^{-1} leading to the following equation when $N = M$

$$\Delta\vec{x} = H^{-1} \cdot \Delta\vec{z} \tag{6.5}$$

The non-linearity of the engine behavior is taken into account by using an iterative Newton-Raphson process where linear GPA is applied iteratively until a converged solution is obtained. The number of component parameters, M, may not be equal. If $N > M$ Equation (4) is under-determined. Typically such a situation leads to an infinite number of least-squares solutions. A pseudo inverse is defined as

$$H^{\#} = H^{T} \cdot (HH^{T})^{-1} \tag{6.6}$$

The solution resulting from this, which is the best in a least square sense, is:

$$\vec{x} = H^{\#} \cdot \vec{z} \tag{6.7}$$

If $N < M$ equation x is over-determined and there are redundant equations. A pseudoinverse matrix is defined as:

$$H^{\#} = (H^{T}H)^{-1} \cdot H^{-T} \tag{6.8}$$

The resulting solution, which is also the best in a least square sense, is:

$$\vec{x} = H^{\#} \cdot \vec{z} \tag{6.9}$$

The convergence of this iterative adaptation calculation process is declared when the performance is very close to the measured performance. The root mean square (RMS) of the difference between predicted and real performance is smaller than $\sigma$when convergence criterion is satisfied.

$$RMS = \sqrt{\frac{\sum(z_{i,predicted} - z_{i,measured})^2}{M}} < \sigma \tag{6.10}$$

where σ is a very small number (σ=0.001 is usually chosen). The prediction error γ_i for each measurable performance parameter is described by the relative difference between the predicted and measured engine performance parameter and expressed with equation 6.11

$$\gamma_i = \frac{z_{i,predicted} - z_{i,measured}}{z_{i,measured}} \cdot 100\% \tag{6.11}$$

(1) Where γ_i is the prediction error for the performance parameter. This diagnostic method is simple and fast in prediction although it has certain requirements that must be met such as

- The influence coefficient matrix (ICM) is an accurate mathematical description of gas turbine performance around a specific operating point.
- Measurement bias and noise free sensors
- Un-correlated (independent) measurements being sensitive to engine degradation.

A disadvantage of the GPA is its dependency on the apriori information of degraded components. To effectively isolate the deteriorated components GPA index is introduced. The GPA index is a measure of the diagnostic accuracy and is defined as:

$$\lambda = \frac{1}{1+\varepsilon} \tag{6.12}$$

where λ is the GPA index and $\varepsilon$is the difference between measured and predicted deviations of engine gas path measurements expressed with the following.

$$\varepsilon = \sum w_i \left| \frac{\Delta z_i - \Delta z_{m,j}}{z_{0,i} - z_{0,j}} \right| \cdot 100\% \tag{6.13}$$

where w_i are the weighting factors taking into account the relative importance of the measurements. To apply the GPA index effectively to gas turbine component fault diagnosis, the maximum number of simultaneously degraded engine components and the component fault cases (CFC) should be assumed. The diagnostic approach that covers all the pre-assumed engine fault cases is shown in figure 6.2 where the highest values of GPA indices indicate the most likely engine degradation test cases.

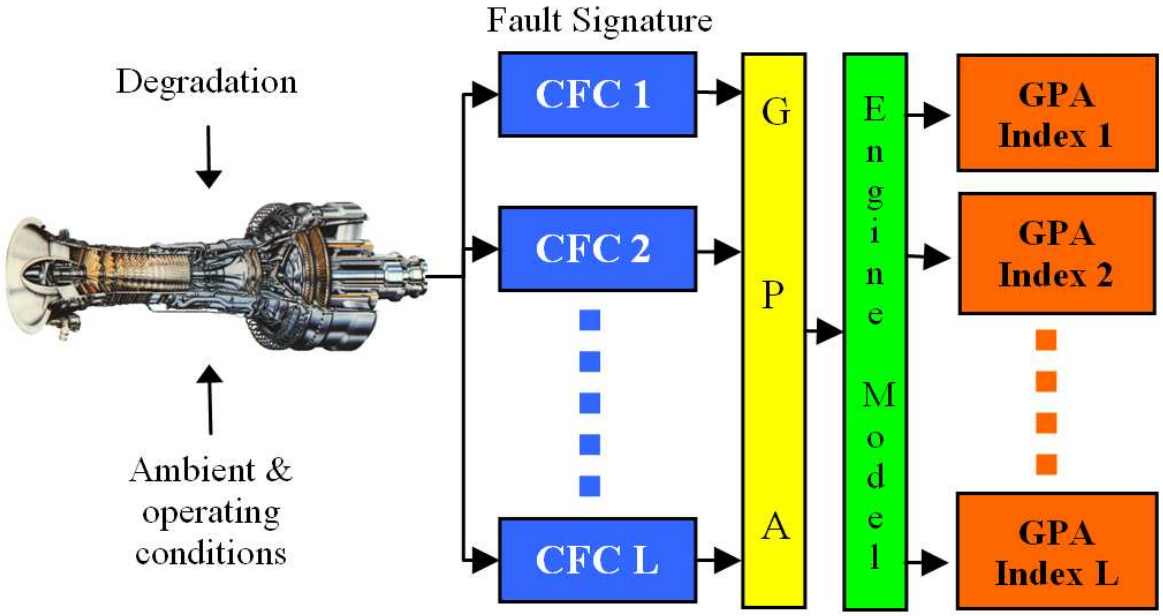

Figure 6.2: GPA diagnostic process chart

In a situation where more than one CFC cases are likely, weighted degradation is suggested and calculated as follows

$$\overline{x_i} = \sum_{j=1}^{Sf} x_{i,j} \cdot \lambda_j / \sum_{j=1}^{Sf} \lambda_j \sqrt{\frac{\sum_{i=1}^{n} error_i^2}{n}} \tag{6.14}$$

where $\overline{x_i}$ is a weighted health parameter, $x_{i,j}$ the i_{th} health parameter predicted in CFC case j, λ_j the GPA index in CFC case $j$and $Sf$the total number of the most likely faults. Summarising this diagnostic system which is based on GPA has been implemented into Cranfield gas turbine performance analysis software PYTHIA [22] developed from TURBOMATCH, the validity of which has been tested over many years.

6.3 Application

The engine chosen for the application of this GPA analysis is the GE LM2500+ aeroderivative gas turbine operating at Manx Electricity Authority. This engine consists of a 17 stage variable geometry compressor [29], a single annular combustor, a two stage high pressure turbine and a two stage high speed power turbine.

Engine Model

When the engine is operating at certain operating conditions, the power output is used as the control parameter and kept constant as environmental conditions change and degradation happens. The requirement for simulating the cooling flows, which are delivered by the compressor to the hot end of the gas turbine, justifies the existence of two compressor bricks in the engine model. In addition there is a burner, a compressor turbine and a power turbine. At the 9th stage of the compressor the bleed flow passes through a heat exchanger for further reducing the temperature of the flow fed to the power turbine.

The developed engine model accurately matches the design point performance of the service engine. For observing the degradation that the gas turbine has experienced during the three month period the selected instrumentation set for diagnostic analysis of the model engine is described in table 6.4.

No	Symbol	Parameter
1	T_1(K)	Ambient temperature
2	P_1(atm)	Ambient pressure
3	P (MW)	Power output
4	PCN (%)	Compressor shaft speed
5	T_7(K)	Compressor exit total temperature
6	P_7(atm)	Compressor exit total pressure
7	T_9(K)	High pressure turbine exit total temperature
8	P_9(atm)	High pressure turbine exit total pressure

Table 6.4: Selected Instrumentation set for Diagnostic Analysis

From a series of available measurements the selected set for this analysis had the same power output at slightly different ambient conditions as described in Table 3. It is noticeworthy that both set of measurements were very close to the design point performance of the engine and the reason for that will be amplified later on this chapter.

Parameters	January 2007	March 2007
T_1(K)	283.45	285.0
P_1(atm)	0.996	0.990
P (MW)	29.3	29.3

Table 6.5: Measurement conditions

Analysis

The objective of this analysis is the application of the diagnostic system described throughout the paper to a real scenario to determine the degradation that this gas turbine has experienced during this period. In the context of this and at such a short time frame the main focus of this diagnosis is to determine the deterioration that the first stages of the compressor have experienced due to fouling. In other words the degradation of the other engine hot end components will be negligible in comparison with the compressor. The considered assumptions of this procedure are enlisted here.

- Up to two components can be simultaneously degraded
- The components among which the faulty compressor will be searched for is Compressor 1 and Turbine 1.
- Adapted engine model for matching the set of measurements close to the design point
- Ambient condition shift present

Performance Adaptation

As previously described the diagnostic analysis is very sensitive to accurate performance simulation, therefore performance adaptation was employed to adapt the engine model to the real engine measurements. Since both set of data were taken close to the design point of the engine's performance it becomes clear that design point performance adaptation could be applied for matching the engine model to the January measurements. The certainty provided by this technique to the engine model is a prerequisite for estimating the degradation of the engine components from the occurred deviations between the January-March measurements.

Initial Correction of Measurements

All the available measurements of March were corrected to the same ambient conditions of the earlier January measurements. As the operating conditions were at the same power output the apparent deviation was due to degradation and mainly due to compressor fouling as the engine hasn't experienced any sort of maintenance action during that period. A comparison between the deviation of the engine performance parameters with and without correction is presented in figure 6.3.

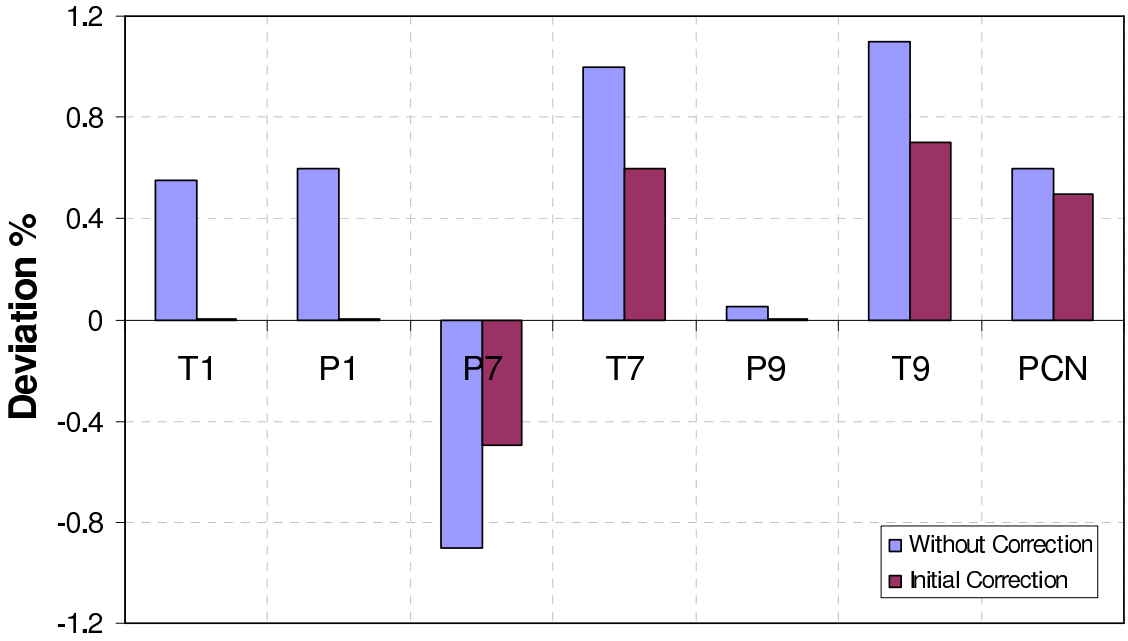

Figure 6.3: Engine parameter deviation with and without corrections

Engine Component Fault Detection

To identify which engine component is responsible for the observed deviation the GPA Index is used. Assuming that the maximum number of simultaneously degraded components can be up to two the component fault cases are listed in table 6.6.

Component Fault Case	Pre-defined faulty components
1	Compressor 1
2	Turbine 1
3	Compressor 1 + Turbine 1

Table 6.6: Fault Cases

The Component Fault Cases with their corresponding GPA index is represented in figure 6.4.

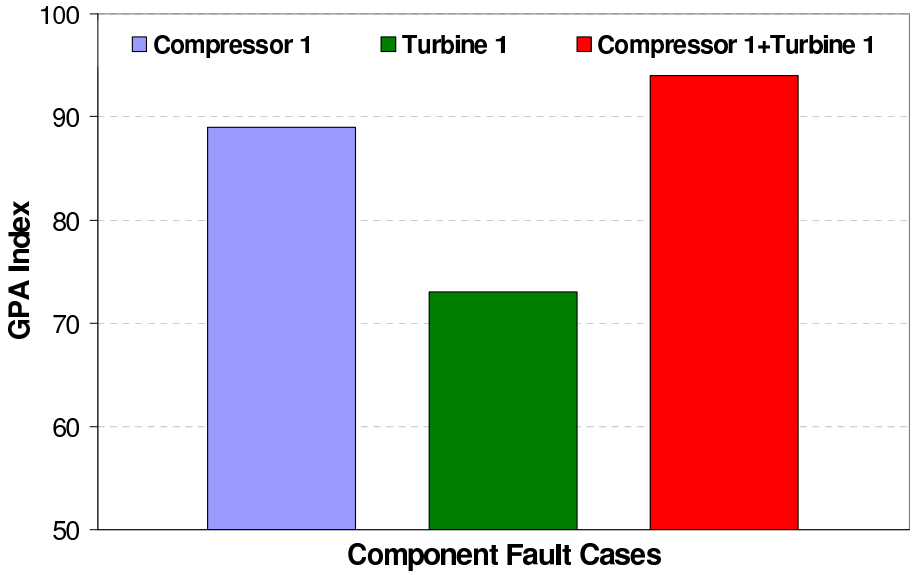

Figure 6.4: Componenet Fault Cases GPA Index

It is evident from Figure 5 that CFC 1 and CFC3 present the highest GPA index therefore there is a deterioration of the compressor and a very small deterioration of the compressor turbine. In order to determine the actual degradation of each component and since two of the CFC are likely responsible for the apparent parameter deviation, the weighted solution is applied. This provides the diagnostic results tabulated in table 6.7.

	Component efficiency	Mass flow capacity
Engine Component	$\Delta\eta$ (%)	$\Delta\Gamma$ (%)
Compressor 1	-0.79	-0.67
Turbine 1	-0.09	0.02

Table 6.7: Componenet Degradation Results

As expected the first stages of the compressor had a drop of 0.79% in isentropic efficiency and a 0.67% reduction in mass flow capacity. The degradation of the compressor turbine is negligible compared to that of the compressor's. The compressor fouling has an immediate effect on the performance of the gas turbine which results in lost power. The engine's control reaction to the above degradation was to add more fuel and run

at slightly higher rotational speed to satisfy the power output, which is the control parameter of this gas turbine configuration.

Gas path analysis is a powerful diagnostic technique and its dependencies on accurate performance simulation and a-priori information about degraded components are compensated by performance adaptation and GPA index respectively. GPA's advantage is that has a fast solution that represents intrinsic relationship between engine performance and aerothermodynamic parameters [27]. GPA and derivatives are powerful but have the disadvantages of requiring a priori info of degraded components, measurement noise and bias free sensors [63]. From the development of an engine model and its adaptation to real engine measurements, which is considered fundamental for such kind of analysis, to the consideration of practical issues of measurement correction and instrumentation selection this GPA method has the capacity to predict component degradation at a reliable level. The analysis showed that during a continuous operation of three months and close to the date of the engine's major overhaul the first stages of the compressor have deteriorated due to fouling. The application of this technique to this real case scenario facilitates gas turbine users with the operation and maintenance decision making of the power plant.

Chapter 7

Conclusions and Future Recommendations

This thesis has focused in the development of a performance off-design adaptation method software programme that can be integrated to a power station's environment as a virtual gas turbine performance and diagnostics tool. The main results can be summarised as follows:

1. A new engine model has been developed in PYTHIA for simulating the performance of the MEA's gas turbines at both design and off-design conditions.

2. The crucial part of progressively refining the engine model, based on the collated service engine data, is accomplished through the design point adaptation method and an application test case has been presented.

3. A novel compressor map generating method has been developed and integrated in PYTHIA software. The compressor map is generated based on a family of coefficients than capture the shape of such a map, therefore enabling the gas turbine user to modify these coefficients and determine a performance map that will meet the design point criteria of a gas turbine.

4. The compressor map generation is extensively being employed by the off-design adaptation method developed.

5. An adaptation method for matching the engine model's performance to that of the service engine of MEA at off-design conditions has been developed. This adaptation process regenerates compressor maps with the appropriate coefficients

and then minimises the difference between the predicted and actual measurements through the genetic algorithms optimiser. The accuracy of this developed method has been validated and tested. The results of the test cases proved that the developed adaptation is an effective and accurate method for single and multiple operating point prediction of a gas turbine's performance at off-design conditions.

6. Convergence time of the adaptation method depends on the genetic algorithms characteristics and the number of off-design operating points that are to be modeled. For a typical single point adaptation this is a matter of seconds where for multiple adaptation this takes a couple of minutes.

7. Gas turbine performance based diagnostics by using the Gas Path Analysis have been used extensively throughout this research for predicting the health of the gas turbines at MEA. An application test case showed that this GPA method can be used for a fast and accurate assessment of a gas turbine's health condition. Performance adaptation and GPA index must be employed in this process for ensuring the accuracy of the diagnosis.

8. All these software capabilities, that have been developed, are integrated in the latest version of PYTHIA that will be delivered to MEA. The software programme will be a virtual gas turbine tool that will have the capacity to load a series of measurements, taken from the control systems, and perform the appropriate actions like measurement corrections,noise reductions, performance adaptation and diagnostics analysis so that trends of the gas turbine's performance over a wide range of operation will aid the power plant's maintenance strategy.

Interesting future research directions worth considering in the context of performance adaptation are:

1. Updating the compressor map generation with more set of equations, that can describe the shape of the compressor map, so that the user can select from a series of equations types, the corresponding level of accuracy and predicted computation time, the one that best matches his criteria.

2. The off-design adaptation currently can employ the compressor map generation for a single compressor brick in the engine model configuration. This feature prompts the further development of the programme so that the adaptation will

be able accommodate more that one compressor bricks with their corresponding compressor performance maps be handled by the generating method.

3. A very key element that affects the flexibility of the off-design adaptation is the extent by which PYTHIA makes full use of turbomatch code. Currently this method has the ability to model up to a specific range lower and upper the point, at which the design point adaptation has been performed. Artificially the adaptation can reach the lowest power level and off-design conditions but this will be performed by a series of simulations and not by a single simulation. Therefore the software should employ extra features from turbomatch code, that are only available at off-design simulations in order to increase the range by which off-design adaptation can be performed.

Bibliography

[1] R. K. Agrawal, B. D. MacIsaac, and H. I. H. Saravanamuttoo. Analysis procedure for the validation of on-site performance measurements of gas turbines. *American Society of Mechanical Engineers (Paper)*, (78 -GT-152), 1978.

[2] M. Mucino. *EngD Thesis:CCGT performance simulation and diagnostis for operations optimisation and risk management.* University of Cranfield, 2007.

[3] S. C. Gullen, P. R. Griffin, and S. Paolucci. Real-time on-line performance diagnostics of heavy-duty industrial gas turbines. *Journal of Engineering for Gas Turbines and Power*, 124(4):910–921, 2002.

[4] L. Vieria, C. Matt, V. Guedes, M. Cruz, and F. Castelloes. Maximization of the profit of a complex combined-cycle cogeneration plant using a professional process simulator. *J. Eng. Gas Turbines Power, Issue 4, paper*, Volume 132, 2010.

[5] C. E. Neilson, D. G. Shafer, and E. Carpentieri. Lm2500 gas turbine fuel nozzle design and combustion test evaluation and emission results with simulated gasified wood product fuels. *Journal of Engineering for Gas Turbines and Power*, 121(4):600–606, 1999.

[6] L. Smith. Axial compressor aerodesign evolution at general electric. *Journal of Turbomachinery*, 124, 2002.

[7] P. Escher and R. Singh. An object oriented diagnostics computer program suitable for industrial gas turbines. *International Congress of Combustion Engines, 21st, Switzerland*, 1995.

[8] A. Alexiou and K. Mathioudakis. Development of gas turbine performance models using a generic simulation tool. *Proceedings of the ASME Turbo Expo*, 1:185–194, 2005.

[9] K. Mathioudakis. Gas turbine test parameters corrections including operation with water injection. *Journal of Engineering for Gas Turbines and Power*, 126(2):334–341, 2004.

[10] A. J. Meacock and A. J. White. The effect of water injection on multispool gas turbine behavior. *Journal of Engineering for Gas Turbines and Power*, 128(1):97–102, 2006.

[11] Philip P. Walsh and Paul Fletcher. *Gas turbine performance [Book].* Oxford, United Kingdom/Fairfield, NJ: Blackwell Science, Ltd./ASME Press, 1998. 130 ref.

[12] NATO Technical Report. Performance prediction and simulation of gas turbine engine operation for aircraft, marine, vehicular and power generation. *Final report of the RTO applied vehicle technology*, 2007.

[13] S. Gulen and R. Smith. A simple mathematical approach to data reconciliation in a single-shaft combined cycle system. *J. Eng. Gas Turbines Power, Issue 2, paper*, 131, 2009.

[14] P. Pilidis. Digital simulation of gas turbine performance. *PhD Thesis, University of Glasgow*, 1983.

[15] E. Tsoutsanis, Y. G. Li, P. Pilidis, and M. Newby. Gas path analysis applied to an aeroderivative gas turbine used for power generation. *International Conference on Condition Monitoring and Machine Failure Prevention Technologies, 5th, Edinburgh, Proceedings*, 2008.

[16] E. Tsoutsanis, Y. G. Li, P. Pilidis, and M. Newby. Gpa diagnostics: An application to an industrial gas tubine. *Cranfield Multi-Strand Conference, 1st, Cranfield*, 2008.

[17] H. I. H. Saravanamuttoo and B. D. MacIsaac. Thermodynamic model for pipeline gas-turbine diagnostics. *Journal of Engineering for Gas Turbines and Power*, pages 875–884, 1983.

[18] P. Zhy and H. I. H. Saravanamuttoo. Simulation of an advanced twin-spool industrial gas turbine. *Journal of Engineering for Gas Turbines and Power*, 1992.

[19] J. Kurzke. How to get component maps of an aircraft gas-turbine's performance calculations. *ASME paper,96-GT-164*, 1996.

[20] E. Tsoutsanis, Y. G. Li, P. Pilidis, and M. Newby. Industry university collaboration: A case study between the manx electricity authority and cranfield university. *Annual Board Meeting of the Institution of Diesel and Gas Turbine Engineers*, 2009.

[21] Y. G. Li, P. Pilidis, and M. A. Newby. An adaptation approach for gas turbine design-point performance simulation. *Journal of Engineering for Gas Turbines and Power*, 128(4):789–795, 2006.

[22] Y. Li M. Mucino. An advanced gas turbine gas path diagnostic system using gpa-index. In *Proceeding of COMADEM*, 2005.

[23] Y. Li. Gas turbine performance and health status estimation using adaptive gas path analysis. *J. Eng. Gas Turbines Power, Issue 4, paper*, 132, 2010.

[24] M. Mucino, J. Ojile, Y. G. Li, and M. Newby. Advanced performance modelling of a single and double pressure once through steam generator. *GT2007-27505, ASME Turbo Expo 2007, Montreal, Canada*, 2007.

[25] W. P. J. Visser, O. Kogenhop, and M. Oostveen. A generic approach for gas turbine adaptive modeling. *Journal of Engineering for Gas Turbines and Power*, 128(1):13–19, 2006.

[26] A. Stamatis, K. Mathioudakis, and K. Papailiou. Adaptive simulation of gas turbine performance. *J. Eng. Gas Turbines Power, Issue 2, paper*, 112, 1990.

[27] H. S. Tan. Fourier neural networks and generalized single hidden layer networks in aircraft engine fault diagnostics. *Journal of Engineering for Gas Turbines and Power*, 128(4):773–782, 2006.

[28] E. Tsoutsanis. *PhD First Year Review:Performance adaptation and virtual gas turbines for power generation applications.* University of Cranfield, 2007.

[29] A. R. Wadia, D. P. Wolf, and F. G. Haaser. Aerodynamic design and testing of an axial flow compressor with pressure ratio of 23.3:1 for the lm2500+ gas turbine. *Journal of Turbomachinery*, 124(3):331–340, 2002.

[30] J. Klapproth, M. Miller, and D. Parker. Aerodynamic development and performance of the cf6-6/lm2500 compressor. *International Symposium on Air Breathing Engines, 4th, Orlando*, pages 243–249, 1979.

[31] C. Kong, J. Ki, and M. Kang. A new scaling method for component maps of gas turbine using system identification. *Journal of Engineering for Gas Turbines and Power*, 125(4):979–985, 2003.

[32] C. Kong, J. Ki, and M. Kang. A new scaling method for component maps of gas turbine using system identification. *ASME Turbo Expo 2002: Power for Land, Sea, and Air (GT2002), Amsterdam, The Netherlands*, 2002.

[33] Y. Yu, L. Chen, F. Sun, and C. Wu. Neural-network based analysis and prediction of a compressor's characteristic performance map. *Applied Energy*, 84(1):48–55, 2007.

[34] C. Kong, S. Kho, and J. Ki. Component map generation of a gas turbine using genetic algorithms. *Journal of Engineering for Gas Turbines and Power*, 128(1):92–96, 2006.

[35] C. Kong, J. Ki, and M. Kang. Fuzzy approaches for searching optimal component matching point in gas turbine performance simulation. *J. Eng. Gas Turbines Power, Issue 6, paper*, 2004.

[36] C. Kong, J. Ki, and C. Lee. Components map generation of gas turbine engine using genetic algorithms and engine performance deck data. *Proceedings of the ASME Turbo Expo*, 4:377–383, 2006.

[37] Y. G. Li and R. Singh. An advanced gas turbine gas path diagnostic system-pythia. *International Symposium of Air Breathing Engines, paper*, 2005.

[38] R. Sekhnton, H. Bassily, and J. Wagner. A comparison of two trending strategies for gas turbine performance prediction. *J. Eng. Gas Turbines Power, Issue 4, paper*, 130, 2008.

[39] E. Lo Gatto, Y. G. Li, and P. Pilidis. Gas turbine off-design performance adaptation using a genetic algorithm. *Proceedings of the ASME Turbo Expo*, 2:551–560, 2006.

[40] W. L. Macmillan. Development of a module type computer program for the calculation of gas turbine off design performance. *PhD Thesis,Cranfield University*, 1974.

[41] J. Ki, C. Kong, S. Kho, J. Kim, I. Ahn, and D. Lee. Development of on-line performance diagnostics program of a helicopter propulsion system. *ASME Turbo Expo 2009: Power for Land, Sea, and Air, Florida, USA*, 2009.

[42] J. Kim, T. Kim, and J. Sohn. Comparative analysis of off-design performance characteristics of single and two-shaft industrial gas turbines. *J. Eng. Gas Turbines Power,*, 2003.

[43] D. Simon and S. Garg. Optimal tuner selection for kalman filter-based aircraft engine performance estimation. *J. Eng. Gas Turbines Power, Issue 3, paper*, 132, 2010.

[44] L. Terfloth and J. Gasteiger. Neural networks and genetic algorithms in drug design. *Drug Discovery Today*, 6(SUPPL.2):S102–S108, 2001.

[45] D.E. Goldberg. *Genetic Algorithms in Search, Optimization and Machine learing.* Addison-Wesley, New York, 1989.

[46] C.R. Reeves and J.E. Rowe. *Genetic Algorithms: Principles and perspectives.* Kluwer, New York, 2002.

[47] M. Mitchell. *An Introductions to Genetic Algorithms.* MIT Press, Boston, 1999.

[48] R.L. Haupt and S.E. Haupt. *Practical Genetic Algorithms.* Wiley, New Jersey, 2004.

[49] S. Kurz, K. Brun, and M. Wollie. Degradation effects on industrial gas turbines. *J. Eng. Gas Turbines Power, Issue 6, paper*, 131, 2009.

[50] Y. G. Li. Performance-analysis-based gas turbine diagnostics: A review. *Proceedings of the Institution of Mechanical Engineers, Part A: Journal of Power and Energy*, 216(5):363–377, 2002.

[51] K. Mathioudakis and T. Tsalavoutas. Uncertainty reduction in gas turbine performance diagnostics by accounting for humidity effects. *Journal of Engineering for Gas Turbines and Power*, 124(4):801–808, 2002.

[52] L. A. Urban. Parameter selection for multiple fault diagnostics of gas turbine engines. *J Eng Power Trans ASME*, 97 Ser A(2):225–230, 1975.

[53] K. Mathioudakis and Ph Kamboukos. Assessment of the effectiveness of gas path diagnostic schemes. *Journal of Engineering for Gas Turbines and Power*, 128(1):57–63, 2006.

[54] Ph Kamboukos and K. Mathioudakis. Comparison of linear and nonlinear gas turbine performance diagnostics. *Journal of Engineering for Gas Turbines and Power*, 127(1):49–56, 2005.

[55] M. Zedda and R. Singh. Gas turbine engine and sensor fault diagnosis using optimisation techniques. *Journal of Propulsion and Power*, pages 1019–1025, 2002.

[56] S. Sampath and R. Singh. An integrated fault diagnostics model using genetic algorithm and neural networks. *Journal of Engineering for Gas Turbines and Power*, 128(1):49–56, 2006.

[57] I. Loboda, S. Yepifanov, and Y. Feldshteyn. Diagnostic analysis of maintenance data of a gas turbine for driving an electric generator. *ASME Turbo Expo 2009: Power for Land, Sea, and Air, Orlando, Florida, USA*, 2009.

[58] A. J. Volponi, H. DePold, R. Ganguli, and C. Daguang. The use of kalman filter and neural network methodologies in gas turbine performance diagnostics: A comparative study. *Journal of Engineering for Gas Turbines and Power*, 125(4):917–924, 2003.

[59] H. R. DePold and F. D. Gass. The application of expert systems and neural networks to gas turbine prognostics and diagnostics. *Journal of Engineering for Gas Turbines and Power*, 121(4):607–612, 1999.

[60] C. Romessis and K. Mathioudakis. Bayesian network approach for gas path fault diagnosis. *Journal of Engineering for Gas Turbines and Power*, 128(1):64–72, 2006.

[61] Y. Lee, D. Mavris, V. Volovoi, M. Yuan, and T. Fisher. A fault diagnosis method for industrial gas turbines using bayesian data analysis. *J. Eng. Gas Turbines Power, paper*, 132, 2010.

[62] S. O. T. Ogaji, L. Marinai, S. Sampath, and R. Singh. Gas turbine fault diagnostics:a fuzzy logic approcah. *Applied energy*, pages 81–89, 2005.

[63] H. I. H. Saravanamuttoo, G. F. C. Rogers, and H. Cohen. *Gas turbine theory*. Prentice Hall, 2001.

Appendix A: Off-Design performance adaptation by GA optimisation developed by LoGatto

The earlier off-design performance adaptation developed by Lo Gatto is summarised here as it has been extensively used for comparison with the new developed off-design adaptation method. The method developed by Lo Gatto [39] uses genetic algorithm for optimising the adaptation procedure through the selection of three scaling factors that are responsible for the "mathematical stretching" of the compressor map as seen in figure 7.1.

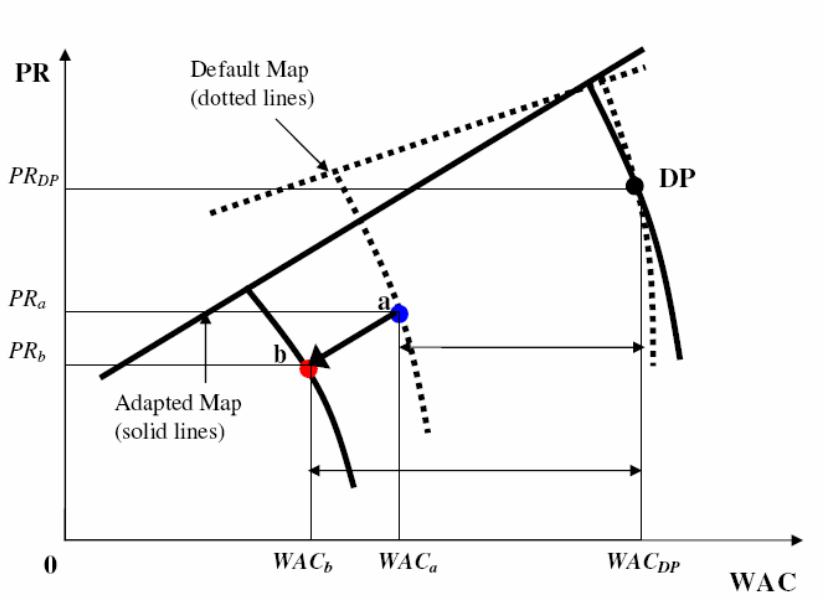

Figure 7.1: Off-Design adaptation Scaling of compressor map [39]

The design point for the default map and the adapted map is the same. The off-design operating point before adaptation labeled "a" and the operating point after adaptation has been performed "b" corresponds to the adapted map and the point at which all the target measurements have been matched.

The three off-design scaling factors employed in this process are listed here:

$$SF_{PR,OD} = \frac{PR_b - PR_{DP}}{PR_a - PR_{DP}} \tag{7.1}$$

$$SF_{WAC,OD} = \frac{WAC_b - WAC_{DP}}{WAC_a - WAC_{DP}} \tag{7.2}$$

$$SF_{ETA,OD} = \frac{ETA_b - ETA_{DP}}{ETA_a - ETA_{DP}} \tag{7.3}$$

Therefore it can be said that each off-design point at the adapted map is a function of the distance between the initial point at the default map and the design point as follows:

$$WAC_b = WAC_{DP} + (WAC_a - WAC_{DP}) * SF_{WAC,OD} \tag{7.4}$$

$$PR_b = PR_{DP} + (PR_a - PR_{DP}) * SF_{PR,OD} \tag{7.5}$$

$$ETA_b = ETA_{DP} + (ETA_a - ETA_{DP}) * SF_{ETA,OD} \tag{7.6}$$

The optimisation procedure follows the same principles with the new developed method, apart from the map generation method. The optimisation procedure is illustrated in figure 7.2.

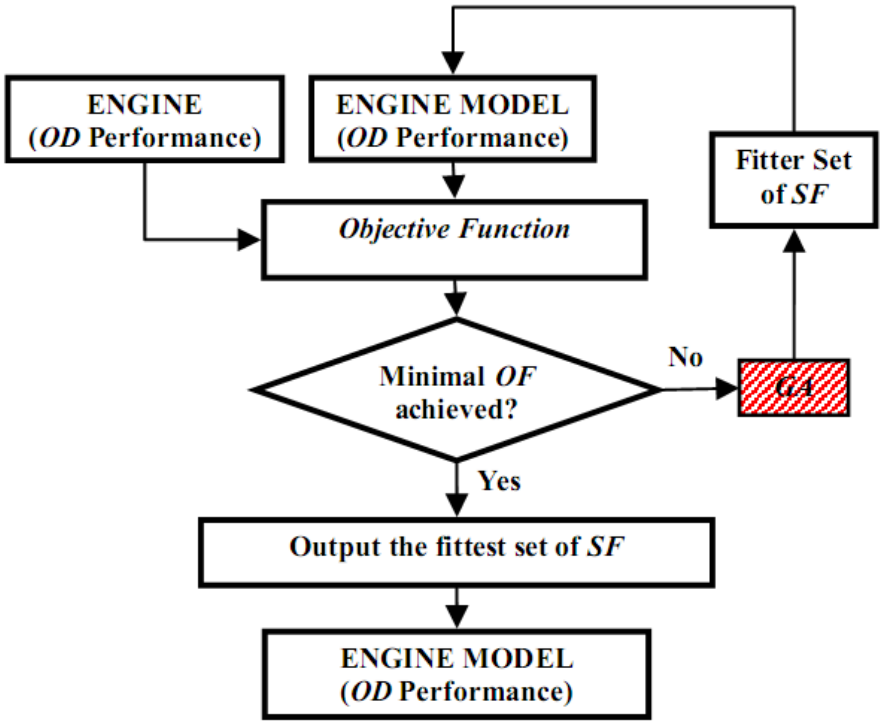

Figure 7.2: Off-Design Adaptation's Flow chart [39]

A series of test cases proved that this adaptation method developed by Lo Gatto is a fast and accurate procedure for single point adaptation. In multiple point adaptation test cases this approach lacks in terms of accuracy and this is mainly due to the nature of the map scaling that is performed. This limitation has been overcome by the new developed off-design adaptation that incorporates a novel compressor map generation method.